1999

Multiple data set integration and GIS techniques used to investigate linear structural controls in the southern Powder River Basin, Wyoming

Heath Patrick Rasco
West Virginia University

Multiple Data Set Integration and GIS Techniques Used to Investigate Linear Structural Controls in the Southern Powder River Basin, Wyoming

Heath P. Rasco

Thesis submitted to the
Eberly College of Arts and Sciences,
West Virginia University
in partial fulfillment of the requirement
for the Degree of

Master of Science
in
Geology

Timothy Warner, Ph.D., Chair
Thomas Wilson, Ph.D.
David Oldham, Ph.D.
David Campagna, Ph.D.

Department of Geology and Geography
West Virginia University
Morgantown, West Virginia

1999

Keywords: Powder River Basin, lineament, data integration, structural controls, GIS applications to geology

Abstract

Multiple Data Set Integration and GIS Techniques Used to Investigate Linear Structural Controls in the Southern Powder River Basin, Wyoming

Heath P. Rasco

Lineaments in the Powder River Basin were mapped and categorized from Landsat TM imagery, a Digital Elevation Model (30 m), and Digital Line Graph (DLG) hydrology files. A GIS program was written using DLG information to eliminate those lineaments that were within 20° of roads and railroads. The DLG and DEM information was further used to stratify the topographic lineaments into slope-breaks, ridge-tops, or valleys. Rose diagrams created for each class of lineaments give important clues on the timing of their formation. The major northwest and northeast trends that these lineaments follow appear to correspond with those identified by previous works. Comparisons with subsurface data suggests that the concentration of lineaments is strongly coincident with gravity and magnetic highs and lows, possibly representing the surface expression of basement-rooted structure. Lastly, the location many reservoirs in the basin also coincide with higher concentration of lineaments over gravity and magnetic highs.

This project was partially funded by the Schumaker Fund, donated by Dr. and Mrs. Robert Schumaker. Also, supplemental funding was given by the American Society for Photogrammetry and Remote Sensing. I would like to thank all of those involved in supporting both of these funds. Their donations has made it possible for continuing research of GIS and geology.

Acknowledgements

This investigation did not occur under academic grant funding. Therefore, all of the data sources needed for this project to occur were either donated, or obtained through donated funds. Among the most crucial of these funds was the Schumaker Fund for academic research in geology. I personally thank Dr. Robert Schumaker and his wife Beverly for their contribution to this study. It was through their fund of $600 that I was able to purchase the Landsat TM image along with the DEM. I also would like to thank Parker Gay at Applied Geophysical, Inc. for his donation of NEWMAG™ high-resolution residual magnetic data. This information was tremendously valuable in correlating the lineaments to subsurface basement structure. Several maps were also donated to this study by two main sources. Jack Uresk at the Rocky Mountain Map Company was able to donate a 2 sheet map (5' x 6') which depicts the structure of the Dakota Formation in the Powder River Basin. This map, created by Barlow and Haun, Incorporated Geologists in 1987, also includes the location of all of the oil fields in the Powder River Basin, as well as well locations. Rod DeBruin, at the Wyoming Geological Survey, is also appreciated for his donation of a Precambrian basement structure map (Blackstone, 1990) and a state geological map of Wyoming. Bob Kucks at the USGS made it possible to obtain the USGS gravity and magnetic data.

This study also entailed a great deal of work on many different software programs. There are many powerful GIS programs that are capable of conducting such an investigation. One of these programs, Arc/Info, was virtually learned in a weekend thanks to the help of Jacquie Snyder, the project manager at the GIS lab at West Virginia University. Kurt Donaldson, GIS lab manager, was also very helpful in this capacity. Many long programs were written to perform many types of GIS functions on these lineaments. One very powerful program, written to give lineaments attributes based on their azimuth in 11.25° increments, was donated by Ping Qin.

Lastly, but certainly not least, the committee members were extremely valuable during the course of this project. Dr. Tim Warner, chairman, remained very patient during my times of cerebral stagnation. Perhaps more compelling was his ability to read and edit the drafts via e-mail from France. Also, thanks goes to Dr. Tom Wilson for obtaining the donation of data from Parker Gay. Any further use of this data must be affirmed through Dr. Wilson. Dr. David Oldham, who was the original designer of this project, was very valuable as a reference in the analysis of the lineament influence on the hydrocarbon reservoirs. Perhaps one of the most profound stages during this project was the stratification of the topographic lineaments based on their topographic properties (i.e. slope-breaks, ridge-tops, and valleys). This was the idea of Dr. David Campagna.

Table of Contents

Table of Figures

List of Tables

Chapter 1: Introduction

Data Integration and Lineament Analysis in Geology

Lineament investigations for geological structural analysis have oftentimes been viewed as untrustworthy. This view perhaps may be caused by the subjectivity of the lineament identification process. Geologists conducting lineament analysis have generally considered all lineaments as equal regardless of their appearances in the data set(s) being used, or else used subjective processes in an attempt to identify major trends. Also, the utilization of multiple data sets in the identification and analysis of lineaments has rarely been employed. This is rather unfortunate, as it appears that surficial data sets, such as satellite imagery, Digital Elevation Models (DEMs), Digital Line Graphs (DLGs) and geological maps integrated with subsurface information such as gravity and magnetic geophysics, seismic reflection geophysics and formation structure maps, provide very powerful capabilities in lineament analysis.

One of the major capabilities in lineament identification made possible using data set integration is the ability to identify lineaments based on their characteristics. This is important issue as combining data may help lend credibility to certain types of lineaments. Identification and classification of various types of lineaments can be carried out manually, automatically, or a combination of both. Once the identification and categorization processes are complete, Geographic Information Systems (GIS) functionality, such as vector and raster spatial analysis and overlay, can be employed for structural analysis and evaluation of significance, using powerful software programs such as ArcView, Arc/Info, and Erdas *Imagine*.

The southern Powder River Basin in Wyoming provides an excellent study area for such an analysis. Many geological features in basin are linearly arranged, including major uplifts, faults, fractures, and folds. The origin and influence of these linear features have been studied in a number of important investigations (Slack, 1981, Marrs and Raines, 1984). These studies have suggested a considerable importance for these linearly arranged structures, as they may affect nearly all of the major hydrocarbon reservoirs. A lineament study utilizing diverse data sets and the power of GIS functionality may

provide a broader and more consistent analysis of the origins, history and influence of these linear features.

The rest of this chapter comprises a description of the study site and an overview of the project objectives.

Study Site Overview and Potential for Lineament Analysis

One of the important interior sedimentary basins in the United States is the Powder River Basin (Figure 1). This area is widely known as a provider of much of the nation's coal from its vast deposits that, at some places, reach thicknesses of over 200 feet. Coincidentally, the Powder River Basin is also a dominant producer of oil and gas from its numerous reservoirs. The Powder River Basin is asymmetric in shape, runs north-south with its axis on the western side, and is surrounded on all sides by structural and physiographic uplifts, which all influenced the formation and evolution of the basin at some time. These major uplifts (Figure 2) include the Bighorn Mountains, Hardin Platform and Porcupine Dome to the northwest; the Miles City Arch to the north and northeast, the Black Hills uplift and monocline to the east, the Hartville Uplift to the southeast, the Laramie Range to the south, and the Casper Arch to the southwest. The surficial area of the basin covers approximately 30,000 km^2 and is a portion of the Laramide intermontane basin province in the Rocky Mountains (Robbins, 1983). The basin received much of its present shape during late Laramide Orogeny, which was during the Late Cretaceous-Early Tertiary (Sharp, 1948). The major oil and gas reservoirs in the Powder River Basin include the aeolian sandstones of the Pennsylvanian-Permian Minnelusa, the Cretaceous alluvial point-bar sandstones of the Dakota (Berg, 1968), the Lower and Upper Muddy channel and marine bar sands, respectively, of Cretaceous age, the Turner channel sandstones of Cretaceous age, and the Shannon, Sussex and Parkman offshore marine bar sands, also of Cretaceous in age (Figure 2). Among the most interesting features of the basin is the pronounced linear arrangement of the vast majority of the oil and gas fields indicating strong structural control. The largest that exhibit this linear arrangement include the Clareton, Fiddler Creek, House Creek, Dead Horse Creek-Barber, Hartzog Draw and the South Coyote fields (Slack, 1981). A few studies have been done in the past to investigate the reason

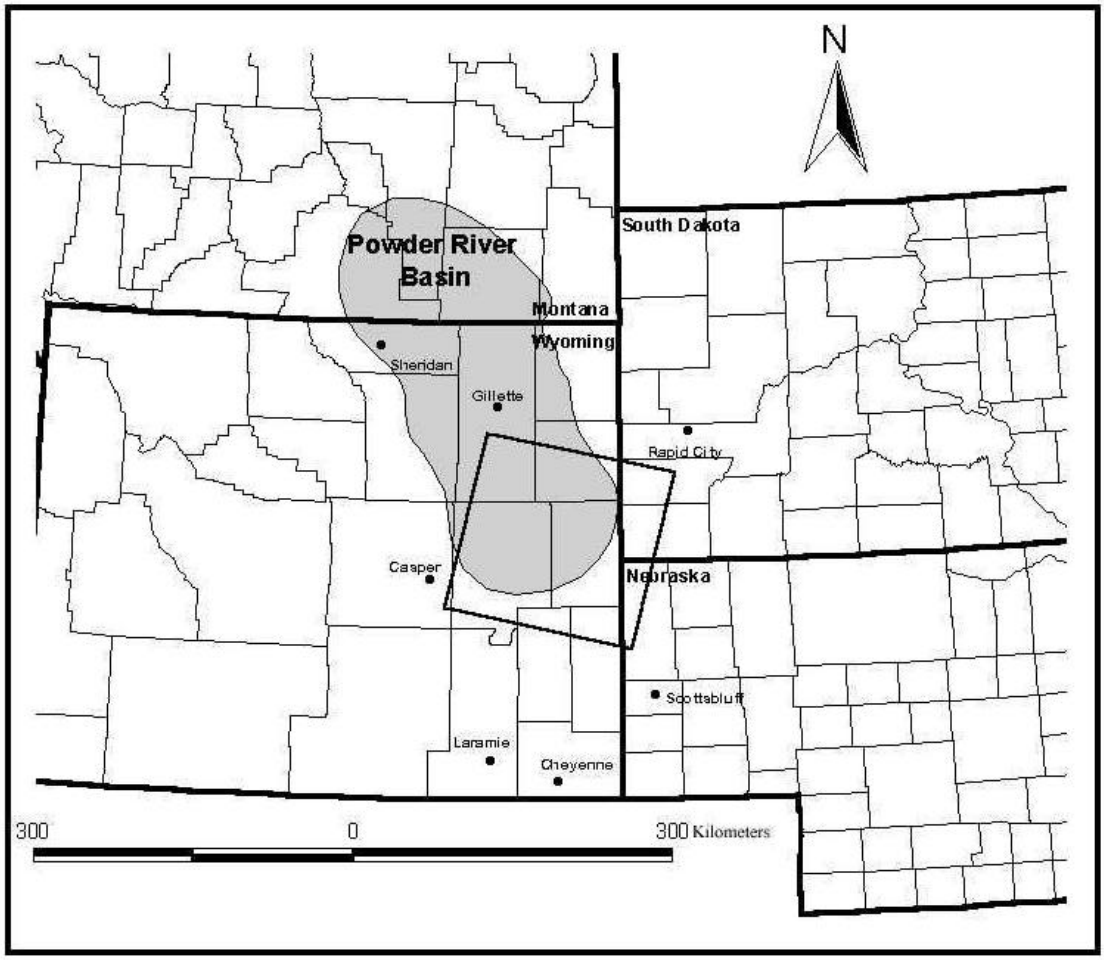

Figure 1: Location of the Powder River Basin and the outline of the study area.

for this pronounced linear arrangement. None of these studies, however, have involved multiple data set integration to investigate structural controls and influences on these fields.

Remote sensing techniques have been shown to be useful tools in analyzing linear framework of structurally complex, as well as remote, areas. When remote sensing techniques are combined with subsurface data sets such as gravity and magnetic data, well data and subsurface structure maps, the result is a very powerful, thorough and inexpensive method for analyzing linear framework and investigating the source and effects of lineaments. A lineament may be defined as a linear or curvilinear zone of structural discordance. Often these represent faults, fractures, sharp anticlinal fold axes, geological rock formation contacts or vertical beds such as flat irons or hogbacks.

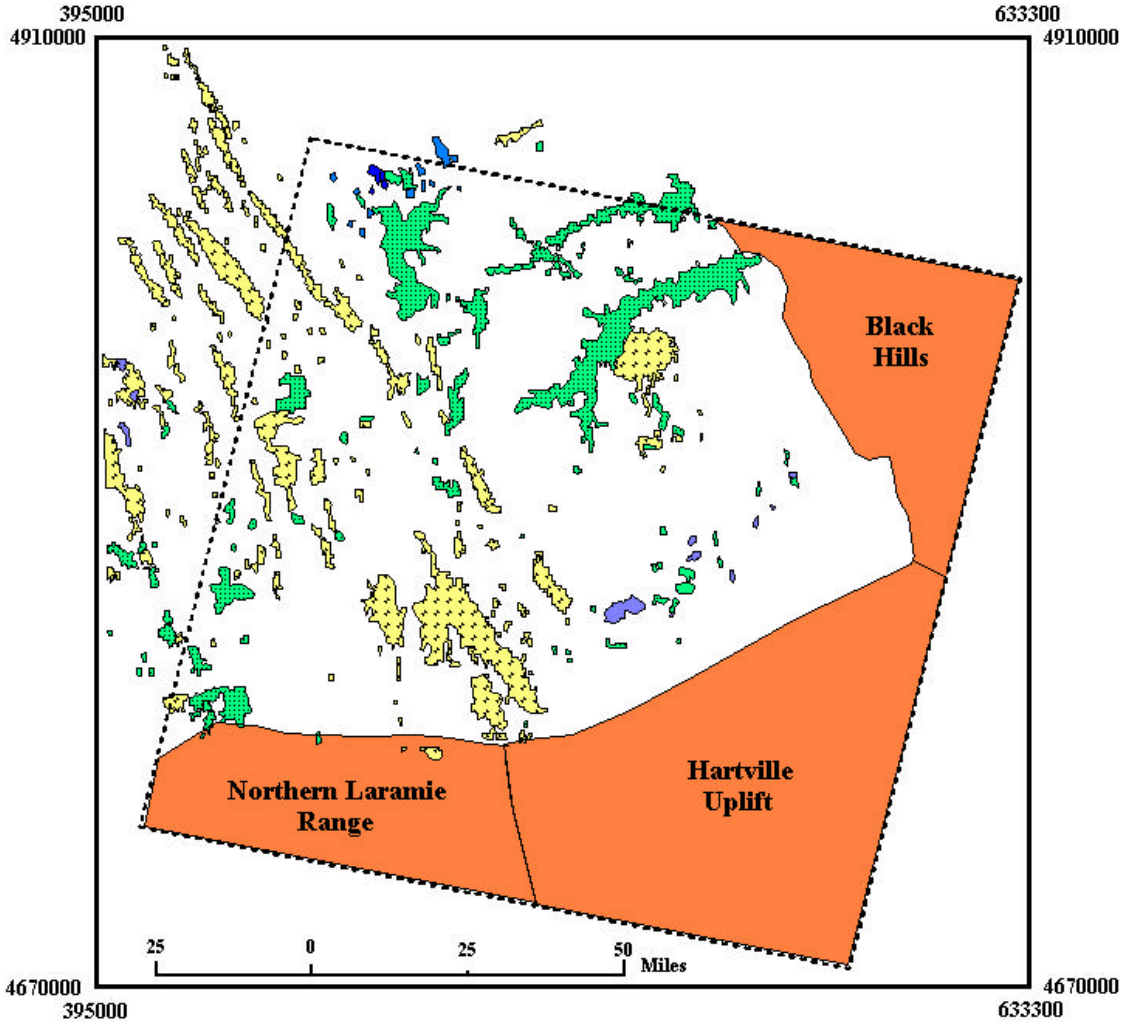

Figure 2: Generalized tectonic map of the Powder River Basin showing the location of major uplifts and hydrocarbon reservoirs. Pennsylvanian-Permian reservoirs are shown in blue, Lower Cretaceous in green, and Upper Cretaceous in yellow. Coordinates are UTM.

Geomorphic indicators of linear structural discordance as viewed from air or space include linearly arranged topographic features such as valleys or ridges and scarps. Other features that are good lineament indicators are linear vegetation growth patterns, abrupt tonal changes in the image, or linear breaks in slope. Digital Elevation Models (DEM) may be very useful tools in automated extraction of these geomorphic indicators.

Tectonic History of the Powder River Basin

The evolution of the Powder River Basin to its present configuration is the result of a structurally complex history. In general, the rocks of the surrounding uplifts and

basement are largely of Precambrian age unconformably overlain by shallow-water marine sedimentary packages with an average thickness of approximately 1 km. The Paleozoic rocks are overlain by Jurassic shallow-water marine sediments, which are interfingered with floodplain deposits that reach a thickness of up to 0.5 km. An epeiric continental seaway covered much of North America, including the basin, during the Cretaceous and deposited more shallow-water marine sediments as well as some coastal plain sediments. These marine sedimentary packages are correlative to those found in the surrounding basins (Mallory, 1972). The Laramide Orogeny, with its counterclockwise change in rotation of stress, significantly impacted the evolution of the basin during the Tertiary (Gries, 1983). Due to Tertiary tectonism in the vicinity of the Powder River Basin, many fluvial and lacustrine sedimentary rocks are indigenous only to the basin. In order to illustrate the influence of structural control on the evolution of the basin, the tectonic history will be presented in sequential fashion.

Precambrian

The Wyoming Precambrian province is the oldest major crustal formation in this area, shown by radiometric dating from detrital zircons from the Beartooth Mountains to be 3.3 Ga (Mueller *et al.*, 1992). From petrographic analysis of the sediments derived from the igneous rocks, this crust was largely composed of orthogneissic (granite) terranes (Condie, 1976). Sedimentation along with volcanism occurred following the crustal formation until 2.9 Ga (Robbins, 1993). The region's first recorded tectonic events, including metamorphism and plutonism in what is now the Bighorn Mountains, Northern Laramie Range and Hartville Uplift, occurred between 3.0-2.9 Ga. Metamorphism continued in the Hartville Uplift until 2.65 Ga, while felsic and mafic plutonism remained active in the Bighorns until 2.75 Ga (Condie, 1976; Hedge *et al.*, 1986; and Snyder *et al.*, 1989). This deformation continued until the end of the Archean (Condie, 1976). A paper by Hedge *et al.* (1986) suggests that the first granitic plutons began to form in the Black Hills region at this time. The above succession may have been derived from the collision with an island arc system (Knight, 1990 and Robbins, 1993).

The earliest Proterozoic tectonic activity was a system of diabase dikes with a dominant northeast trend, as well as subsidiary northwest, east-west, north-northwest, north-northeast and east-northeast trends (Condie, 1976; Love and Christiansen, 1985; Hedge *et al.*, 1986; Snyder *et al.*, 1989; and Robbins, 1993). Following these structures, granitic intrusions began to form in the Hartville Uplift area around 2.1-1.9 Ga. During the period from 1.7-1.6 Ga, intrusions in the Black Hills and the Hartville Uplift regions (Hedge *et al.*, 1986) may have formed from a partial subduction of the crust under a volcanic arc in the southeast portion of the basin (Robbins, 1993). Stewart (1976) and Winston (1988) investigated the last documented tectonic event in the Precambrian Era. Their findings suggest that rifting was initiated at approximately 0.85 Ga and formed a passive margin by 0.65 Ga. This extensional event may be the reason for a system of northeast-trending near-vertical normal faults in the southern portion of the basin parallel to the Hartville Uplift (Mitchell and Rogers, 1993).

The domination of structural linear features in the northeast direction has been a focus of many types of studies in the past (Slack, 1981, and Maughan, 1983). These studies have suggested that northeast-trending lineaments may be derived from reactivation of the Precambrian basement shear zone faults. Slack (1981) suggests that the dominance of northeast trending lineaments is analogous to the shear zone formed from the development of an Atlantic-type margin at around 1.7 Ga (Robbins, 1993). This view, however, is not supported by the presence of the aforementioned intrusions in the Black Hills region. These basement structures are also not indicated on the Wyoming State basement structure map, which was generated from well data (Blackstone, 1990).

Paleozoic Era

The Powder River Basin was cycled above and below sea level throughout the Paleozoic. This was largely due to the apparent lack of relief in the area at this time (Robbins, 1993). The major tectonic events of the Paleozoic in this region were related to the ancestral Rocky Mountain orogeny. Maughan (1990) chronicled the events surrounding this orogeny. Upwarping of the craton occurred around 365 and 330 Ma. These upwarping events are believed to be precursors to the ancestral Rocky Mountain orogeny. There were three subsequent events that were part of the orogeny; one from the

Mississipian to Early Pennsylvanian, one during Middle Pennsylvanian time and one from Late Pennsylvanian to Early Permian (Maughan, 1990). Slack (1981) states that reactivation along these Precambrian faults may have occurred during the tectonic events in the Pennsylvanian. The ancestral Rocky Mountain orogeny was completed by the Late Permian (Robbins, 1993).

Mesozoic Era

Sea level again fluctuated as evident from Triassic and Jurassic rocks in the basin. There were four main marine transgressions from the west into the nonmarine depositional environment that characterized the basin at that time (Johnson, 1992 and 1993). The only apparent tectonic activity during this period was the broad flexing of the craton (Robbins, 1993). This relative quiescence continued until the Early Cretaceous. Slack (1981) states that strata present in the Powder River Basin were affected by increased structural activity and subsequent formation of the Belle Fourche Arch, which trends roughly east-west across the center portion of the basin, caused by reactivation of basement faults. It is believed that the formation of this arch was likely related to the Sevier Orogeny continuing further to the west (Robbins, 1993).

Deformation related to the Laramide Orogeny started in the Rocky Mountain region in the Late Cretaceous around Campanian (80-60 Ma) time. Uplifts along thrust faults, as well as arches, belong to three main trends in the Rocky Mountain region according to age: north-south, northwest-southeast and east-west. Structures following these trends belonging to the Laramide Orogeny are assumed to be the result of counterclockwise changes in the direction of compressive stress as the Farallon plate was being subducted at a low angle under the North American plate (Gries, 1983). During the Late Cretaceous, the Hartville Uplift began to rise toward the southeastern part of the basin (Robbins, 1993). Also developing at this time is the Black Hills Uplift along the east flank of the basin, which is actually a large monocline that dips as high as 45° to the west with structural relief up to 6,000 ft. (Slack, 1981). The Laramie Range began to develop in the very latest Cretaceous as east-west compression led to thrusting of Precambrian crystalline rocks over the west flank of the Denver Basin (Gries, 1983).

Cenozoic Era

Most of the tectonic activity that formed the present shape of the Powder River Basin occurred during the Tertiary. A shifting in direction of compressive stress toward the southwest during the Paleocene initiated the formation of the most important structural regimes in the Powder River Basin (Figure 3). The major tectonic activity was in the northern foreland area where folds and thrusts were oriented northwest due to shortening on the northeast axes (Brown, 1981). Among the northwest trending structures adjacent to the Powder River Basin are the Bighorn Mountains, which developed in the Middle Paleocene, and the Casper Arch, which developed during the very latest Paleocene (Gries, 1983).

At the beginning of the Eocene, Laramide compressive stress became almost directly north-south (Figure 3). This caused the formation of many east-west trending structures including the Uinta Mountains. The effect that this stress regime had on the

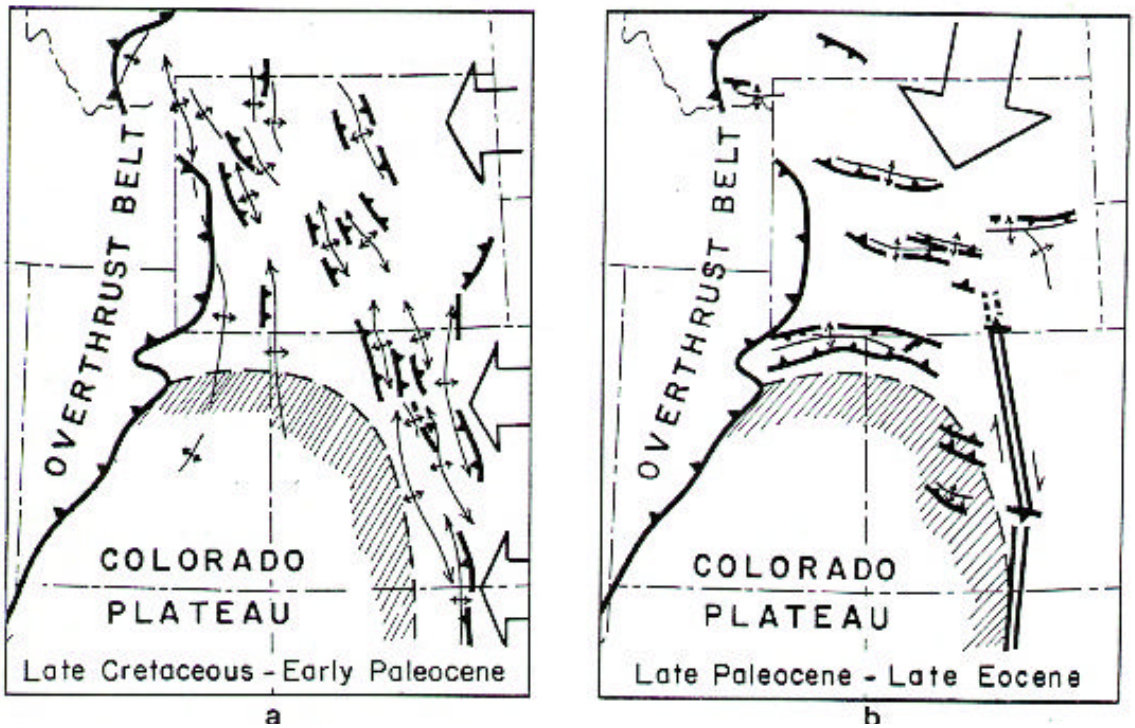

Figure 3: Timing of compressional stress during the Laramide Orogeny (Gries, 1983):

a. Westerly direction of stress caused the formation of north-south-trending uplifts and thrusts with broad arches plunging off to the north. These structures appear to be stacked along the Colorado Plateau.

b. Late Laramide compression shifted to north-south which yielded the formation of east-west-trending uplifts and associated structures.

Powder River Basin is quite important. The Owl Creek Range was developed just to the west of the basin during the Early Eocene and connects to the northwest-trending Casper Arch. Due to the continuation of this north-south compressive stress, at perhaps the most strongest tectonic pulse, the northern Laramie Range was thrust over the southern portion of the Casper Arch and the south flank of the Powder River Basin (Gries, 1983). Also, the northern portion of the Black Hills was undergoing plutonism, including the intrusion of laccoliths, dikes and sills. Terrestrial sedimentation occurred during the Oligocene in the Powder River Basin. The basin has developed much of its present relief from erosion (Robbins, 1993).

Summary of Tectonic History

In summary, the Powder River Basin has undergone intense metamorphism and plutonism in the Archean through the Proterozoic. Toward the end of the Proterozoic, findings suggest a rifting event that lead to the formation of an Atlantic-type passive margin by 0.65 Ga. The first signs of dominant northeast and northwest structures were established. Sea level fluctuated above and below the basin throughout the Paleozoic; the only tectonic activity in the area at this time was from the Ancestral Rocky Mountain Orogeny, which may have caused reactivation of Precambrian faults. Sea level again fluctuated throughout almost all of the Mesozoic, due to the presence of a major continental seaway. The destruction of this major seaway is recorded in the very thick succession of Late Cretaceous terrigenous rocks. Counterclockwise rotation of stress related to the Laramide Orogeny is represented in the form of many reactivated basement faults and new structures that trend north-south, northwest-southeast, to east-west in that order of age. The basin has retained much of its present shape since the Laramide Orogeny.

The Powder River Basin is therefore a very significant basin with a very rich and complex structural and tectonic history. This complex history has resulted in an equally complex expression in the surface geology. A remote sensing analysis, and especially one that integrates GIS spatial analysis (i.e. overlay), has the potential to provide a valuable overview of the surface features, and help unravel their significance.

Purpose of Study

The purpose of this investigation is to investigate various lineament analysis techniques using GIS spatial analysis functionality with the Powder River Basin as a test area. Many lineament studies in the past have been shown to be very subjective, especially when based on only a few data sets. Also, lineaments have, in the past, been viewed as equal regardless of their appearance (Slack, 1981 and Marrs and Raines, 1984). This investigation has a number of subsidiary aims, as listed below:

- Manually identify and classify lineaments from different surface data sets based on their topographic or visual appearance.
- Employ GIS functionality with a Digital Elevation Model (DEM) to automatically categorize the identified lineaments into classes based on topographic characteristics.
- Compare lineaments with subsurface data sets.
- Illustrate the importance of multiple data set integration in lineament analysis.
- Investigate the possible relationship of lineaments to hydrocarbon reservoirs in the Powder River Basin.

Stratification of lineaments based on their topographic appearance has potential significance, as lineaments that are positive topographic features may have different structural implications than negative topographic features. This stratification may shed some light on which type of lineaments portray the most influence on structural patterns, and furthermore, control of hydrocarbon reservoirs. Thus, one result from this investigation will be the illustration of the DEM as a useful, and perhaps necessary, tool in automated lineament categorization of the topographic lineaments.

This type of investigation may develop to be a most productive, thorough and inexpensive method to analyzing lineaments and may eliminate some of the considerable speculation that arises from correlating lineaments to tectonic events. It is a general rule of thumb that the more data sets used to study a particular problem, the better the result. This type of study can also be applied to similar regions in the world in order to gain understanding of the structural geology and maybe hydrocarbon potential.

Chapter 2: Literature Review

Lineament Identification in Remote Sensing

Linear features observed on satellite images and aerial photography have been studied for a considerable length of time. These features are commonly termed lineaments, and although different authors have defined them in various ways there is general agreement (Hoppin, 1974, O'Leary *et al.*, 1976, and Rowan and Bowers, 1995) that they include:

- Topographic features, such as alignment of drainages, ridges or escarpments.
- Tonal features, such as anomalous linear features or changes in image tone.
- Geological features, such as abrupt discontinuities in geological formations.
- Combinations of the above.

Lineaments are commonly interpreted as surface expressions of rock fractures. They have therefore been used in hydrological (Parizek, *et al.*, 1990, Yin and Brook, 1992, and Hardcastle, 1995), mineral (Rowan and Wetlaufer, 1975, and Rowan and Bowers, 1995) and hydrocarbon exploration (Dix and Jackson, 1981, Mah *et al.*, 1995). Lineaments may have particular significance in hydrocarbon exploration as an indicator of zones of high permeability and/or less pressure that may serve as pathways for hydrocarbon migration, and thus targets for increased production. In addition, they may represent faults that control basin development and distribution of reservoir.

In recent studies (Warner, 1997, and Warner, 1998), in was found that lineaments had importance in both structural and stratigraphic traps in two test sites in the Appalachian Basin. It was found that lineaments that paralleled the structure of the Burning Springs anticline were related to hydrocarbon production, whereas those that were cross-strike were related to soil gas accumulations. Thus it appears that lineament interpretation should be treated with caution, as different lineaments may not all have the same significance, even in the same area. Lineament studies of hydrocarbon reservoirs using Landsat imagery have also proven to be successful in the Denver Basin (Merin and Moore, 1986) where fracture reservoirs were found to develop preferentially at lineament intersections.

Lineament Studies in the Powder River Basin

Major structural lineaments have been studied in various parts of the Powder River Basin. Potential trends have been interpreted from structural offsets in the Black Hills monocline and topographic expression on contour maps (Slack, 1981) and from Landsat imagery (Marrs and Raines, 1984). Slack (1981) studied major structural offsets in the Black Hills monocline and postulated that the linear framework that developed in the basement of this region should also be present in the basement underneath the basin. He was able to correlate the structural offsets to the Belle Fourche Arch, a broad arch that trends northeast through the center of the basin. The offsets were interpreted to have developed from reactivation of the basement faults along the arch, which have total displacement each of less than 40 ft. He concluded that the major northeast-trending lineaments formed from this basement block rejuvenation control the location of the major hydrocarbon reservoirs in the basin.

Marrs and Raines (1984) mapped lineaments from Landsat imagery in order to determine the linear framework of the Powder River Basin. Lineaments were grouped into trends while other sets were eliminated altogether if they were neither dominate nor significant. The major linear trends were grouped into larger linear zones. The linear zones mapped trend northeast with a seemingly conjugate northwest set. These linear zones were postulated to have controlled the location of many hydrocarbon reservoirs in the basin. When compared to the major linear zones mapped by Slack (1981), many of the zones do not match. Aside from this, the selective statistical method used by Marrs and Raines (1984) has been the source of controversy and the subject of many subsuquent discussions including Michael and Merin (1986).

Despite the proposal that the major linear zones control the location of the hydrocarbon reservoirs, as suggested by these two major lineament studies in the basin, an analysis of multiple subsurface data sets to prove this has not carried out. In particular, detailed information about the basement and its involvement in the development of structural linear features and reservoir control has not been used. The development and use of higher resolution magnetic geophysical data may offer other useful insights into this problem of the effects of lineaments at depth.

Geophysical Studies in the Powder River Basin

Geophysical surveys have been extensively carried out in the Powder River Basin in the form of 2-D and 3-D seismic reflection. There are thousands of seismic lines that run through the basin due to the interest of oil and gas companies. Past studies of the basin involving seismic data have been conducted to determine structural geology and tectonic history, but with a major focus on the effect of hydrocarbon migration and entrapment. The area near the Casper Arch has been studied by Gries (1983) and Ray and Berg (1985). Their findings show the dramatic effects and influences of the northern Laramie Range thrust over the Casper Arch and the southern portion of the Powder River Basin. Furthermore, McMillen (1990) has studied the extent of Cambrian sedimentary rocks in the basin related to extensional tectonics. Lastly, Robbins and Grow (1990) used seismic data to study basement lithologies in the basin.

Gravity and magnetic studies are not as common in the Powder River Basin, but research performed by Gay (1995) with high-resolution magnetics may change that. Kleinkopf and Redden (1975) as well as Duval, Pitkin and Macke (1977) have undertaken gravity and magnetic studies in the past. Robbins (1993) completed a gravity and magnetic geophysical investigation of the Powder River Basin using a series of total intensity magnetic maps and residual gravity maps.

The use of subsurface geophysical information for structural analysis is a very powerful tool. However, the correlation between features seen on the surface to those seen underground can be even more powerful and reliable. The importance of this method of data integration has already proven its worth in many areas of the world.

Geophysics and Remote Sensing Integration

Remote sensing can be very useful in mapping and analyzing structural geology, especially in remote regions. However, subsurface geophysical methods are among the best supplement to surface interpretations made from satellite or aerial image. Examples of investigations integrating remote sensing and geophysics include the studies conducted by Campagna and Levandowski (1993) and Levandowski, Cetin and Reichard (1993).

Campagna and Levandowski (1993) used Landsat images supported with gravity geophysics to investigate the relationship between the Lake Mead fault zone and the Las

Vegas shear zone in the region of the Overton Arm of Lake Mead, Nevada. This area is not only a structural low, but also a topographic low covered by Lake Mead. A Complete Bouger Anomaly (CBA) map of the same area shows gravity low, bounded by the two left-lateral fault segments. These combinations of observations suggests the presence of a pull apart basin that formed due to a step in the strike slip fault system, and illustrates the power of combining diverse data sets.

Through the support of hydrocarbon exploration in eastern Nevada, Levandowski *et al.*, (1993) investigated the effectiveness of remote sensing, enhanced by gravity data, as a tool for analyzing extensional faulting associated with unconsolidated valley fill sediments in the Basin and Range Province. Faults were mapped based on geomorphic characteristics from aerial photographs. These faults were then overlain on a CBA map to determine if these faults corresponded with 1) a horizontal density contrast and 2) sufficient structural relief present in that density contrast. The authors were able to identify major boundary faults from steep gradient changes on the CBA map. The significance of this study was that combining remote sensing and gravity geophysical data might be more reliable as an exploration tool in the Basin and Range Province than either data set on its own.

Geophysical data is of particular value in remote sensing studies. Remote sensing is a science that is generally limited to the surface of the earth. Subsurface geophysics provides a means of lending credibility to geomorphic features seen in surficial remote sensing. An additional ancillary data set, that can be very useful in understanding the geomorphology of an area, is a digital elevation data (DEM). Many geomorphic features such as valleys, ridges and escarpments are very important structural indicators that can be extracted from a DEM. Methods of topographic extraction will be discussed in the following section.

Automated Feature Extraction from DEM

Many recent studies have shown the DEM to be very useful in geological analysis, particularly structural analysis. DEMs are also very useful in aiding the classification of landforms for many purposes such as recognition of geomorphological patterns, watershed characteristics and valley heads. A very important study by

Chorowicz *et al* (1989) described a technique by which geological and geomorpological features could be recognized from DEMs. Elementary objects such as crests, thalwegs and various other slope types were classified by checking for slope changes characteristic of the above classes in many directions. Douglas (1986) illustrated various techniques to locate such topographic features as ridges, channels, watersheds and drainage patterns from DEMs. The main problem with this approach was that depressions and other flat areas that hinder water flow were not fully identified. A method of extracting these depressions was developed by Jenson and Domingue (1988). Building on this premise, separation of wet flat areas (swamps) from dry flat areas (plateaus) using DEMs has been carried out by Warner *et al.* (1991). Hydrologic flow modeling and drainage networking has been carried out by combining valley finding algorithms with algorithms that analyze the profiles of those valleys (Chorowicz *et al*, 1992).

More recent advances have been made in using the DEM as a means for extracting information and characteristics on geological structure. McMahon and North (1993) developed a method in which measurements can be made on faults observed in images of 3-D combinations of DEMs and subsurface data. The regional stress domain of a particular area can also be investigated with DEMs, as shown by Beaver *et al.,* (1992). Their work uses the DEM to analyze structural symmetries of features such as folds, faults and fractures based on given characteristics and appearance on the DEM. The end product is claimed to be a reliable description of the stress regime in a given area. This approach, however, has its weaknesses in areas of complex tectonic histories. DEMs have also been used to map geomorphologic features based on detection and manipulation of certain node points (Neves and Thiessen, 1993). The node points are stretched out and converted to vectors. These vectors are then examined for coplanar alignments and plotted as planes on the original DEM for correlation to known geological structures. The significance of this work is the development of a method for extracting the major planar structural features that might ordinarily be lost in a regular 2-D analysis. Most recently, difference in topographic characteristics of strike-slip faults and dip-slip faults have been used to distinguish dip-slip faults from strike-slip faults (Florinsky, 1996). Faults that showed changes solely in the horizontal curvature were interpreted as strike-slip, while faults that showed changes on the vertical curvature were interpreted as

dip-slip. Oblique and gaping faults had changes on both horizontal and vertical curvatures.

Extraction of topographic feature information from DEMs has become increasingly popular in structural analysis. In fact, some investigations solely rely on the geomorphic information seen on the DEM. These studies often include some variation of involvement with GIS functionality (Berquist, 1996, and Linn, 1996). GIS functionality, such as spatial analysis, has also become more popular in structural geology in general. The use of GIS functionality for structural analysis is discussed below.

GIS Functionality in Analysis of Geological Structure

Geographical Information Systems (GIS) have become increasingly powerful due to improvements in both hardware and software. With this increase in the power of GIS, many fields in both geography and geology have found new uses for GIS. One of the geological fields that have recently benefited from GIS input is structural geology. Many of the recent technological advances in structural geology involving GIS rely on the construction of large databases containing structural information about features such as faults, folds and fractures. This information can then be used in the construction of geological structure maps as has been illustrated by Berquist (1996), Ross (1997) and Jaworski (1997). Once data about these structural features is entered into a GIS package, data manipulation for detailed analysis can take place. Linn (1996) used ArcView to illustrate the ease of using layer overlay in performing rapid and accurate geological analysis and mapmaking. In support of hydrocarbon exploration, Oldow (1996) developed a digital database of structural features, derived from many map sheets, as well as aeromagnetic and gravity geophysical data for Venezuela. Through spatial analysis of these data sets using GIS software packages, geologists were able to make rapid assessments of hydrocarbon potential in areas of Venezuela when it would otherwise take months.

Both raster and vector based GIS software were integrated in the development of a basement structural model for the Oriente (Amazon) of Ecuador (Fishman and Bhatt, 1996). In this study, an existing geological map for Ecuador was digitized into vector coverage and overlain with contoured gravity data in Erdas *Imagine*. Topography was

also digitized and used for topographic terrain corrections of the gravity data as well as further topographic analysis. When all of these products were used together, pre-Cretaceous high angle reverse faulting in Ecuador became more evident.

Chapter 3: Methodology

Definition of a Lineament

In order to conduct a lineament investigation, a working definition of the term lineament must be chosen. For the purposes of this study, lineaments are defined as linear, or curvilinear, zones of structural discordance. Lineaments on the surface are assumed to represent such geological features as faults, fractures, sharp anticlinal fold axes, rock unit contacts, vertical beds, or a linear arrangement of the above. The method of detecting lineaments varies, depending on the types of data used to identify them. The data sets employed in this study were a Landsat TM image, a Digital Elevation Model (DEM) with postings on a 30-meter interval, and hydrographic data from Digital Line Graph (DLG) files. As is discussed below, each data set was enhanced in different ways in order to identify lineaments.

Two main methods of classifying and categorizing lineaments were also investigated. The first approach was a manual one in which a trained interpreter classified lineaments based on their appearance in the various data sets. The second method is an automated approach in which the manual interpretation is limited to the identification of lineaments; the categorization of the lineaments is carried out automatically based on topographic or other associations.

Identifying Lineaments on Landsat TM Image

The Landsat TM imagery was purchased from the U.S. Geological Survey EROS Data Center. The image (path 34-row 30) was acquired on 12 October 1987. This time of year is a "leaf-off" vegetation condition for this portion of the Northwest, and was assumed to be the most suitable for geological analysis. The coordinates are as follows:

Table 1: Landsat TM Image Location

Corner	Latitude	Longitude
Northwest	44°03'47"N	105°39'38"W
Northeast	43°43'59"N	103°24'00"W

Southeast	42°15’47”N	103°55’59”W
Southwest	42°35’06”N	106°08’31W

The pixel size of the image is 28.5 meters, the nominal spatial resolution of Landsat imagery. The image was of very good quality with no clouds present to obscure observation, however, there was a slight dusting of snow on the higher elevations.

Image Enhancement

The Landsat TM image was digitally enhanced in order to facilitate the process of identifying lineaments. After experimenting with different filter kernels, the best enhancement was found to be a 5 X 5 modified Laplacian edge enhancement filter with the following matrix:

-1	-1	-1	-1	-1
-1	-1	-1	-1	-1
-1	-1	49	-1	-1
-1	-1	-1	-1	-1
-1	-1	-1	-1	-1

The band combination found to be most useful was a standard false color composite with Band 2 (green) displayed on the blue gun, Band 3 (red) displayed on the green gun, and Band 4 (near-IR) displayed on the red gun. This band combination made it easier to identify linear patterns of vegetation, which could represent deeper soils associated with geological zones of weakness and erosion susceptibility. Only one other band combination, a true color display, was found to be somewhat useful in aiding the identification process.

Description of Landsat Image Lineament Classes

Once the image was enhanced, an Arc/Info vector file was created as a transparent overlay. This editable vector file served as the lineament layer for on-screen digitizing. Lineaments were visually separated into two main classes. The first class was that of topographic lineaments. The characteristics of topographic lineaments include features such as ridges, valleys, and prominent scarps oriented in a linear or curvilinear fashion (Figure 4a). Alignment of these linear or curvilinear features was regarded as

confirmatory evidence, but was not required to be present. Also included in this class were front range thrust faults implied at the edge of mountain ranges (Figure 4b). The second class of lineaments identified from the image was tonal anomalies and linear vegetation patterns (Figure 5). Zones with a distinct linear distribution of vegetation defined this class. Linear distribution of vegetation could possibly represent a zone of geological weakness, such as associated with faults and fractures. Erosion is more active in geologically weak zones where water can penetrate. In the semi-arid steppe environment of the field area, plant growth tends to be enhanced by the presence of more reliable water.

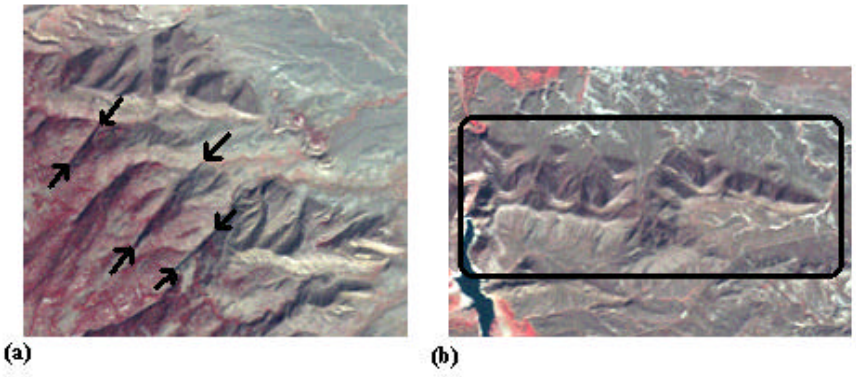

Figure 4: (a) Small subset image of the Landsat TM image that shows some examples of topographic lineaments in the form of aligned valleys and ridges. Arrows indicate end points of the lineaments. (b) Another small subset of the Landsat TM image that depicts the flat irons representing the front range fault. Within the box is the actual zone of interest. The lineament in this case would be mapped along the base of the flat irons.

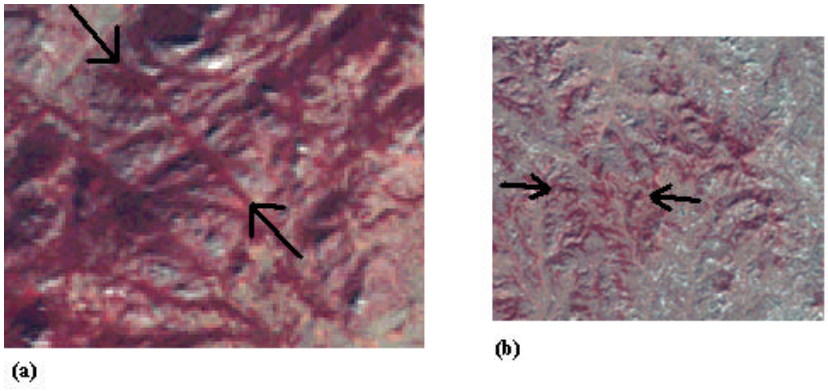

Figure 5: (a) Small image subset that shows a linear pattern of vegetation growth (bounded by arrows). The vegetation is shown in red due to the high reflectance in infrared light, which is displayed as red on the image. (b) This subset shows the characteristics of abrupt linear tonal changes, again bounded by the arrows.

Identifying Lineaments from DEM

The DEM image of 30-meter intervals was also purchased from the U.S. Geological Survey. The DEM covered an area slightly larger than that of the Landsat TM image. This is due to the near-polar orbit of the Landsat spacecraft, which produces an image slightly rotated with respect to north. The DEM, on the other hand, and was formatted to include the entire imaged area as well as the blank buffer region produced in geocoding the satellite image. Lineaments identified from the DEM were strictly topographic in character. Of course, these lineaments can either be geological or cultural. For example, a road-cut, a cultural feature, would appear as a linear topographic change in slope.

Image Enhancement of the DEM

In order to identify linear topographic features from the DEM, two shaded relief images were generated, with sun angles 90° apart. The first shaded relief image created had a solar azimuth (sun angle) of 225°, which is from the southwest, and a solar elevation of 45°. An ambient light setting of 0.20 was used, which produces a good contrast. The ambient light setting is simply a scaling factor in the *Imagine* (Erdas, 1998) topographic program. A vector layer was created to overlay this image. Lineaments were visually identified, and then digitized on-screen.

The second shaded relief image from the DEM was created with all of the same properties as the first, except that the solar azimuth was set at 315°, or from the southeast. The vector layer used to record the 225° lineaments was overlain onto the 315° image, and the additional lineaments identified were added to the same file by on-screen editing. The final vector layer was a single file of topographic lineaments from the two DEM lineament interpretations.

Description of DEM Lineaments

The lineaments identified from the shaded relief images created from the DEM were strictly topographic. Features that produce linear topographic alignments include fault scarps, fractures, front range thrust faults, geologic rock unit contacts, linear ridges

and valleys, as well as cultural features such as road cuts, roads and railroads. Both shaded relief images enhanced a distinct pattern of north-south-trending linear features, which are artifacts from the profile lines digitized during the creation process of the DEM. These artifacts were excluded during the lineament identification process and thus should not have added noise to the vector file.

Identification of Drainage Anomalies from DLGs

DLG files, distributed on CDs by the U.S. Geological Survey, are a particularly valuable source of vector cartographic information. Each DLG disk holds files for roads, railroads, miscellaneous transportation and hydrology. The files are separated into coverages based on the regions covered by the equivalent 1:100,000 scale maps. The appropriate 1:100,000 scale maps for the study area, based on the map coordinates of the Landsat TM image, were downloaded from a CD obtained from the USGS Depository at the WVU Wise Library. This involved the selection of sixteen individual maps within the field area, which were joined using Arc/Info commands. The DLG data was then displayed in Erdas *Imagine* 8.3. A new vector layer was created to overlay the hydrographic data so that on-screen digitization of drainage anomalies could take place.

Description of a Drainage Anomaly

For the purposes of the investigation, a drainage anomaly was defined as an abrupt linear or curvilinear change in the established flow pattern of a stream or river system. The alignment of several streams, stream segments, or of linear or curvilinear changes in stream flow, was regarded as particularly strong evidence for a drainage anomaly.

Lineament Processing

Once all lineament identification was complete, an Erdas *Imagine* 8.3 Spatial Modeler program was written to eliminate those lineaments that were potentially of cultural origin. The Spatial Modeler Program is a powerful icon-based macro-language scripting tool. The Spatial Modeler is developed mostly around raster functionality. Consequently, prior to developing models, the vector lineament files rasterized to

produce 1-bit raster coverage, on the same grid as the Landsat image. This step generated a file with lineaments coded as 1, and the background at 0. The same steps were also applied to convert the railroad and road DLG files to raster coverages.

The model constructed to eliminate cultural lineaments is shown in Figure 6. In this model, the 1-bit DLG file (roads or railroads) and lineament file serve as input images. The first process gives each road or railroad a four-pixel buffer, giving a total width of eight pixels for each transportation feature. This buffer zone allows for slight errors in projection between the two files as well as any fuzziness in the location of lineaments, or operator error. For example, if the person digitizing the lineaments is within an average of plus or minus four pixels of the actual lineament, then the buffer covers that error. Once this step has been completed, the buffered road or railroad file is compared with the lineament file. Lineaments or lineament segments that cross this buffer zone are deleted. Since the aim is to delete lineaments that parallel the road or

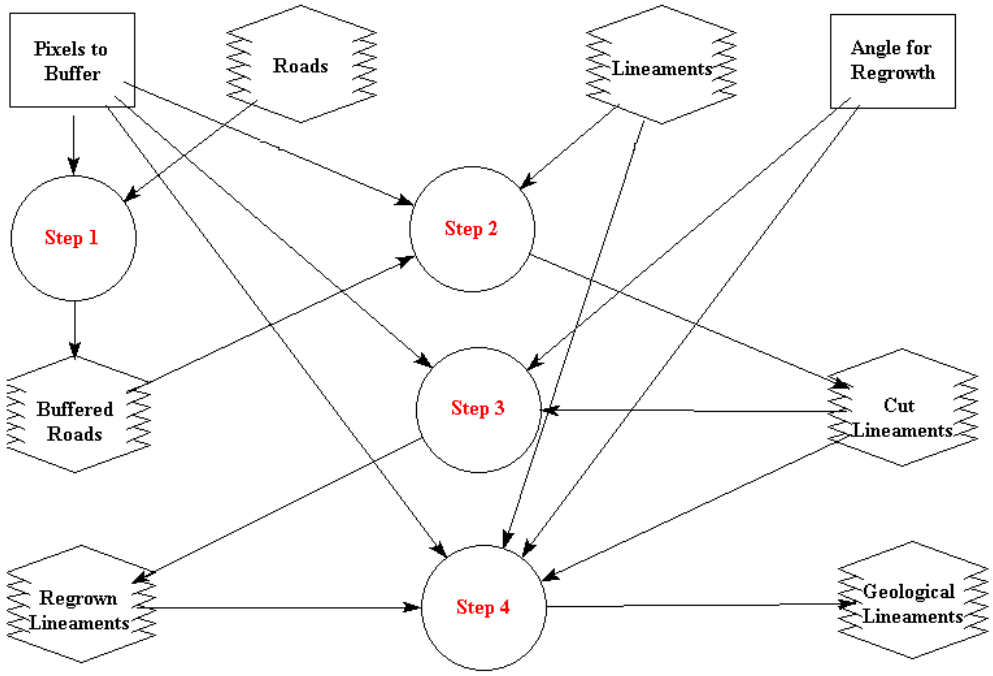

Figure 6: Flow diagram to show the development of the Erdas Spatial Model constructed to eliminate cultural lineaments. The arrows indicate the direction of which step is performed next. Step 1 is the buffering process, Step 2 is the removal of lineaments crossing the road buffers, Step 3 is the lineament regrowth based on the angle supplied, and Step 4 takes the changes from the original lineament file.

railroad, and not those that simply cross such features, another step is added. This step is a linear regrowth of lineament segments. The amount of pixel regrowth is based on the width of the buffer zone, and the maximum angle assumed to be associated with a subparallel relationship between the lineament and the road or railroad. The length of the regrowth is then calculated by simple geometric relationships: Buffer length (in pixels)/Sine of the maximum angle. Based on a number of empirical experiments with different angles, 20° was found to be an optimum maximum angle. Lineaments that are completely deleted are not regrown; roads that cross at high angles are reconnected and entirely restored (Figure 7).

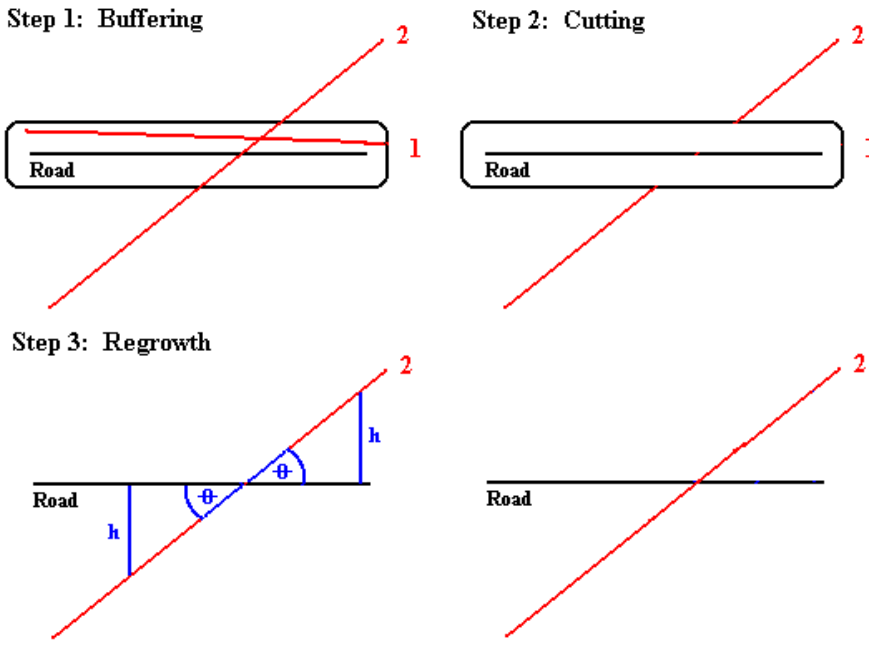

Figure 7: Conceptual diagram that depicts the processes involved in removing cultural lineaments (for example, Lineament 1 in red) and regrowing geological lineaments (for example, Lineament 2 in red). Regrowth is based on angular difference between the road and the lineament.

Once lineaments at angles greater than 20° are regrown, the model compares the original lineament file and the cut and regrown lineament file to generate a final lineament file. This final step is required to eliminate spurious regrowth into areas where no lineament was digitized. This occurs because no attempt is made during the regrowth to check if this lineament was cut in the buffer overlay step, instead all lineaments are regrown.

Many geological structures form ideal avenues for the construction of roads and railroads. In this regard, many cultural lineaments may actually overlay geological lineaments. The key to deciding whether a lineament should be removed because it represents only a cultural feature is provided by the DEM.

Rose Diagram Generation

Lineament patterns were summarized using rose diagrams (Figures 11, 13, 15, 17, 18) . When lineament processing was complete, the final "geological" lineament file was converted back to a vector format. This can be done in two different ways. The first way is to simply vectorize the final raster image using ARC functionality available through *Imagine*. This procedure was found to add pseudo nodes and consequently requires repeated "cleaning" and "building" in Arc/Info. The pseudo node problem was found to be greatest with large files, and thus the vectorization approach works best with smaller lineament files. The second method is to overlay the original lineament vector layer on the final lineament raster layer and manually delete those lineaments that were removed on the raster image. This method was used with the larger lineament files (Landsat and DEM derived) to avoid the pseudo node problem.

The ARC/Info UNGENERATE Command

Once the final lineament file was in vector format, the next step was to apply the Arc command, UNGENERATE, to the layer. This command gives coordinate values for each node associated with a particular lineament. The output coordinates are within the cartographic coordinate system of the original file and are in text format. This text file was then imported into Microsoft Excel where the data were reformatted and overall length and azimuth (0 to 180°) for each lineament calculated.

StereoNett Software

The StereoNett (Duyster, 1999) structural geology software has a spreadsheet database in which strike and dip of planar features or azimuth and plunge of lineaments can be entered and recognized. This software is free for academic uses, but a donation must be made for private sector use. For this study, 90° were added to each azimuth

angle to compensate for the difference between the 0° mark in Excel and the 0° mark in StereoNett. Next, a plunge value of 0° was added to each lineament along with an L to signify to the software that the structural feature was a lineament. Rose diagrams of the strike of these lineaments as well as frequency were generated. Each rose diagram displays frequency information in 7.5° intervals, and their results are fully analyzed later.

Automated Lineament Categorization

A central aim of this investigation was to study automated approaches in the categorization of lineaments. The DEM and the hydrology DLG data were used to stratify the lineaments into the classes of slope-break, valley, and ridge lineaments. The slope-break and the ridge-top information was obtained from the DEM. The valley information was obtained from the DLG. It is assumed that all river segments represent incised topographic lows and are thus valleys.

Slope-break Lineament Categorization

Slope breaks, or abrupt changes in topography, can in some cases represent faults or other structural features. An example of a surface profile associated with a fault is shown in Figure 8. Cultural lineaments often follow geological "avenues", such as valleys, as they are ideal passageways in rough terrain. Therefore, road-cuts associated with these cultural lineaments will be displayed as a slope-break in the DEM.

The DEM Information was used in the automated categorization of slope-break

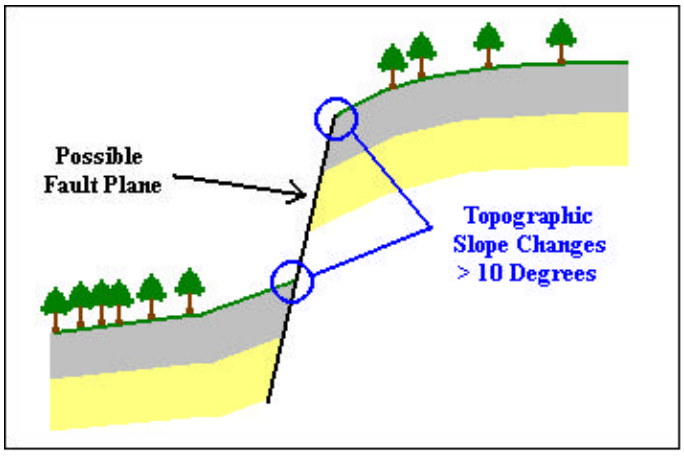

Figure 8: Schematic diagram of slope changes associated with a fault.

lineaments. Slope was calculated from the DEM data using the Erdas Imagine SLOPE program (Erdas, 1997). This program uses a 3 by 3 window to calculate average slope from pairs of pixels in the window. Srinivasan and Engel (1991) have pointed out this approach does not consider the center pixel, and may lead to inaccuracies in a landscape with numerous small pits or ridges. However, in this data set, the topography appears to be relatively smooth, and thus this was not considered a problem. The image produced by the *Imagine* SLOPE program has values ranging from 0-90°, representing flat terrain to sheer cliffs. Lineaments in the topographic and tonal anomalies and linear vegetation lineament files were categorized by direction using *Imagine* Spatial Models. Sixteen directions, which on average represent intervals of 11.25°, were identified. This directional lineament file, as well as the slope file, was used in another model that checked the difference in slope on each side of the lineament. The model selected a matrix that was elongate in a perpendicular direction to the lineament to quantify the difference in slope on either side of the lineament. If the value in slope difference across a lineament in the resulting image was over 10° across a 90-meter swath, then the lineament was assumed to represent a structural slope break, and was stored in a separate file. The value of 10° was chosen after finding less success of classification with higher angles.

Ridge-top Lineament Categorization

Another very important category of lineaments that can be identified through automated feature extraction is that of ridge-top lineaments, or any positive topographic feature. The DEM is the source of information for the categorization of these lineaments, as was the case with slope-break categorization. Thus the first step in the two programs is very similar. Using the Spatial Modeler in Erdas *Imagine*, a program was designed to identify the average direction of lineament intervals. Each lineament pixel was assigned a value ranging from 1 to 16, based on 11.25° angular increments from 0-180°, by evaluating the lineament direction in a 9 x 9 window. In the next process, a 9 x 9 matrix, with zero in all matrix cells except in a direction perpendicular to the lineament, was selected and the mean value of that matrix is calculated. In this way the mean value of a linear profile perpendicular to the lineament is determined from the DEM and assigned to

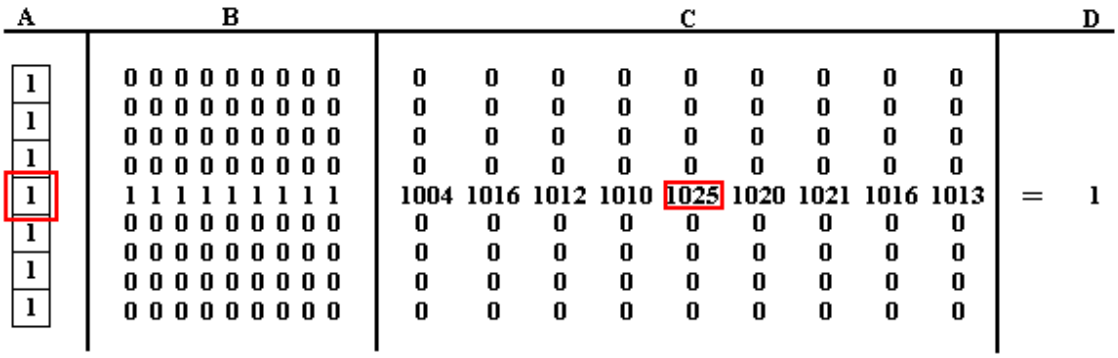

Figure 9: Diagram showing step-wise process of ridge categorization. Step A identifies the direction of the lineament pixel (vertical in this case). In step B, a matrix is selected that has non-zero values perpendicular to the lineament direction. Step C shows example results after passing the matrix over the coincident DEM values for the particular lineament. In this example, the center pixel of 1025 meters is greater than the mean of the perpendicular row (1015 meters). Therefore that pixel is coded as 1 in Step D, signifying a ridge-top.

the pixel location on that lineament (Figure 9). This mean value was then compared to the elevation of the original lineament pixel, which is located at the center of the matrix. If the center pixel of the DEM was greater than that of the mean value for the 9 x 9 matrix, then it was labeled as a ridge-top, or other positive topographic feature, and assigned a value of 1. If the center pixel was less than the mean value of the 9 x 9 matrix, then it was coded as non-ridgetop, or 0.

Valley Lineament Categorization

Lineaments associated with linearly arranged topographic valleys do not necessarily have to be categorized from the DEM, because the hydrology files from the DLG represent a very reliable source of rivers, and by inference, river valleys. The categorization method for valley lineaments was modified from the cultural lineament extraction method. The first step in this process was to give a four-pixel buffer around each river or stream. The assumption is that rivers and streams form the center of valleys. This is generally more valid for narrow, deep valleys characterized by downcutting than broad valleys with meandering streams. In the study area meandering rivers are not common. The *Imagine* buffering routine outputs a series of coded rings around the buffered object, in this case a stream. For example, with a four-pixel buffer zone, the stream itself is coded as 0, the first buffer zone is coded 1, the second buffer is

coded 2, the third buffer is coded as 3, the fourth is coded as 4, and everything else is given a value of 5. This buffered image was modified in the valley lineament analysis so that the stream itself was also coded as 1, and everything coded as 5 (i.e. more than 4 pixels from a river) was recoded 0. The buffered hydrology files were then multiplied with the lineament files. The lineament files are coded such that a pixel belonging to a lineament is 1 and the background 0. All values greater than 0 in the product image would therefore be lineaments, or lineament segments that were mapped as linear topographic valleys.

Those lineaments that cross valleys in a perpendicular, or near perpendicular, direction would also, in this case, be considered as valley lineaments. The importance to this is that most lineaments identified in this study appeared as more than one class. For example, a lineament may be identified initially as a slope-break, but one segment of the same lineament may appear to be the controlling factor of a valley.

Chapter 4: Lineament Classification Results

Results of Lineament Identification from all Data Sets

Many lineament studies tend to involve identification from one main data source (Slack, 1981, and Marrs and Raines, 1984). Also consistent with these studies is the consideration of all identified lineaments as equal, regardless of the various ways in which they might appear on the data set being used. However, in this work, lineaments were identified from multiple data sets, including Landsat TM imagery, DEMs and DLG data. Lineaments were divided into different classes, such as topographic or vegetation lineaments. Different lineament classes potentially reflect different types of structural features, and therefore may show different patterns. The next sections of this chapter discuss the lineaments in the following groups: the topographic lineaments and linear tonal anomalies and vegetation patterns from the Landsat TM image; the lineaments identified from the DEM; and the linear drainage anomalies from the DLG. The following table illustrates the data source used in the identification of each lineament class.

Table 2: Data Sources for Lineament Identification.

Landsat TM Image	**DEM (30 m intervals)**	**DLG Hydrology Files**
Topographic Lineaments	DEM Lineaments	Drainage Anomalies
Tonal Anomalies and Linear Vegetation		

Topographic Lineaments Derived from the Landsat Image

Many types of surficial geological features contributed to the identification of the topographic lineaments. These structures include ridges, valleys, faults, fractures, rock unit contacts, vertical beds, or alignment of two or more of the above. The overlay of the DLG cultural features over the topographic lineaments indicated that some lineaments were cultural in origin. The most common cultural features mapped as lineaments were found to be small road or railroad cuts in mountainous areas. These were successfully

removed from the final lineament data through the cultural lineament elimination process. A map of the final topographic lineament class is shown in Figure 10.

The rose diagram created from these lineaments (Figure 11) shows the highest occurrence of lineaments in a east-west orientation. The largest of the 7.5° petals

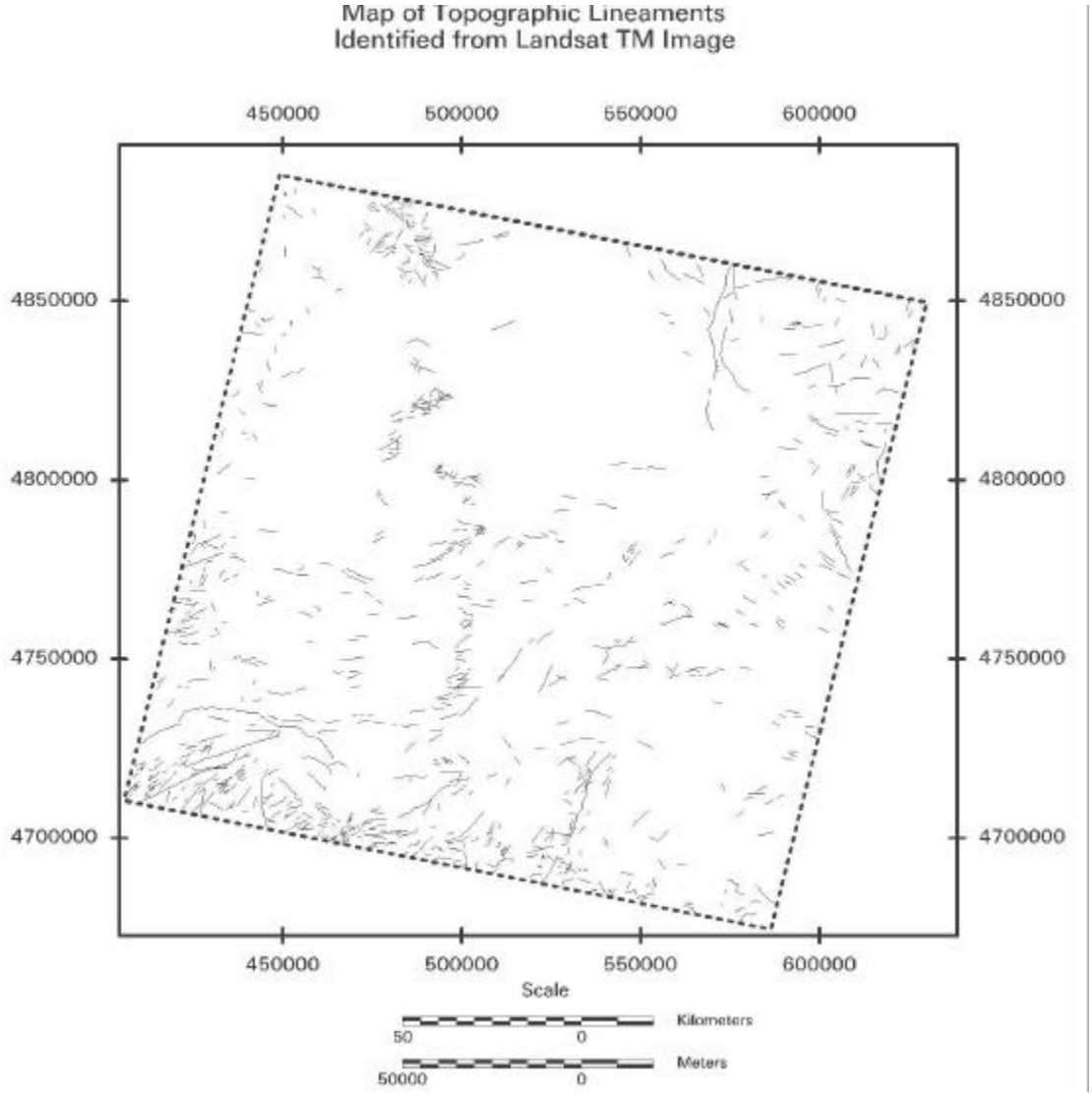

Figure 10: Map showing the locations of the Topographic Lineaments. Coordinate system is UTM Zone 13.

represents 74 lineaments, or 7% of the 970 total. This primary east-west trend is bracketed by a broad trend of lineaments oriented between 60° and 120°. Of particular interest is the suggestion of a conjugate set of northwest-southeast and northeast-southwest lineaments. There are very few lineaments that trend north-south.

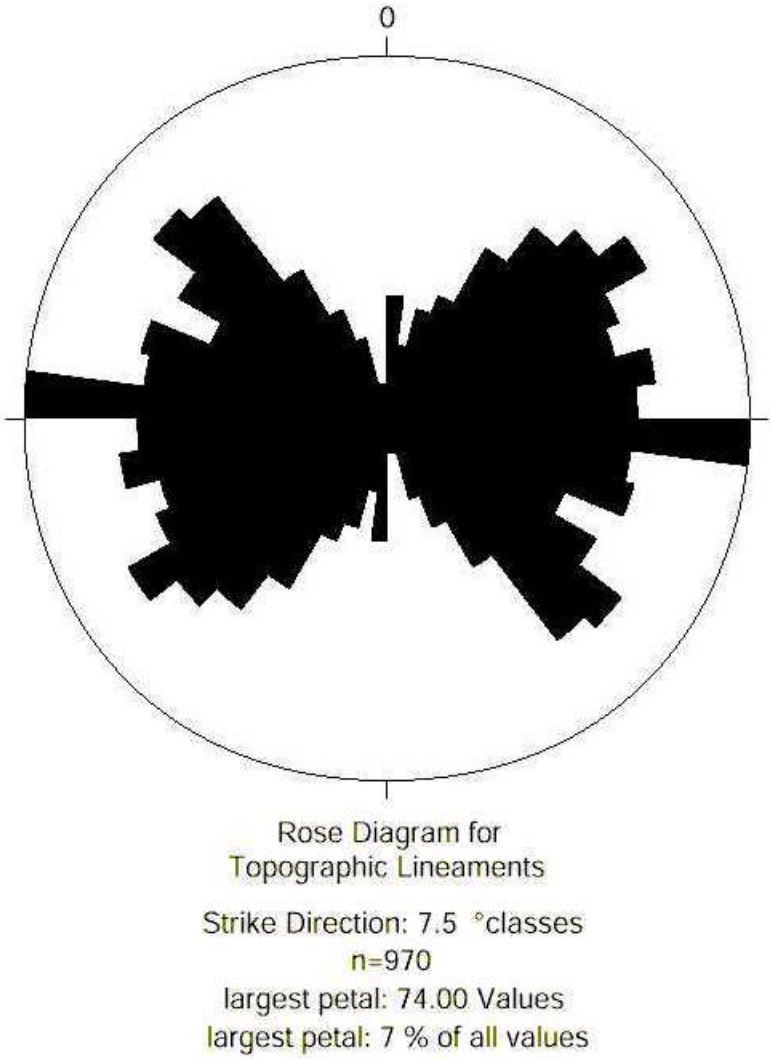

Figure 11: Rose diagram for the Topographic Lineaments.

Linear Tonal Anomalies and Vegetation Lineaments Derived from the Landsat Image

The most common lineaments identified in the linear tonal anomalies and vegetation class were those of linear vegetation patterns. In this semi-arid region, vegetation growing in a linear fashion was easily seen in the standard false color composite image, in which near-IR is displayed as red. The faults and fractures in the mountainous regions within the field area, the Black Hills and the northern Laramie Range, were the most common places where linear vegetation growth patterns were observed. Cultural lineament removal was not found to be necessary with the linear

vegetation class; however, it was an important step with the linear tonal anomalies. The overlay with cultural features indicated that many rural or unpaved roads were accidentally classified as tonal anomalies. This region of the Powder River Basin has many unpaved roads, as not only is it a major farming area of the U.S., but also a major hydrocarbon producer. The dirt roads that run between oil well pads in the larger oil fields follow a grid pattern that is very easily confused with linear tonal anomalies. Fortunately, the DLG road files included minor roads between the well pads, and thus were effective for removing lineaments that paralleled these roads. The resulting map of the linear tonal anomalies and vegetation lineaments can be seen in Figure 12.

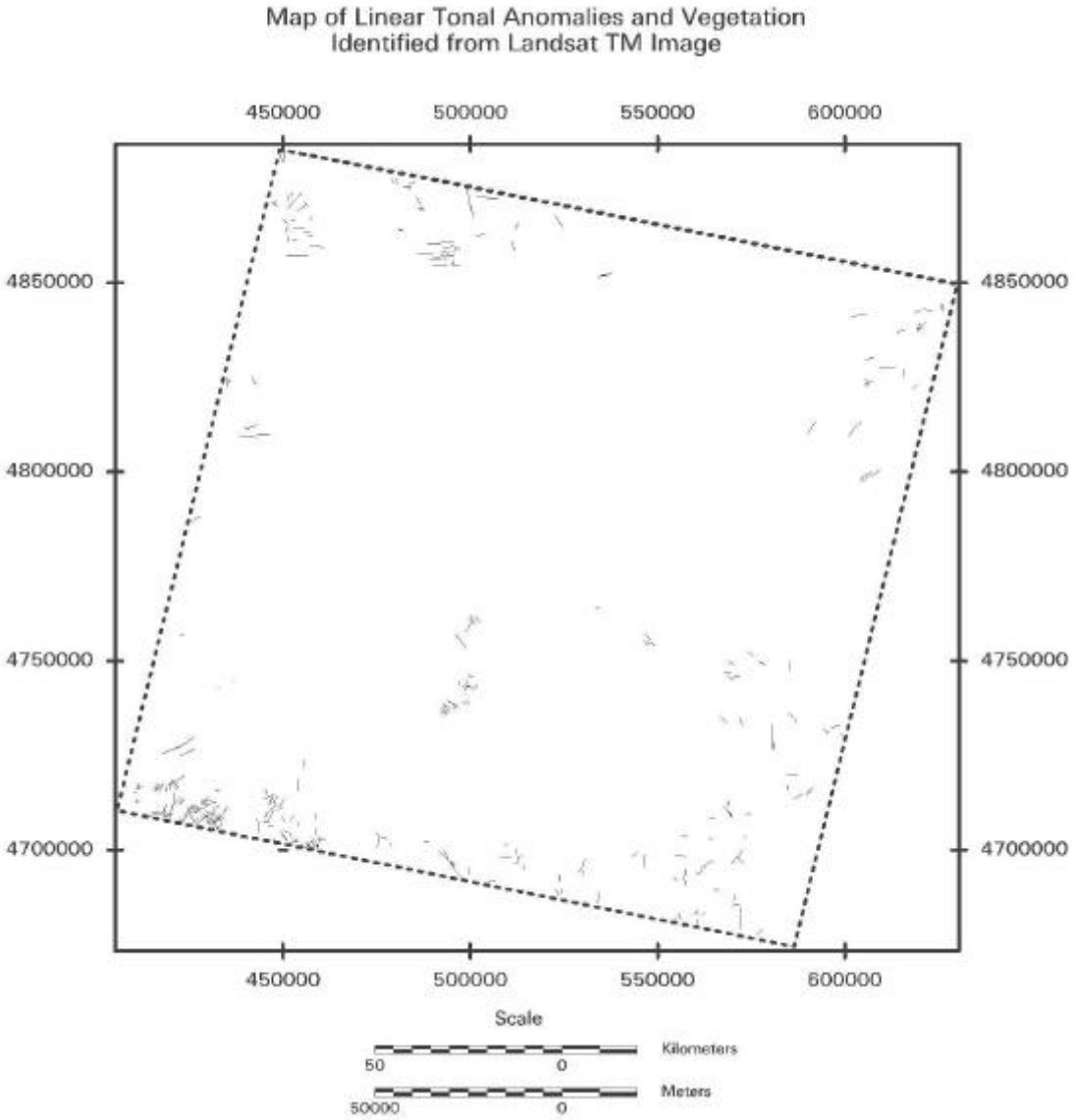

Figure 12: Map showing the locations of the Linear Tonal Anomalies and Vegetation Lineaments.

From analysis of the rose diagram for this class of lineaments (Figure 13), the largest petal trends east-west and represents 8%, or 26 lineaments, out of a total of 310 lineaments. This petal appears isolated from the rest of the major petals, which mostly trend northeast-southwest at approximately 45°. Another noteworthy, but isolated petal is one that trends northwest-southeast at approximately -40°. This isolated petal could possibly represent a conjugate set of fractures to the northwest-southeast lineaments. The last major lineament trend seen in this diagram is that of near north-south orientation. This could possibly represent another set of lineaments complementary to the east-west lineaments.

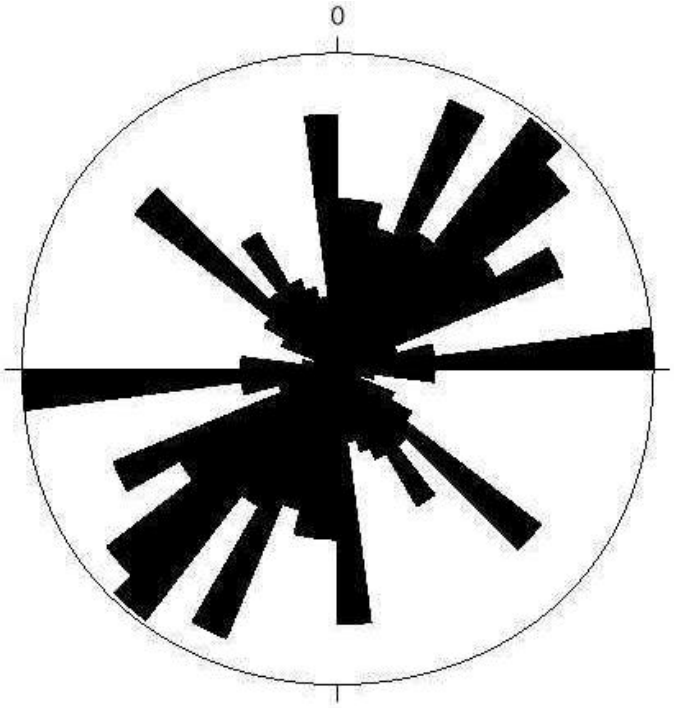

Figure 13: Rose diagram for the Linear Tonal Anomalies and Vegetation Lineaments.

Lineaments Identified from the DEM

The lineaments obtained from the DEM were identified from two shaded relief images with a solar azimuth of 225° and 315° respectively. The two lineament interpretations were subsequently combined to form a single lineament map (Figure 14). These lineaments are strictly topographic and most commonly represent breaks in slope, as these are perhaps the easiest topographic features to observe on the DEM. These

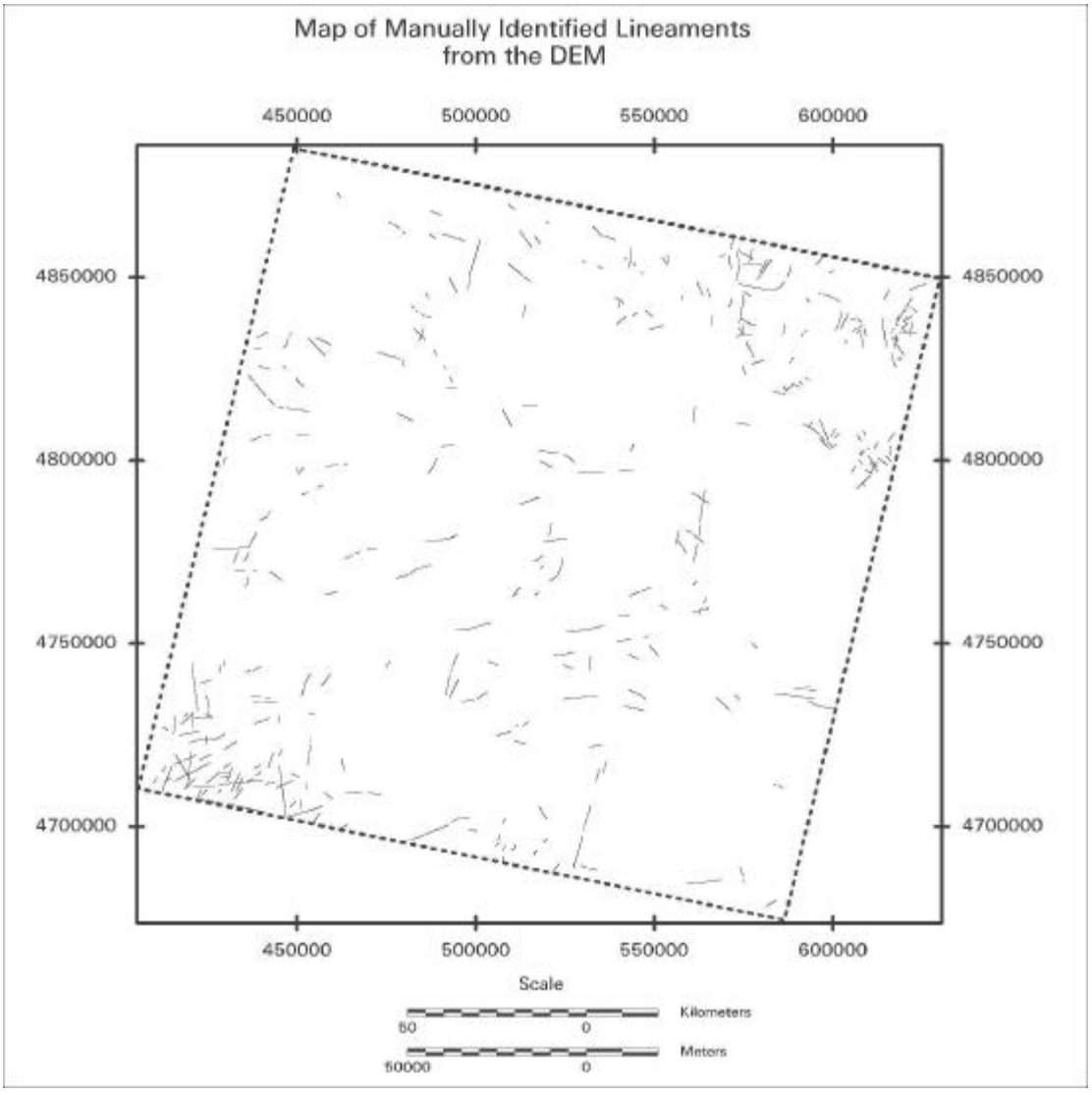

Figure 14: Map showing the locations of DEM Lineaments.

breaks in slope are commonly sharp ridges or steep valleys that create a linear profile in the shaded relief image. Elimination of cultural lineaments from this lineament file posed an interesting dilemma. Road cuts tend to be displayed in the shaded relief image as linear features, as they are, in essence, slope-breaks. If these roads were either deliberately or accidentally sited along geological "avenues," such as faults or fractures, then the associated lineaments should not be removed. Adding to the complexity of the interpretation, there were several cases in which portions of lineaments were removed because they were associated with cultural features. The remaining sections of these lineaments did not overlay roads or railroads. In this event, that particular road may have followed a geological lineament.

The rose diagram for these lineaments (Figure 15) shows the major petal oriented northeast-southwest at 45°. This major petal represents 8%, or 28 lineaments out of 338. This same northwest-southeast orientation is strongly followed by the majority of the lineaments, as is indicated by the number of petals in the northeast and southwest

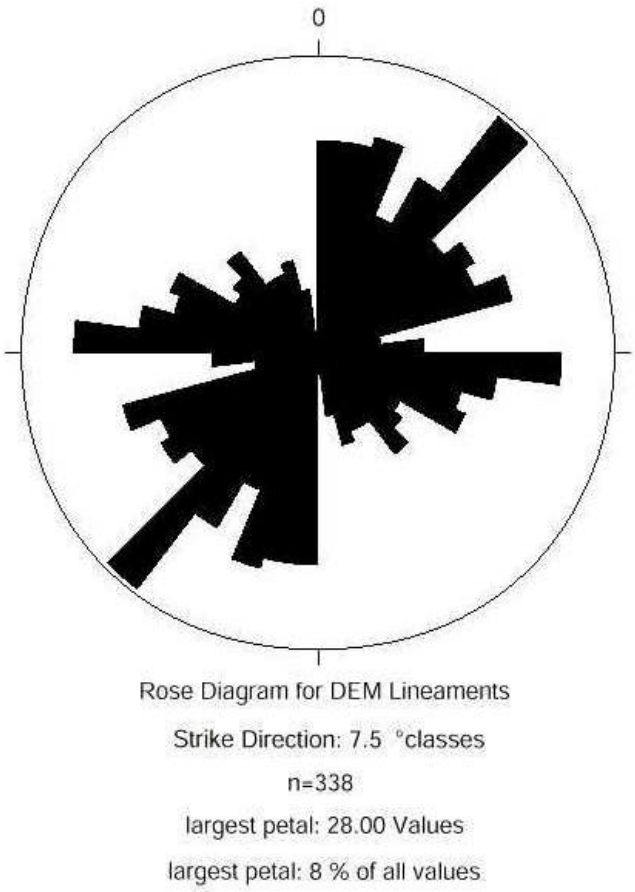

Figure 15: Rose diagram for the DEM Lineaments.

quadrants. Another major trend direction indicated by the petal orientation is approximately east-west. By comparison, very few lineaments trend northwest-southeast.

Drainage Anomalies

Linear drainage anomalies were mapped from the hydrology information files in the DLG (Figure 16). Any abnormal linear change in an established drainage pattern was digitized as a drainage anomaly. The anomalies were often aligned with anomalies in other streams. Under the assumption that roads or railroads would not interfere with

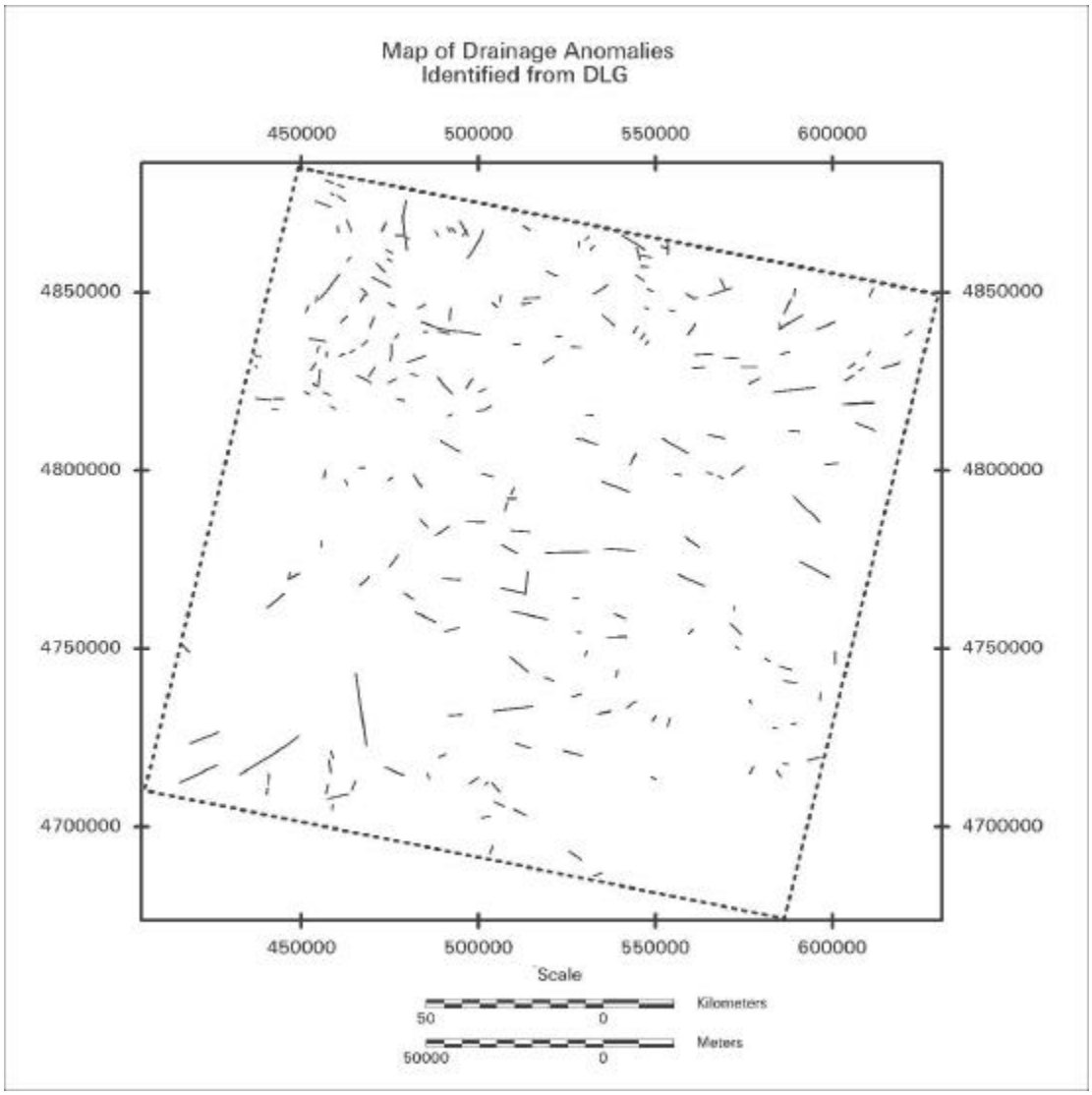

Figure 16: Map showing the locations of the Drainage Anomalies.

drainage flow appreciably, these lineaments were not treated to the cultural lineament removal process.

The rose diagram for these lineaments (Figure 17) shows a major petal trending east-northeast at approximately 70°. This petal represents 11%, or 24 lineaments out of a total of 203. A second important orientation in this diagram is east-west. All other trends are relatively minor.

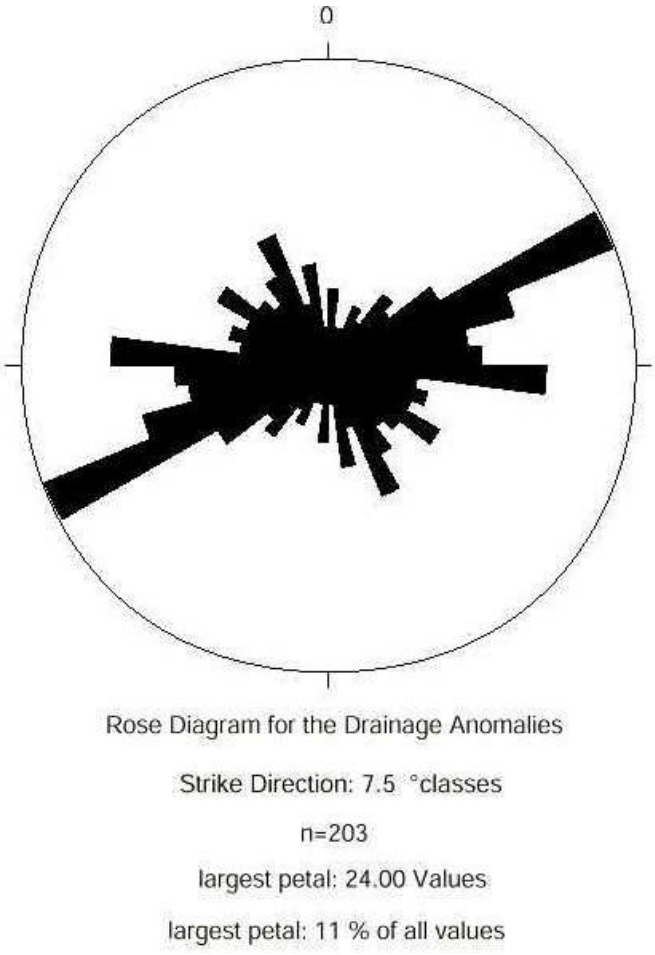

Figure 17: Rose diagram for the Drainage Anomalies.

Comparison of Manually Classified Lineaments to Combined Lineament Dataset

A central focus of this investigation is to evaluate the importance of the classification of lineaments compared to an approach that considers all lineaments of equal value. A rose diagram was therefore created from a dataset produced by combining

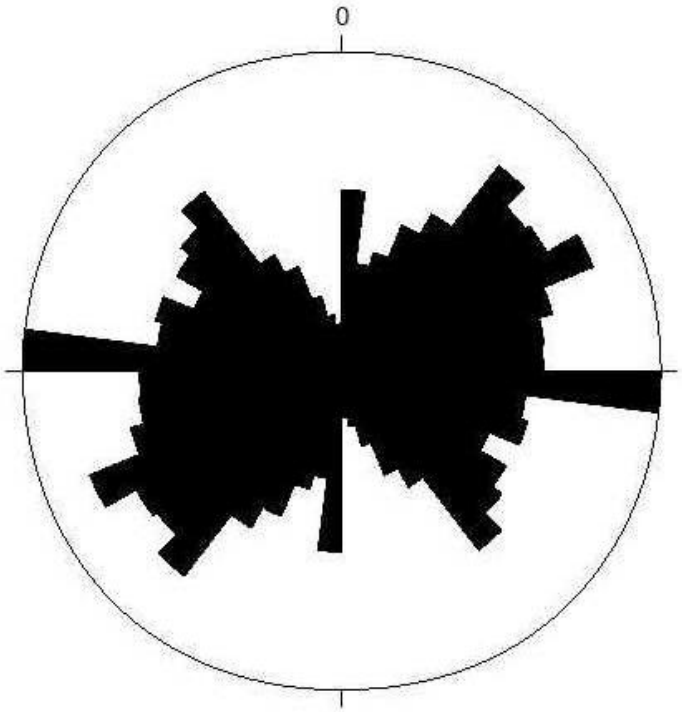

Figure 18: Rose diagram for all combined lineaments.

all the lineaments from the Landsat, DEM and DLG sources (Figure 18). The rose diagram shows a major east-west trending petal with 7%, or 136, of the 1821 lineaments. This petal, however, is mostly isolated. The majority of the petals lie between 45° and 135° with a slight majority trending northeast-southwest. Another isolated petal trends north-south. Use of this diagram alone for determining the dominant trend direction would not show the details of the trends of the individual coverages – especially in the important northwest and northeast trend directions. Furthermore, lineament orientations identified from rose diagrams from separate classes of lineaments may shed some light on the history and origins of those lineaments that otherwise could not be extracted from a rose diagram of all lineaments. This is significant as one class of lineaments may be the major controlling factor in the location of hydrocarbon reservoirs.

Relationship of Lineament Trends to Previous Works

The major trends of all the combined lineaments within this study are in four main directions (Figure 18). There is a major east-west trend followed by these lineaments along with subsidiary northeast-southwest and northwest-southeast trends, possibly representing conjugate fracture sets, and a small amount following a north-south trend. Of particular interest is how these trends relate to the major trend directions identified from previous works in the Powder River Basin, specifically Slack (1981) and Marrs and Raines (1984).

Slack (1981) identified major linear trend directions from offsets seen topographically and in the Black Hills Monocline (Figure 19a). He related these linear trends to the Belle Fourche Arch, which is a very subtle and broad northeast trending structure just north of the area of interest for this study. The only linear trends that continue into the study area are the Fiddler Creek and Clareton Trend (marked FC and CT in Figure 19a). Evidence for these two linear trends continuing further into the field area can possibly be indicated by two relatively large northeast magnetic trends seen in the magnetic data in Figure 36. If these trends are, in fact, viable in the field area, then it may be that the secondary northeasterly trend seen in this study coincide with the Fiddler Creek and Clareton Trend.

The major northeast and northwest lineament trends mapped out by Marrs and Raines (1984) from Landsat imagery using concentration and direction statistics can be seen in Figure 19b. The Natrona/Ross trend may actually be a continuation of Slack's Fiddler Creek trend and does coincide with northeast-trending magnetic highs in Figure 36. Other trends that extend into the field area are the Arminto/Upton, Casper/Bill, Orpha/Redbird, and the northwest-trending Buffalo/Douglas. The northeast trends seen obtained from their investigation may very well correspond to the reoccurrence of northeast trends seen in the rose diagrams for all classes of lineaments in this study Figures 11, 13, 15, 17, and 18). Therefore, it seems that there is good correlation between the studies of lineament trends in the northeast direction. Furthermore, the Buffalo/Douglas trend may coincide with northwest trends seen in the Landsat-derived lineaments and the drainage anomalies (Figures 11, 13, and 17).

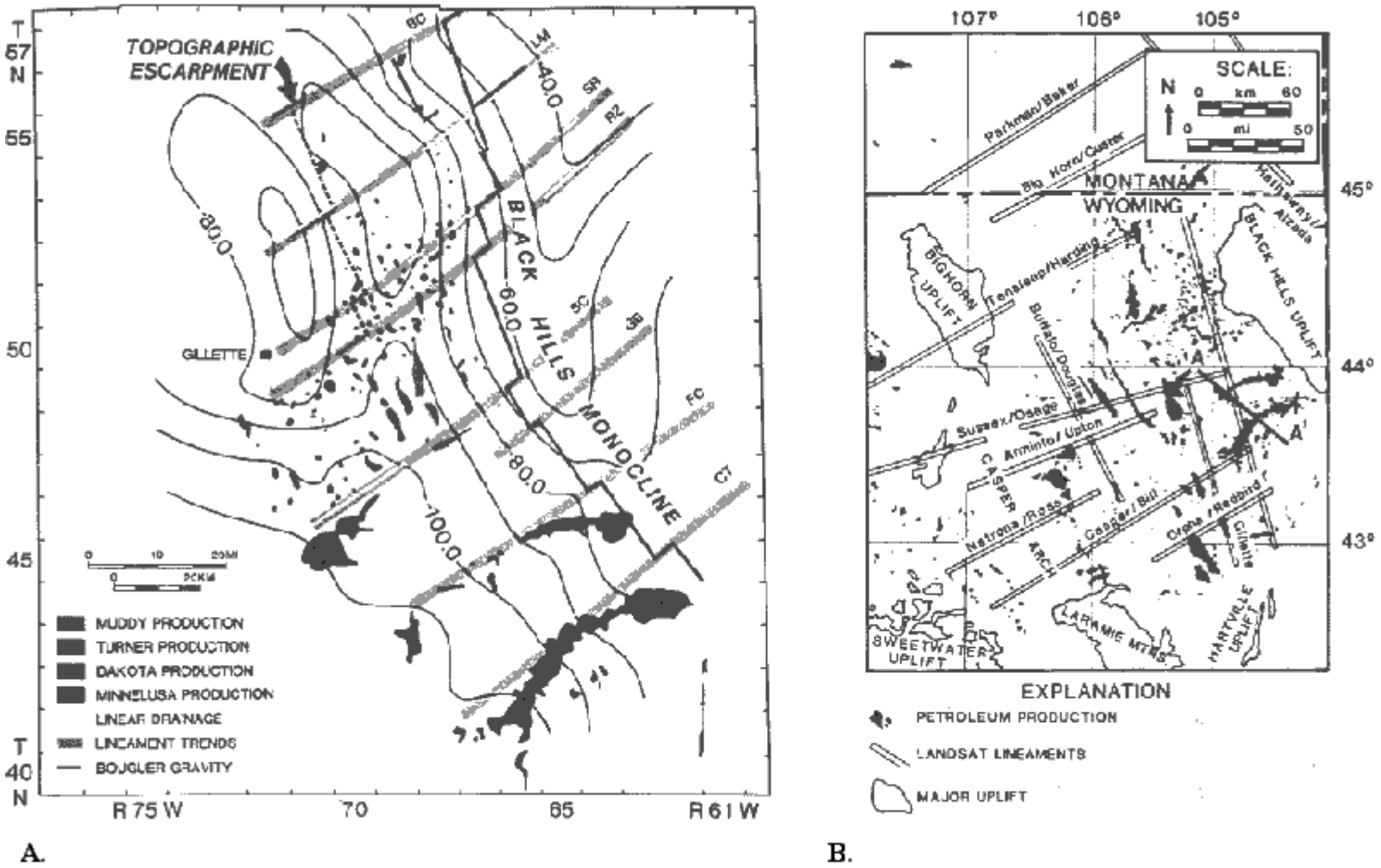

: Lineaments trends from previous works. A) Major lineament trends from Slack (1981) overlain onBouger gravity data. B) Marrs and Raines (1984).

Results of Automated Lineament Categorization from DEM and DLG

Manual lineament classification can oftentimes be very time consuming and adds subjectivity to the process. There were several cases in this investigation in which manual classification was difficult, especially in situations where a lineament could be assigned to more than one class. Automated lineament categorization of already digitized lineaments by topographic characteristics may alleviate this problem. Automated categorization can be based on topographic classes generated from DLG and DEM data, such as slope-breaks, ridge-tops and river valleys. This procedure was applied to the combined lineament data set discussed in the previous section.

Slope-Break Lineament Classification from DEM

Lineaments belonging to the topographic and tonal anomalies and linear vegetation patterns classes, and also associated with topographic breaks in slope over 10°, were identified from the DEM data. Slope-breaks are very important topographic features because faults are commonly characterized by changes of surface slope. The lineaments with a difference in slope greater than 10° on either side of the lineament are shown in Figure 20. This 10° mark appeared to be the most effective for slope-break analysis from comparison with those of lesser angles. There appeared to be no change in the resulting slope-break lineament images where less than 10° was used. The resulting image of slope-break lineaments was overlain onto the DEM for an evaluation of the accuracy. All lineaments checked against the DEM slope information were found to be indeed associated with slope changes greater than 10°. The automatic slope categorization is done on a pixel by pixel basis, and not on an individual lineament basis. Consequently in most cases it was only parts of lineaments that were identified as being associated with slope breaks. This suggests that most lineaments were associated with more than one topographic expression, or the 10° minimum slope change was too high.

From analysis of the original lineament maps, it appears that most of the slope-break lineaments belonged to those originally assigned to the topographic class of lineaments. This is expected, as there were many more topographic lineaments. Slope-break lineaments represent only a small portion of the total topographic lineaments,

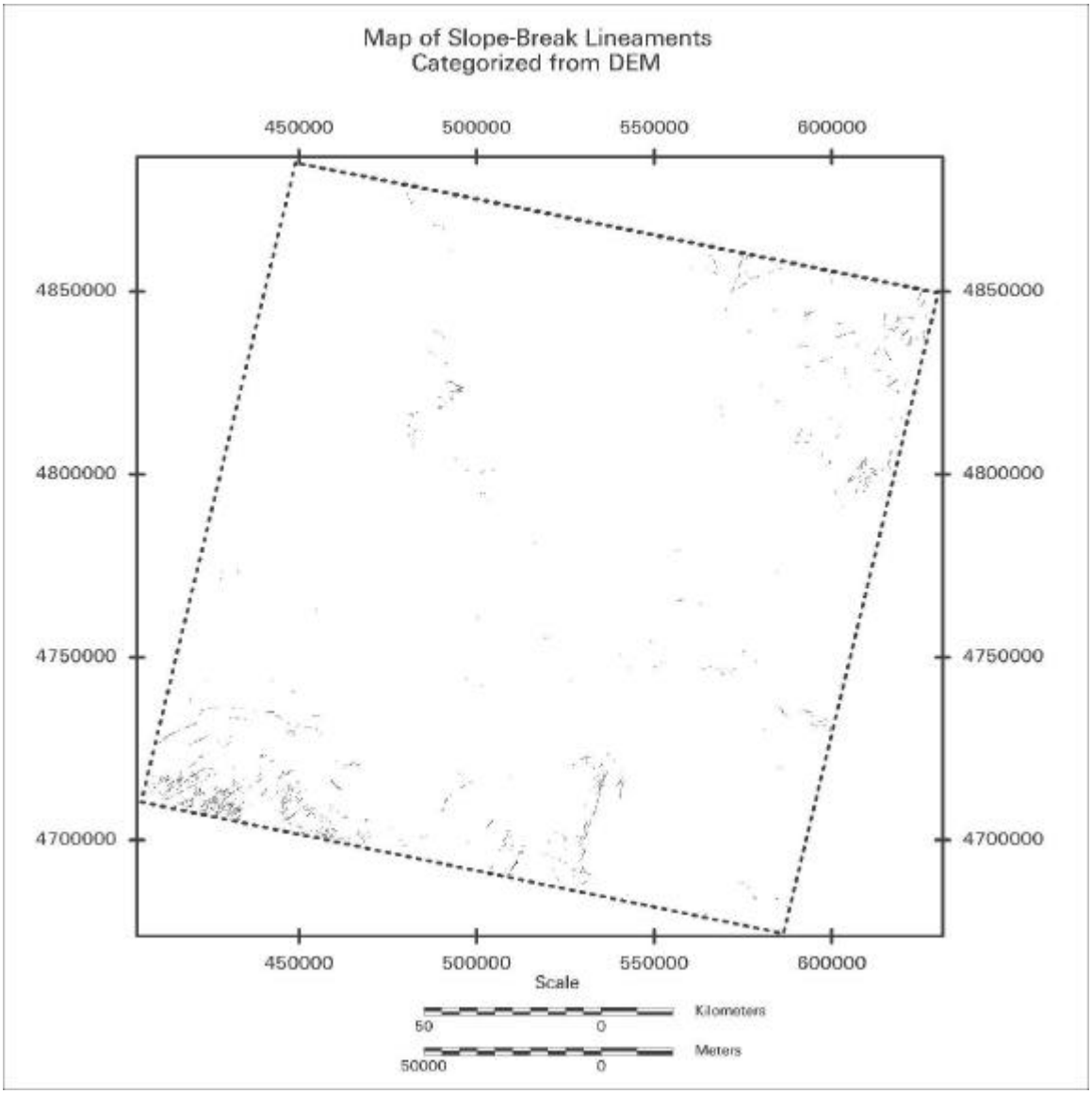

Figure 20: Map showing the locations of the slope-break lineaments.

however. Common occurrences of topographic slope-break lineaments appear to be prevalent in mountainous areas, such as the northern Laramie Range and the Black Hills, where extreme changes in slope are expected. In fact, a portion of the major east-west trending front range fault of the northern Laramie Range was successfully classified as a slope-break lineament.

Slightly less than half of the linear tonal anomalies and vegetation lineaments were classified as slope-breaks. The significance of this may be that geomorphic features that show linear tonal change, such as escarpments, are common slope-break

representations of lineaments. Therefore, the value of evaluating linear tonal anomalies as slope-breaks seems to be high.

Ridge-Top Lineament Classification from DEM

DEM information was used to automatically identify ridge-top lineaments in the Landsat and DEM-derived lineaments (Figure 21). Lineament pixels were classified as ridge-tops if their elevation value was higher than the mean elevation values of a

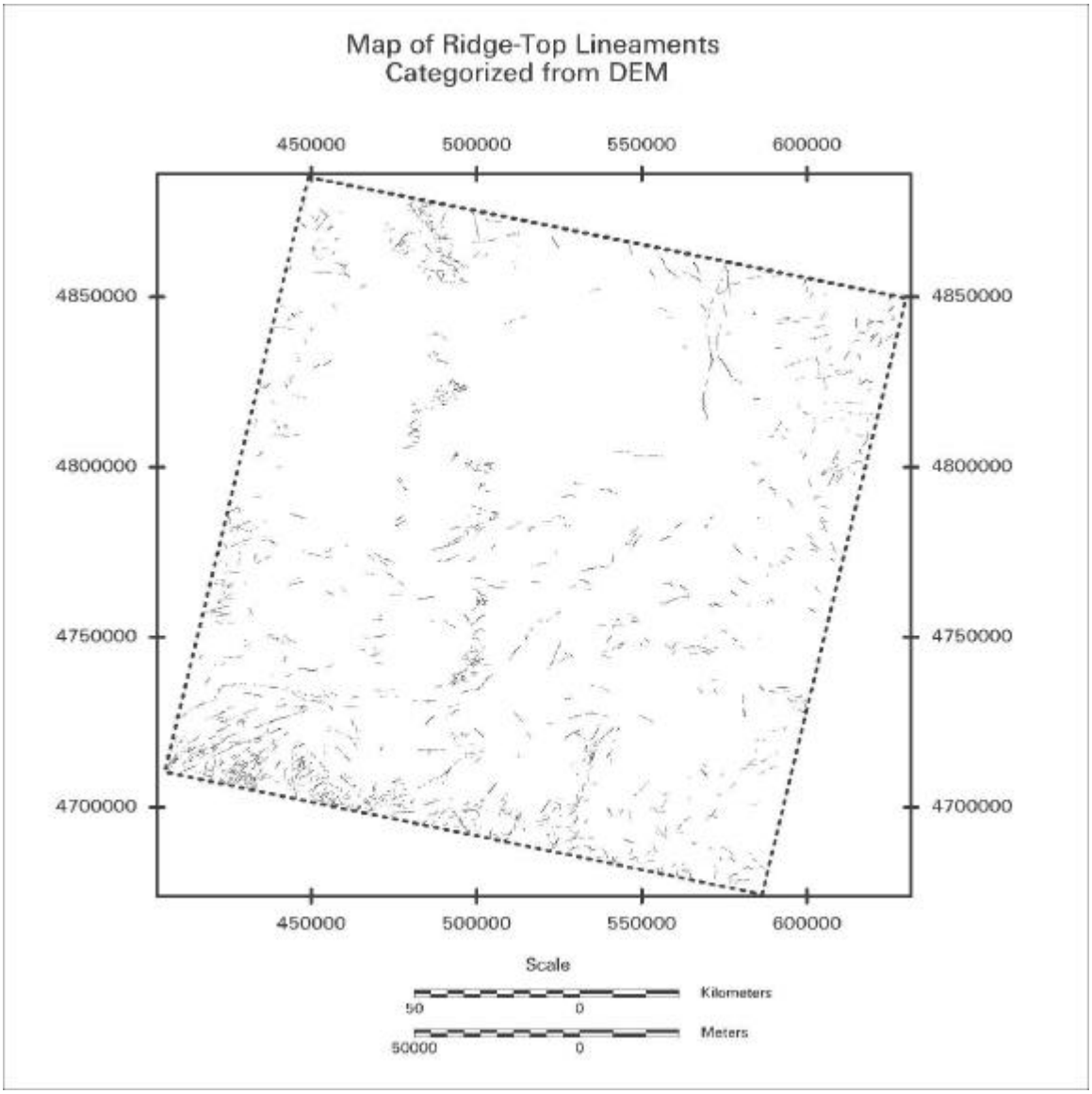

Figure 21: Map showing the locations of the Ridge-Top Lineaments.

perpendicular matrix. The vast majority of the topographic lineaments were categorized as ridge-top lineaments. This is expected, as the most common manually identified topographic lineaments were linearly aligned ridges.

The categorized lineaments were overlain onto the DEM for accuracy analysis. A close inspection of the ridge top lineaments overlain on the DEM suggests that the categorization is very accurate. As with the slope-break lineaments, the ridge-top lineaments appear somewhat segmented because lineaments did not consistently follow ridge lines.

The linear tonal anomalies identified on the Landsat image included crests of barren ridges that are linear in shape. Not many barren ridge-tops were present in the Landsat image. Therefore, a number of the manually identified linear tonal anomalies and vegetation lineaments were automatically categorized as ridge-top lineaments. Thus automatic categorization of the linear tonal anomalies and vegetation lineaments can be an important step if barren ridges are not dominant in the field area.

Valley Lineament Classification from DLG

The hydrology data within the DLG files were used to identify the lineaments, or segments of lineaments, that were associated with valleys in topographic lineaments and the linear tonal anomalies and vegetation lineaments (Figure 22). The procedure is based on the assumption that the stream location gives a good representation of the shape of the valley. This assumption should be reasonably appropriate in mountainous areas where downcutting streams and steep valleys are more prevalent.

Many of the lineaments automatically classified as valley lineaments appear to be highly segmented (Figure 22). This is a result of the fact that lineaments that cross the valleys at 90° to the valleys were not excluded. These segments were kept in the valley lineament data set in order to investigate whether they controlled small linear changes in the valley. In this regard, a lineament may be categorized as a slope-break in one portion, but as a valley in another.

Slightly less than half of all the topographic lineaments were categorized as valley lineaments. In the original manual mapping of topographic lineaments, there were many

linear valleys, or aligned valleys, which were identified. Therefore the high number of lineaments categorized as valleys is not surprising.

Most of the lineaments belonging to the linear tonal anomalies and vegetation class were categorized as valleys. The valley lineaments were overlain onto the Landsat

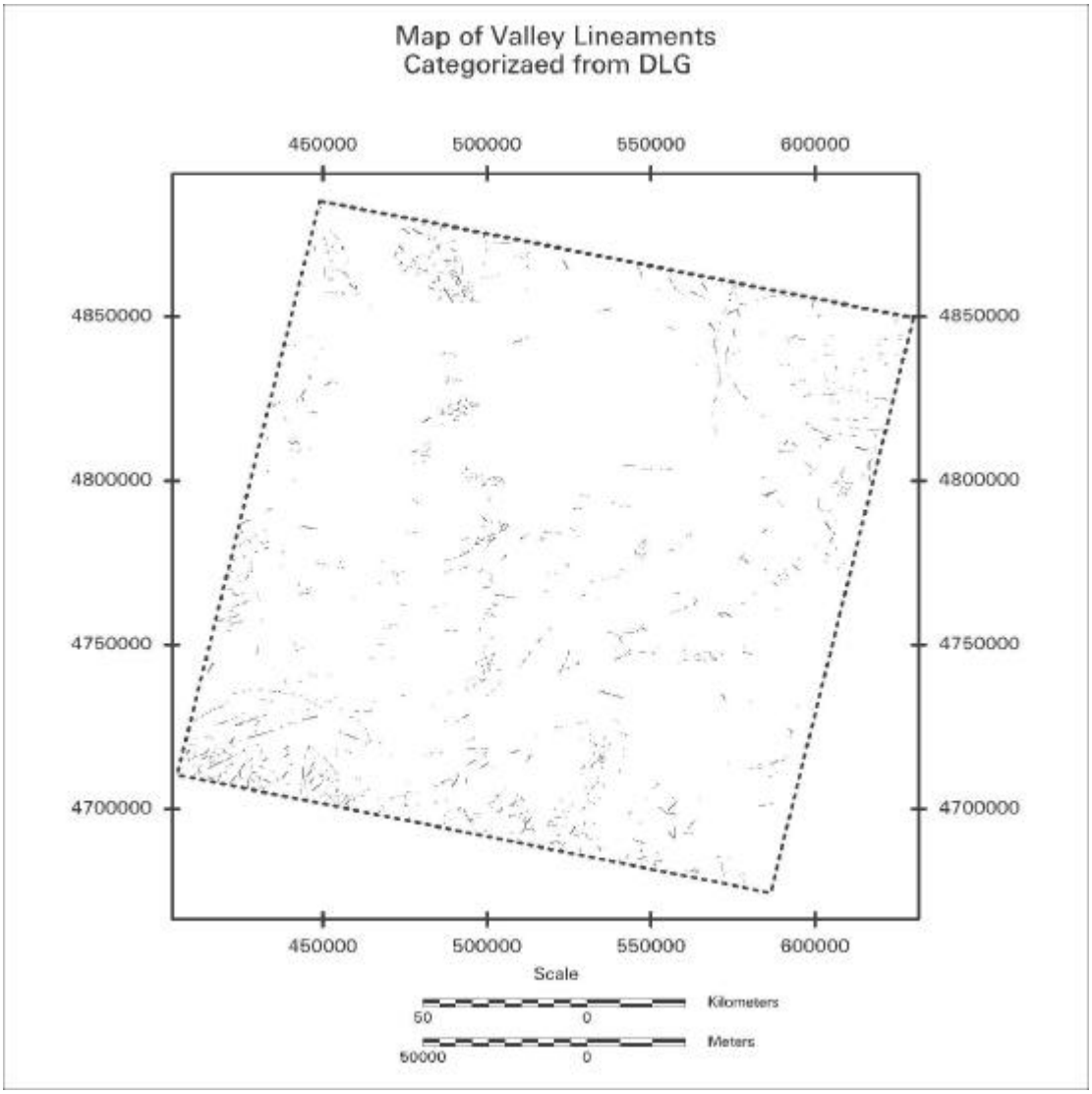

Figure 22: Map showing the locations of the Valley Lineaments.

image to try to understand this association. A strong correspondence between the valley lineaments and the linear patterns of vegetation was found. Relatively abundant green vegetation is one of the main characteristics of river valleys in semi-arid regions. However, a linear growth of vegetation may also represent faults and fractures, as water

is more abundant in those areas. Therefore, categorizing this class of lineaments appears to be valuable in regions having a semi-arid steppe climate.

Summary of Automated Categorization

The automated approach to categorizing, and thus stratifying, lineaments based on their topographic characteristics is very important. In areas where the structural geology and geomorphology is relatively understood, further categorization of lineaments could prove to be very useful. For example, valley lineaments may be more important in areas where subsurface salt tectonics, and subsequent drainage anomalies, are common. Lineament categorization can also be very important in flat drainage areas like the Mississippi valley region. In such an area, slope-break lineaments may be the considered the most important as there are very few solid rock outcrops where faults and fractures are exposed.

In this investigation, automated categorization was found to be very accurate. When all categorized lineaments were added together and compared with the original manually derived lineaments, very few segments were left unclassified. Those unclassified lineaments could represent random linear patterns of vegetation or perhaps rural roads not included in the DLG information. The majority of the topographic lineaments were categorized as ridge-top and valley, and only a relatively minor proportion was associated with the slope-break class. Slope-break topographic lineaments were only common in the mountainous areas. Most lineaments belonging to the linear tonal anomalies and vegetation were classified as either valleys, from the common occurrence of linear vegetation patterns in intermontane valleys, or slope-breaks, associated with the presence of escarpments near the edges of mountainous areas.

Lineament categorization was also valuable in the categorization of the linear tonal anomalies and vegetation lineaments. This categorization led to the identification of such geomorphologic features as escarpments.

Chapter 5: Structural Significance from Lineament Results

Implied Origins and Timing of Lineaments

The Powder River Basin developed much of its present geometry during the Laramide Orogeny, which took place in Late Cretaceous to Early Tertiary time (Robbins, 1993). The Laramide Orogeny consisted of a counterclockwise rotation of compressional stress (Gries, 1983). It may be assumed that many of the surficial lineaments identified from the Landsat TM image, DEM and DLG should follow trends associated with Tertiary tectonism. By relating known and unknown subsurface structural features, as seen from gravity and magnetic geophysical maps as well as subsurface structure maps, with the locations of the identified lineaments, credibility can be given to certain types of lineaments. Therefore, certain types of lineaments may be identified as better indicators of subsurface structure. Also, the orientations of these lineaments are important as they may infer an approximate timing of their formation.

Topographic Lineaments

The topographic lineaments identified from Landsat imagery were overlain on USGS total intensity gravity data (2 km spacing), USGS total intensity magnetic data (2 km spacing), and NEWMAG™ high-resolution residual magnetic data (0.8-1.6 km spacing) (Appendix A). Also, comparisons were made with a detailed subsurface structure map of the Dakota Formation. Gravity highs are generally assumed to represent positive basement structure, where there is an increase in denser rocks closer to the surface. Errors could result in interpretation of gravity data where very dense sedimentary packages of rocks are present. Magnetic highs are slightly different, and perhaps more reliable, as they reflect the abundance of magnetic minerals in rocks below the earth's surface. The higher the basement structure, the higher the magnetic reading, if there is homogeneity in the magnetic concentration. Possible errors in interpretations can be encountered when there are intrusions of mafic or ultramafic rocks. These rocks contain much more magnetic minerals and thus give the appearance that they are closer to

the surface. Furthermore, gravity data can be used to complement magnetic data to determine basement structure.

Many correlations of subsurface structure with lineaments can be inferred from the USGS gravity data (Figure 23). The most notable is that of the Black Hills area. Several major north-south trending lineaments were mapped near the Black Hills in the northeast portion of the study area. These lineaments appear to correlate very well with a strong gravity high associated with the Black Hills uplift. These lineaments are aligned

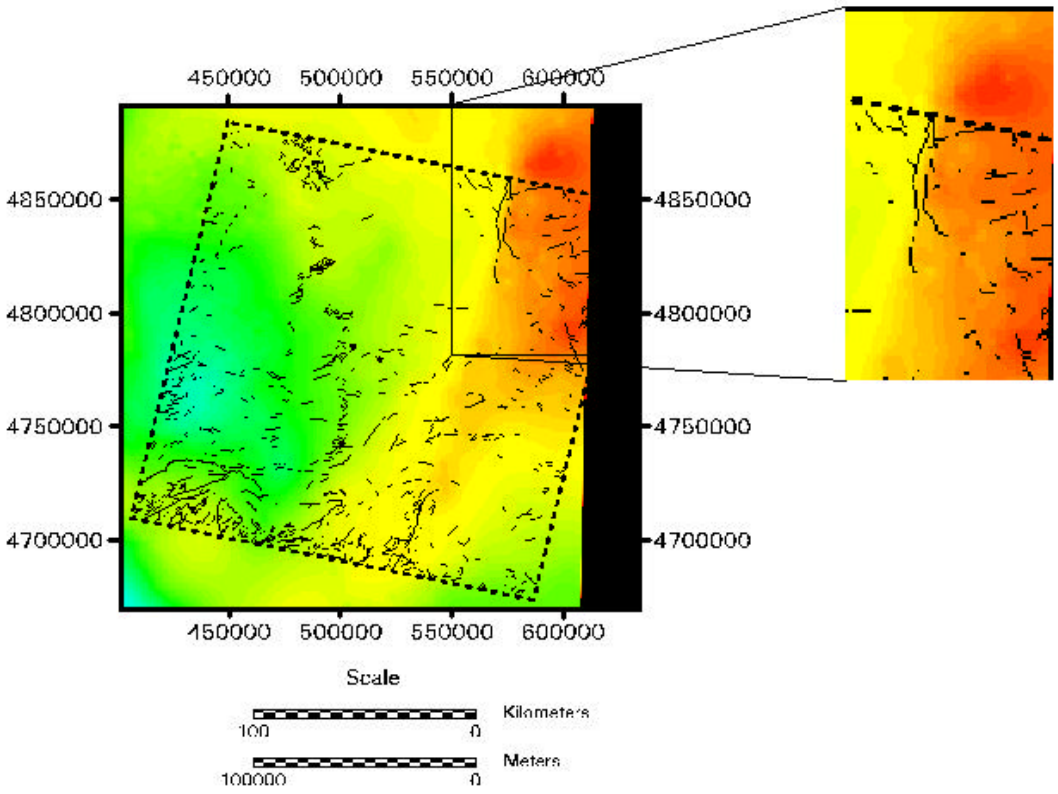

Figure 23: Map showing the location of Landsat-derived topographic lineaments within the study area overlaid on the USGS total intensity gravity data. The inset is of the gravity high near the Black Hills. Legend in Appendix A.

with the sharp gradient between the gravity high and the eastern portion of the basin. Therefore, these lineaments could represent the surface expression of a major fault. Another strong correlation can be seen in the southwestern portion of the study area near the northern Laramie Range. A major east-west-trending low-angle thrust fault is known to exist here (Gries, 1983). Two major east-west-trending lineaments were mapped at

this location and appear to coincide with the steepest part of the gravity gradient between the Laramie Range and the basin. Furthermore, many lineaments can be seen in an arcuate pattern near the central portion of the study area. This pattern of lineaments follows a gravity gradient that defines the region where the basin becomes deeper.

The magnetic data provides further insight in to the relationship between the lineaments and subsurface structure. Many of these features were not seen in the overlay with the USGS total intensity gravity data. The USGS total intensity magnetic data shows a bend in a linear magnetic trend from the east-central portion of the study area to the southwest. A strong correlation is seen between this magnetic bend and the identified lineaments (Figure 24a). This arcuate magnetic gradient is very well represented topographically on the surface, as shown by the lineament pattern. The NEWMAG™ residual magnetic data shows this trend as a series of localized highs and lows centered around the topographic lineaments (Figure 25a). A small, but intense, magnetic high can be seen just southeast of the arcuate trend (Figure 24b). This magnetic high appears to be part of a significant linear trend. Many lineaments mark this feature as well; however, one major lineament appears to separate the two halves of this magnetic high. Apparent movement along this feature may well indicate a right-lateral strike-slip fault as a result of counterclockwise rotation. Another striking magnetic feature is found in the northwest of the study area. This feature is a small, but well defined, circular magnetic high (Figure 24c). A large number of lineaments appear to parallel the northeastern half of this feature oriented. The NEWMAG™ residual data shows this feature as a very intense high with very sharp north-south trending gradients on either side (Figure 25b). The feature may represent a localized basement high, as there are older sandstones that appear at the surface in this area (Love and Weitz, 1951). Therefore, the lineaments associated with this feature may represent jointing in the brittle sedimentary rocks. Lastly, although not apparent in the USGS data, the NEWMAG™ residual data depicts localized magnetic highs along the western flank of the Black Hills in the northeast region of the study area (Figure 25c). The topographic lineaments in this area bracket part of the feature with parallel to sub parallel alignment.

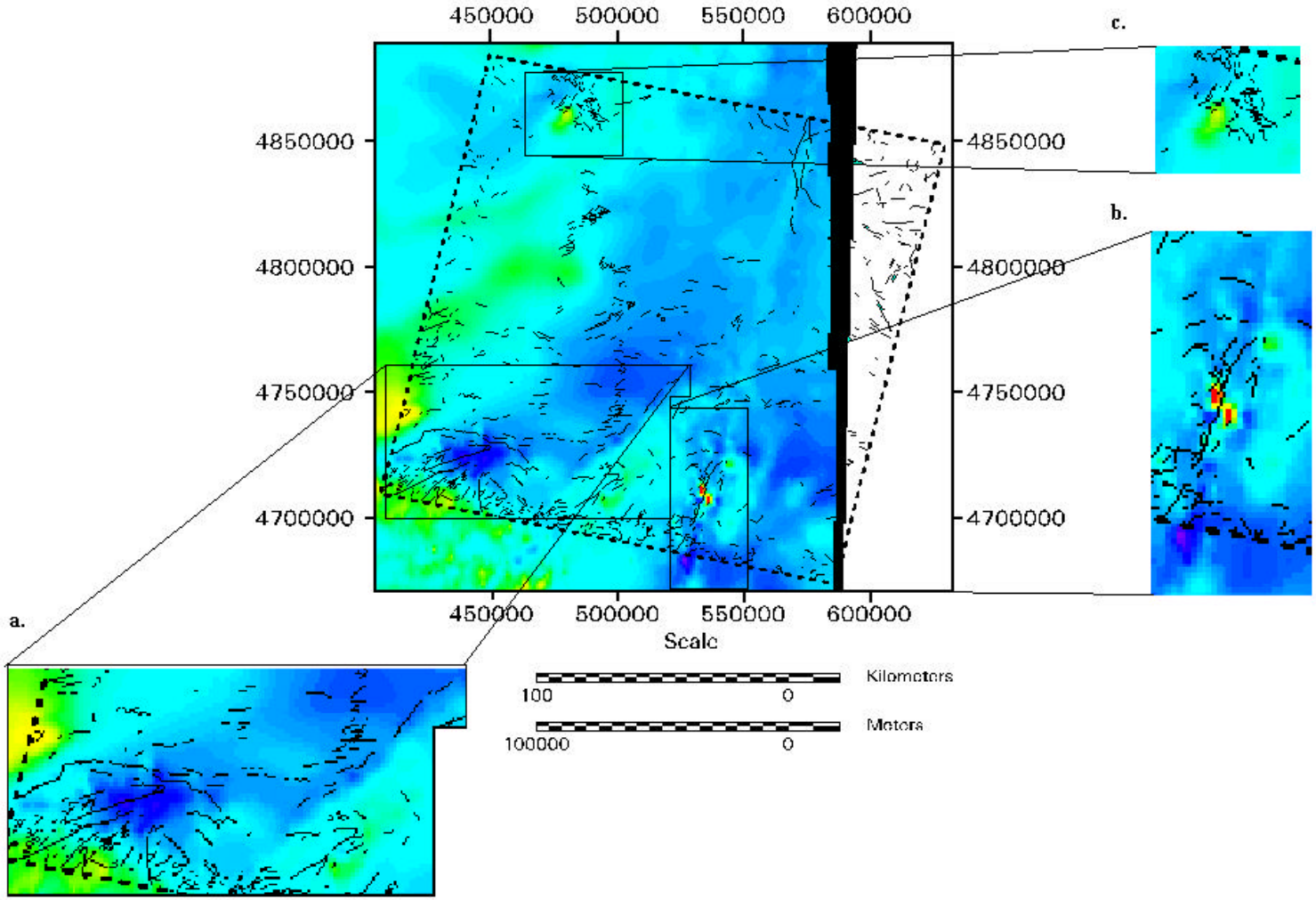

: Topographic lineaments overlaid on USGS total intensity magnetic data. a) Zone of large bend in a magnetic trend. b) Zone of linear
Legend in Appendix A.

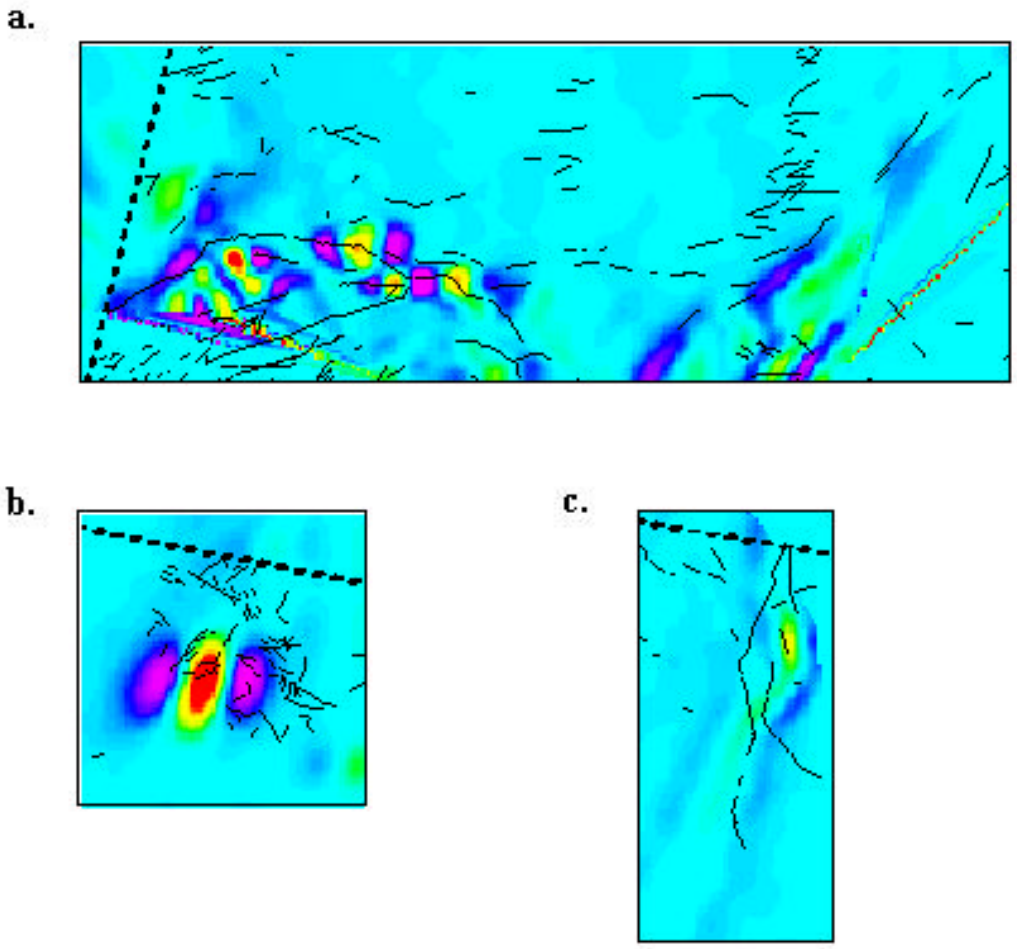

Figure 25: Topographic lineaments overlaid on NEWMAG™ high-resolution residual magnetic data. a) Zone of large bend in a magnetic trend that shows the trend is a series of magnetic highs. b) Small circular magnetic high with very sharp north-south-trending gradients on either side. c) Curvilinear magnetic high associated with the Black Hills. Index figure of NEWMAG™ data and legend in Appendix A.

The dominant trend direction for the topographic lineaments obtained from the rose diagram is east-west. There are also slightly smaller trends in the northwest-southeast and northeast-southwest directions. These orientations suggest that the linear topographic features, if they formed perpendicular and oblique to the major stress direction, developed during the later part of the Laramide Orogeny, or Early-Mid Tertiary, when compressive stress was approximately north-south (Gries, 1893).

Of all of the correlations between lineaments and the geophysical data, only the circular magnetic high (Figure 24c and Figure 25b) could not be associated with features in Dakota Formation structure map. The arcuate magnetic trend corresponds to two well-

mapped thrust faults associated with the northern Laramie Range and the Hartville Uplift. Therefore, it appears that the topographic lineaments, mapped from linear ridges and valleys, are excellent indicators of subsurface structure.

Tonal Anomalies and Linear Vegetation Patterns

The linear tonal anomalies and vegetation lineaments are much fewer in number than the topographic lineaments, and appeared to have few obvious correlations with trends in the geophysical data. From analysis of the overlay of lineaments on the USGS total intensity gravity data and magnetic data, the only notable correlation with structure patterns is in the northern Laramie Range, in the southwestern portion of the study area, and the Black Hills, toward the northeastern portion of the study area (Figure 26 and 27, respectively). These are areas of exposed crystalline rocks at the surface and are

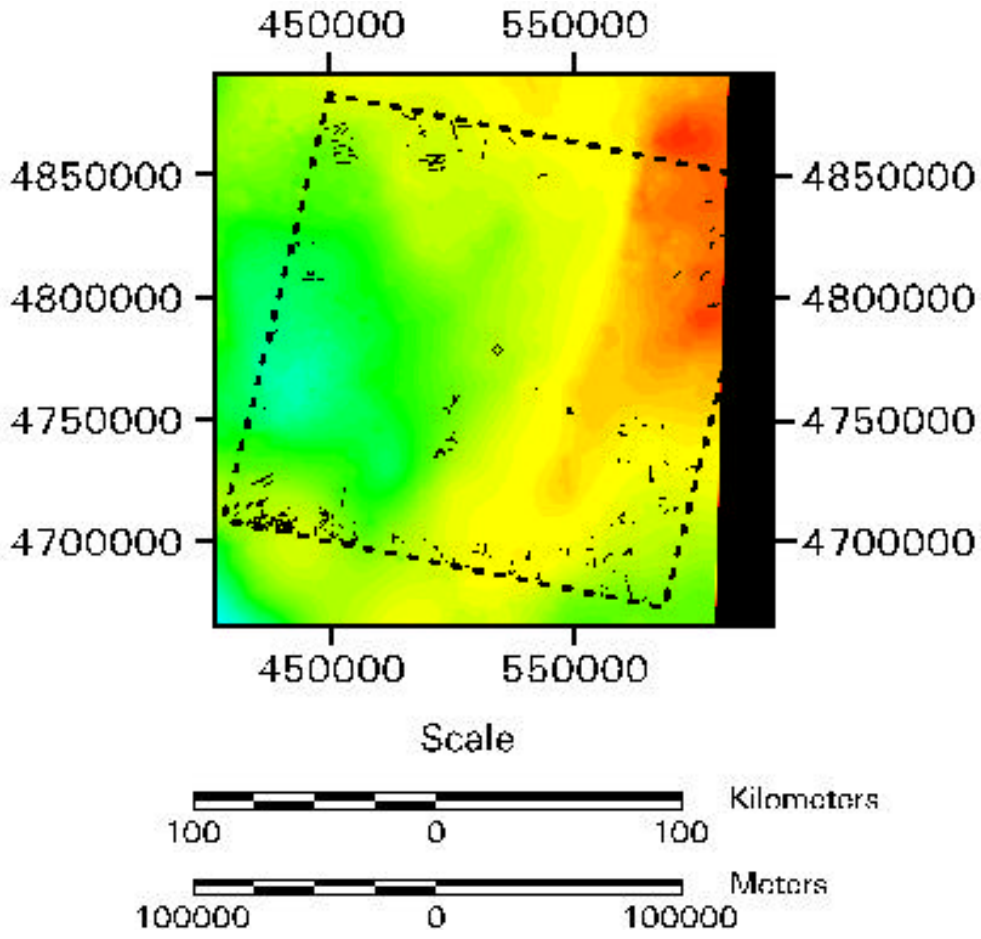

Figure 26: Linear tonal and vegetation anomalies overlaid on USGS total intensity gravity data. Legend in Appendix A.

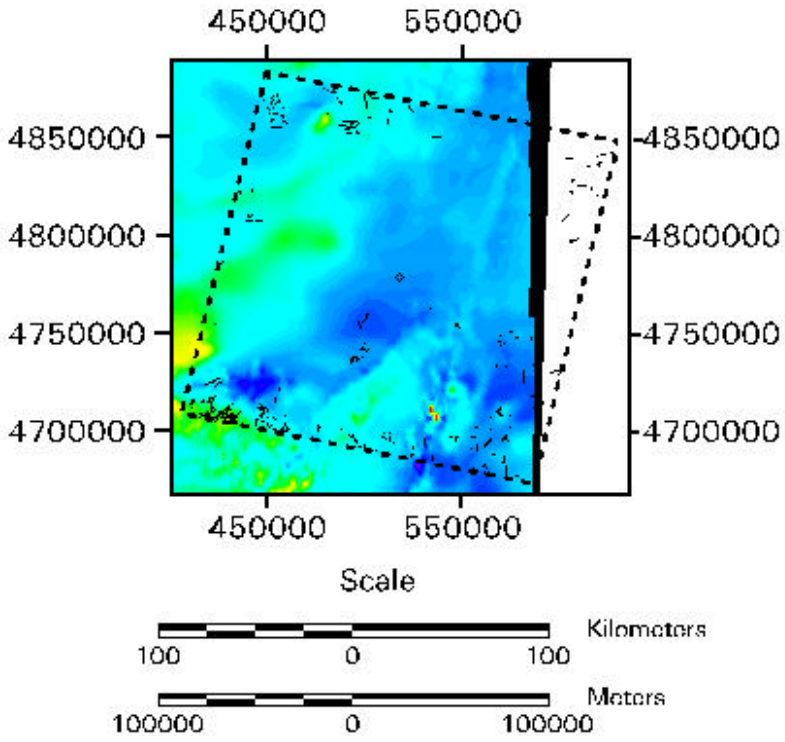

Figure 27: Linear tonal and vegetation anomalies on USGS total intensity magnetic data. Legend in Appendix A.

expected to contain joint and fracture sets. The linear tonal and vegetation anomalies appear to follow the fracturing present in the exposed basement rocks, but not in the basin itself, as evident from the geophysical data. From comparison with the Dakota structure map, there are only a few minor faults that correlate with linear tonal anomalies and vegetation lineaments. Therefore, it seems that these lineaments should probably be included with the topographic lineaments or discarded.

The major trend direction of these lineaments, indicated by the rose diagram, is strongly oriented to the northeast. According to Gries (1983), this orientation of the lineaments places them as developing during the very early Laramide Orogeny, or Late Laramide, depending on whether or not these lineaments represent structures formed at oblique angles to the orientation of north-south stress. In summary, it is suggested that these lineaments are more reliable in mapping surface structure in exposed rock, rather than subsurface structure.

DEM Lineaments

Lineaments identified from the DEM were overlain on to the gravity and magnetic data to shed light on the origins and timing of these lineaments (Figure 28). Since these lineaments are by definition topographic in origin, they may be redundant, considering that topographic lineaments were also identified from the Landsat TM image. DEM lineaments of the Laramie Range (Figure 28a), the Black Hills (Figure 28b), and the faulted magnetic high in the southeast portion of the study area (Figure 29b) give similar, but by no means identical, patterns to those identified from the Landsat imagery. Furthermore, there are some correlations of the DEM lineaments with subsurface structure that are not seen with the Landsat topographic lineaments. One example is the presence of lineaments along the continuation of the magnetic linear trend related to the Black Hills uplift, as seen on the USGS total intensity magnetic data (Figure 29a) and the NEWMAG™ high-resolution residual magnetic data (Figure 28c).

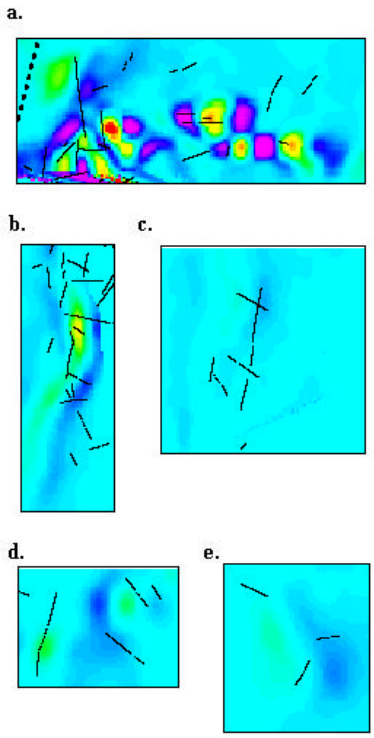

Figure 28: a) DEM lineaments overlaid on to NEWMAG™ data of the northern Laramie Range. b) Black Hills uplift. c) Small linear magnetic high at southern tip of the Black Hills uplift. d) Two small magnetic highs separated by a low marked well by lineaments. e) Small magnetic gradient that is indicated at the surface by the lineaments. Index figure of NEWMAG™ data and legend in Appendix A.

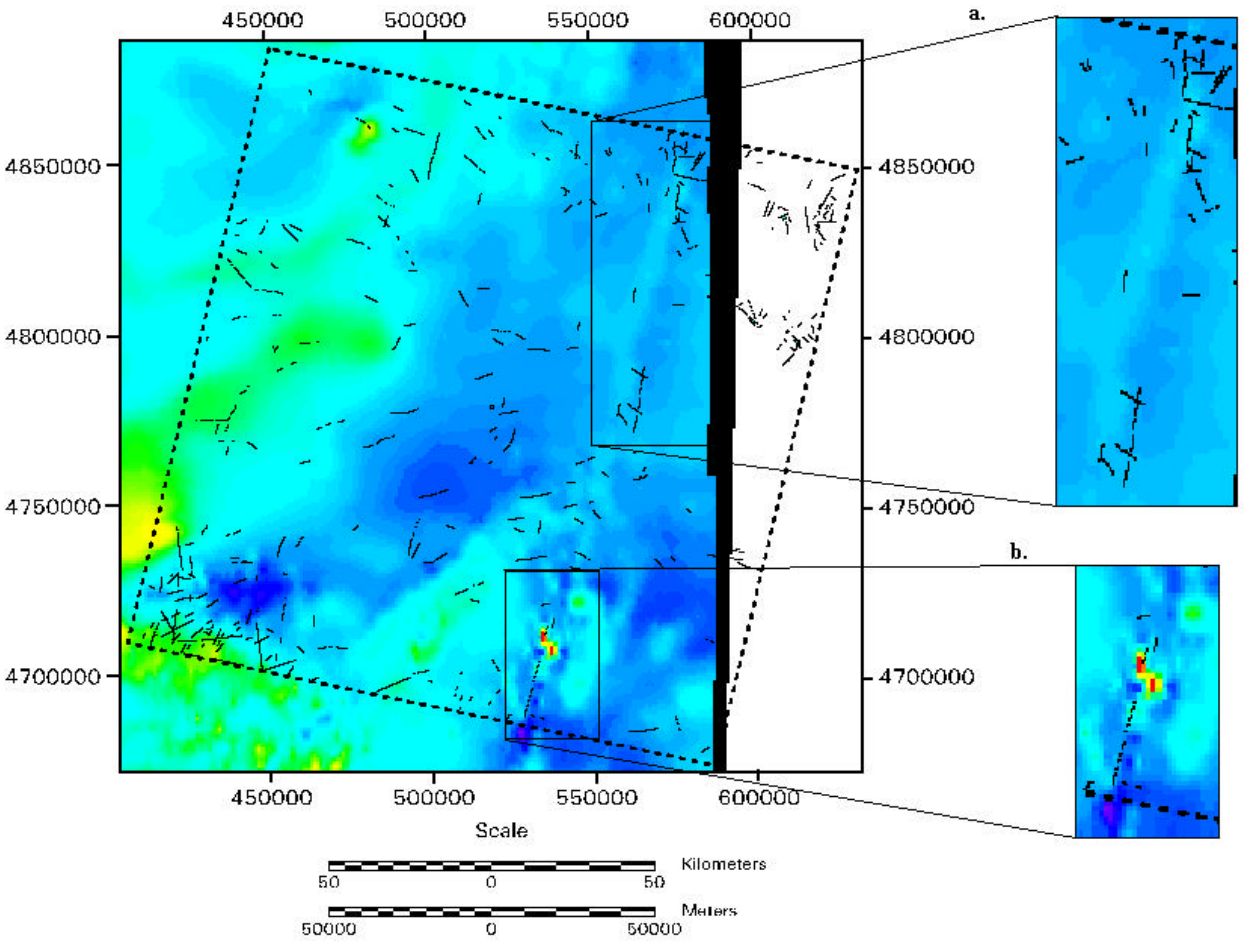

: Map showing DEM lineaments overlaid on USGS total intensity magnetic data. a) Area magmnetic linear trend associated with the Black Hills uplift with lineaments identified from b) Two magnetic highs to the southeast of the study area as part of the same linear trend. Legend in Appendix A.

Another case where DEM lineaments correspond to a magnetic high is seen in the north central portion of the study area. USGS magnetic data does not show the high at all, however, NEWMAG™ data does (Figure 28d). This feature is actually two small magnetic highs, both of which are associated with the lineaments on the surface, and a sharp magnetic low separating the two highs. The last example of a significant magnetic high that corresponds to a series of lineaments is in the central portion of the study area. Although not identifiable on the USGS magnetic data, it is detectable on the NEWMAG™ data (Figure 28e). The lineaments identified from the DEM seem to mark the gradient between this subtle high and low.

The DEM lineaments appear to be a useful class, and therefore worthwhile mapping. Perhaps the main utilization of these lineaments is as a supplement to the topographic lineaments because these lineaments follow trends that were not documented by the topographic class of lineaments identified from the Landsat TM image. The rose diagram for these lineaments shows a strong northeast-southwest trend. This is strikingly different from the related topographic lineaments, which have a substantial east-west trend. Perhaps the majority of these DEM lineaments represent an older set of topographic lineaments formed during the Late Cretaceous (Gries, 1993).

Drainage Anomalies

The linear drainage anomalies identified from the hydrology files of the DLG were displayed on the USGS gravity (Figure 30) and magnetic data (Figure 31). Figure 30 appears to suggest that unlike the Landsat-derived lineaments, the drainage anomalies only correspond to areas of uplift, such as the Black Hills in the northeast of the study area, but there are some dispersed in the basin area as well. The total intensity magnetic data shows interesting structural features associated with the drainage anomalies (Figure 31). For example, a small circular pattern of drainage anomalies can be seen in the very northern portion of the study area (outlined by box in Figure 31). This circular pattern of drainage anomalies corresponds to a circular-shaped magnetic gradient. Another arcuate pattern of drainage anomalies can be seen in the west-central portion of the study area (outlined by box in Figure 31). This series of drainage anomalies appears to mark the gradient between the magnetic high to the west and the corresponding low to the east.

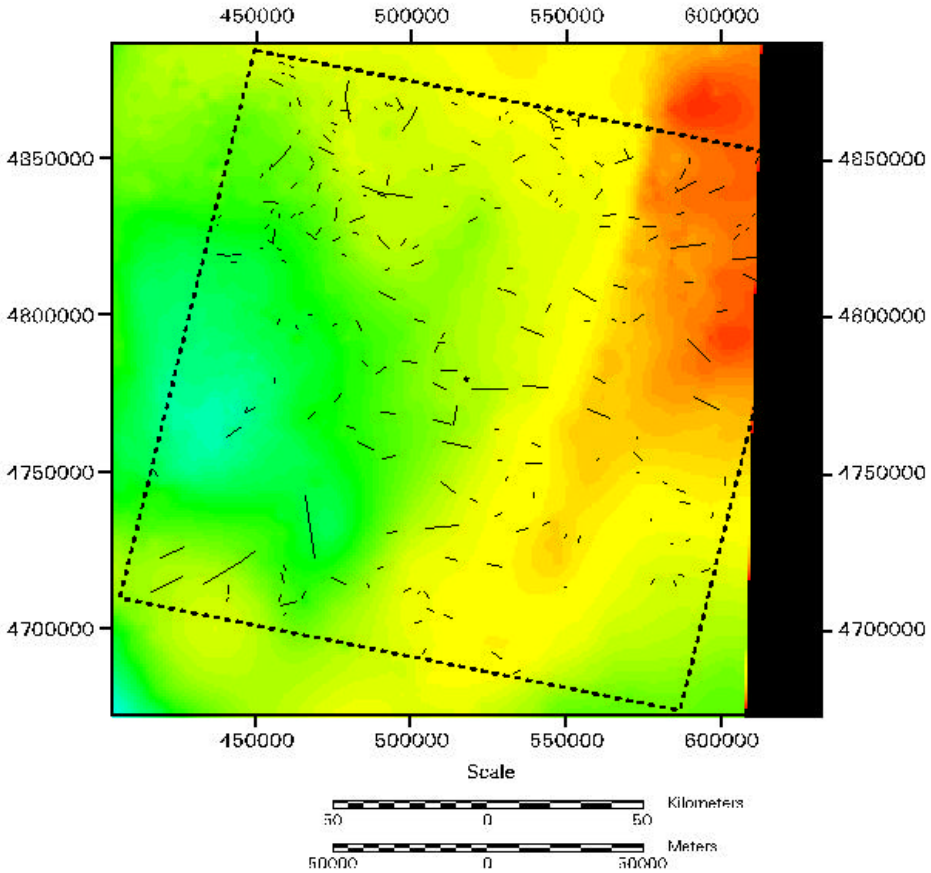

Figure 29: Map showing the locations of drainage anomalies overlaid on the USGS gravity data. Legend in Appendix A.

Also, many drainage anomalies seem to relate to the highs seen in the northwest portion of the study area.

The drainage anomalies have a trend direction of east-northeast. Following Gries (1983), the formation of these anomalies could have been approximately Middle to Late Tertiary in age.

Summary of Structural Significance and Timing of Lineaments

Comparing the lineaments identified from the various data sets with subsurface information has yielded interesting and striking results. These results have provided valuable insight as to which group of lineaments appear to be the most useful and correlative to subsurface structure. The topographic lineaments, identified from the Landsat image, appear to be the most coincident with subsurface structure, implied by

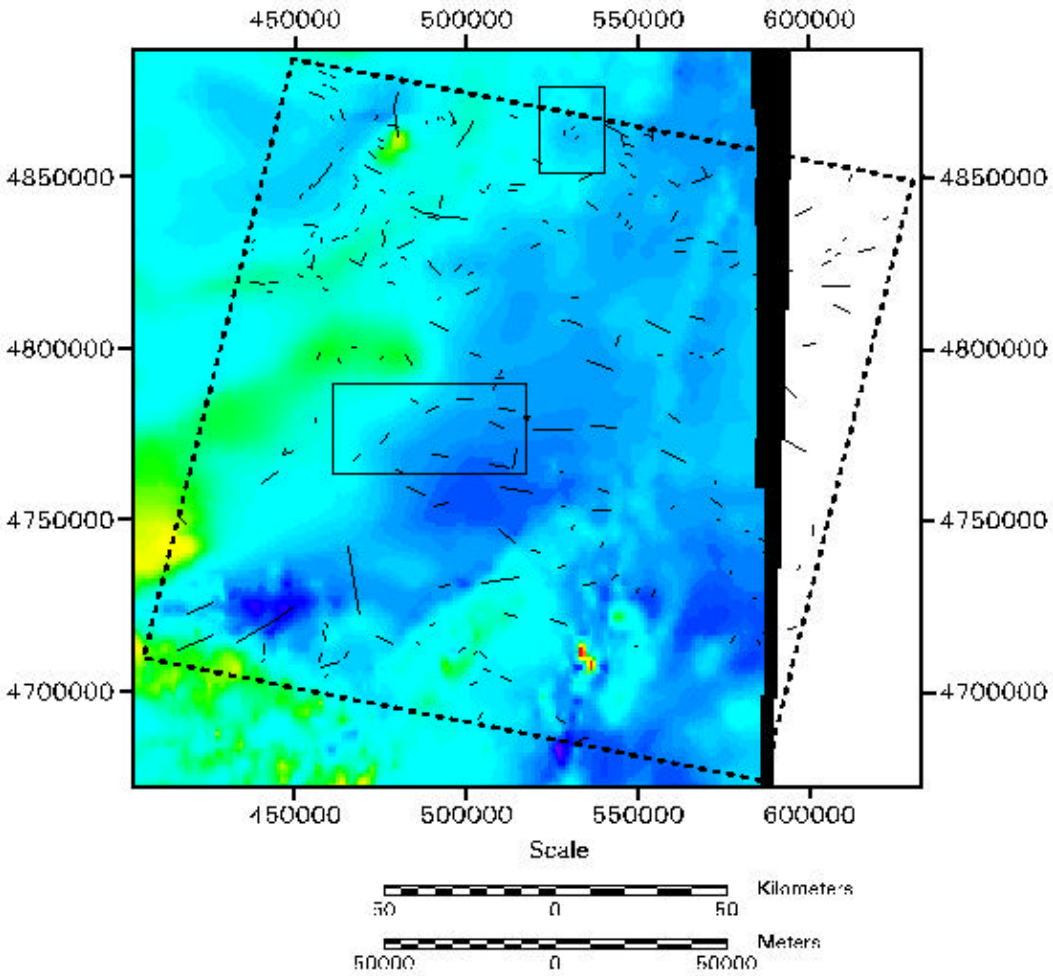

Figure 31: Map showing the location of the linear drainage anomalies overlaid on the USGS total intensity magnetic data. Legend in Appendix A.

gravity and magnetic highs. The lineaments identified from the DEM also correspond to subsurface structure. These lineaments are topographic in nature and appear to supplement the topographic lineaments identified from the Landsat image. The drainage anomalies also appear to coincide with subsurface structure. Therefore, these lineaments could possibly represent surface expressions of these geophysical highs. The linear tonal anomalies and vegetation lineaments did not, however, show associations with subsurface structure. Nevertheless, their usefulness in identifying surface structure, such as joint and fracture sets, appears to be evident by their concentration in exposed brittle rock.

The general age of the lineaments, combining results from the rose diagrams and work completed by Gries (1983), appears to indicate that the topographic lineaments,

with a strong east-west and seemingly conjugate trend directions of northeast and northwest, are the result of the development or reactivation of structures during the Late Laramide, when the tectonic stress was strongest (Robbins, 1993). Those topographic lineaments identified from the DEM indicate development during the Late Cretaceous. Therefore, these topographic lineaments may well be slightly older and closely related to the topographic lineaments identified from the Landsat image as indicated by the secondary orientation of east-west in the rose diagram. The age of the drainage anomalies may be the most perplexing. These lineaments may have mostly developed in Late Cretaceous during very the Early Laramide Orogeny, if they represent structures formed at acute angles to stress or in the Middle-Late Paleocene at the very last while Laramide deformation was near southward in the Powder River Basin. Lastly, the northeast-trending linear tonal anomalies and vegetation lineaments, which mark surficial structures, may have been the earliest structures to develop during the Late Cretaceous.

The concentration of lineaments is higher in areas of exposed brittle rock, typically coinciding with uplifts. Figure 32 shows rose diagrams for all lineaments in the Black Hills, Hartville Uplift, and Northern Laramie Range. Assuming these lineaments represent fractures and faults developed either at acute angles or perpendicular to the compressive stress during the Laramide Orogeny, they should yield clues on the timing and deformation of these uplifts. The north-south trending Black Hills are understood to have developed during the Early Laramide Orogeny (Gries, 1983). A strong, but isolated east-west primary trend and a secondary northeast-southwest trend, suggest that the Black Hills were strongly deformed during the later stages of the Laramide Orogeny. The Hartville Uplift is another Early Laramide structure (Gries, 1983) with a northeast-southwest trend. The rose diagram for this region shows that the concentration of lineament trends between 45° and 135° support this, if they represent conjugate fracture sets at acute angles to the westward stress direction. A strong east-west trend may by the result of later Laramide deformation when the tectonic pulse was the greatest and oriented southward. Lastly, the lineaments in the Northern Laramie Range show a strong northwest-southeast trend, which is the same as the uplift, with significant trends east-west and between 30° and 60°. These trends would also be consistent with Middle-Late Laramide deformation as the rotation of compressive stress, according to Gries (1983),

was oriented to the southwest and south. These trends would therefore represent structures formed at perpendicular and acute angles to the stress.

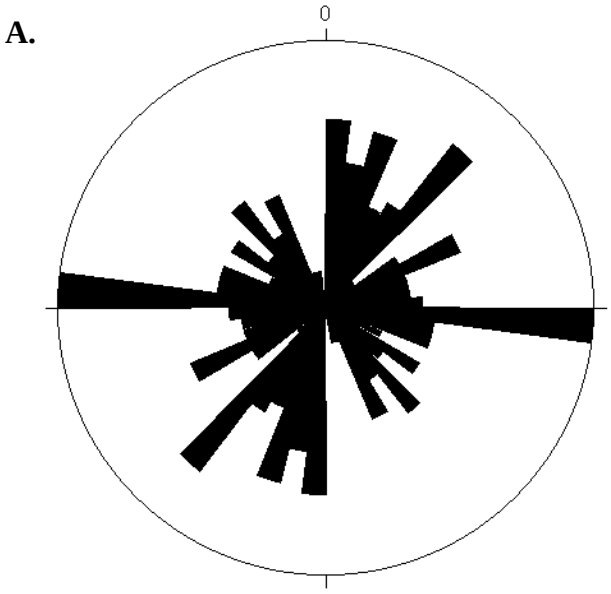

Black Hills Lineaments
Strike Direction: 7.5° classes
n = 435
largest petal: 44.00 values
largest petal: 10% of values

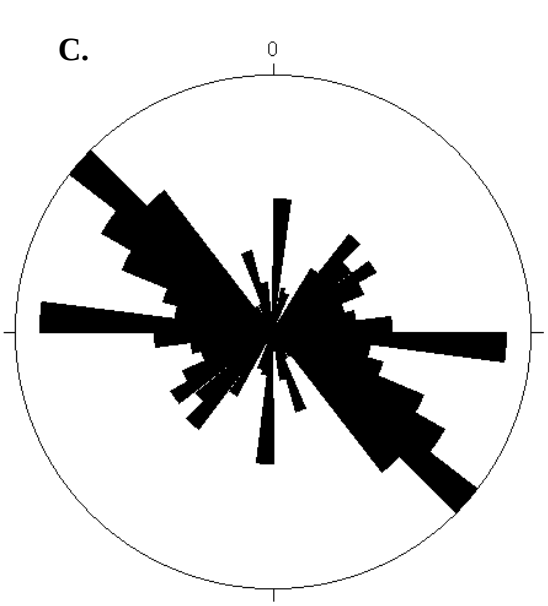

Northern Laramie Range Lineaments
Strike Direction: 7.5° classes
n = 1000
largest petal: 104.00 values
largest petal: 10% of all values

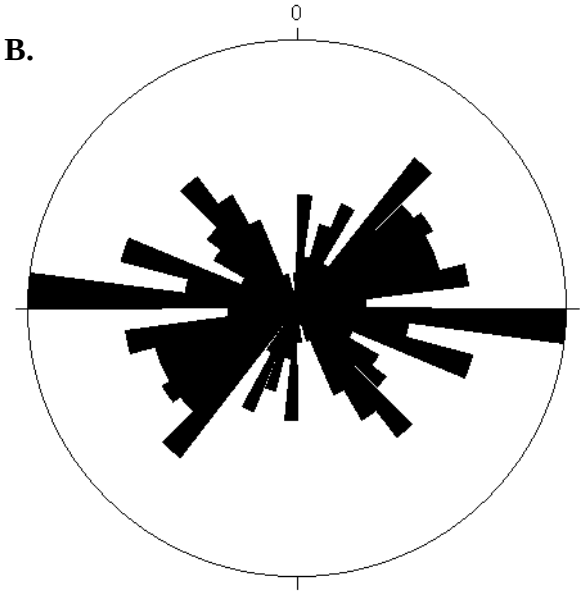

Hartville Uplift Lineaments
Strike Direction: 7.5° classes
n = 636
largest petal: 62.00 values
largest petal: 9% of all values

Figure 32: Rose diagrams showing major trends of lineaments occurring in the uplifted regions within the study area. The rose diagrams are in the relationship that the uplifts occur to each other. A) Rose diagram for the Black Hills lineaments. B) Rose diagram for the Hartville Uplift lineaments. C) Rose diagram for the Northern Laramie Range Lineaments.

Chapter 6: Relationship of Lineaments to Hydrocarbon Reservoir Location

Background of Hydrocarbon Reservoirs

The employment of the powerful GIS functionality of overlay has been shown in the previous chapter to be a very informative tool for the analysis of lineaments and subsurface structure. Subsurface structure, of course, is crucial in the entrapment of hydrocarbons. Whether or not these entrapments are stratigraphic, structural, or a combination of both, overlaying lineaments and oil field locations with subsurface geophysics gives useful insights in understanding the distribution of the reservoirs.

The Powder River Basin is a very large producer of oil and gas and contains many linearly arranged oil fields. These oil fields largely belong to three main time intervals: Pennsylvanian-Permian, Lower Cretaceous, and Upper Cretaceous. The major producing intervals and their producing formations are shown in Figure 33. The major Pennsylvanian-Permian producing zone is the Minnelusa Formation, an aeolian sandstone, and the Minnekahta Limestone. The productive formations belonging to the Lower Cretaceous are the Mowry Shale, Newcastle Sandstone, Muddy Sandstone, Skull Creek Shale, Dakota Sandstone, Fall River Sandstone and the Lakota Sandstone. Lastly, those productive formations of the Upper Cretaceous rocks are the Lance Formation, Lewis Shale, Teapot Sandstone, Parkman Sandstone, Steele Shale, Sussex Sandstone, Niobrara Formation, Turner Sandstone, Greenhorn Formation and Frontier Formation (DeBruin and Boyd, 1990).

The identified lineaments may not directly, or even indirectly, affect the hydrocarbon reservoirs of these three main age groups. However, as was shown in the previous chapter, many lineaments occur over major basement features interpreted from the gravity and magnetic geophysical data. The lineaments appear to represent the surficial expression of these features. Therefore, the combination of geophysical data with the lineaments becomes a useful and inexpensive method of understanding the structures involved in hydrocarbon entrapment.

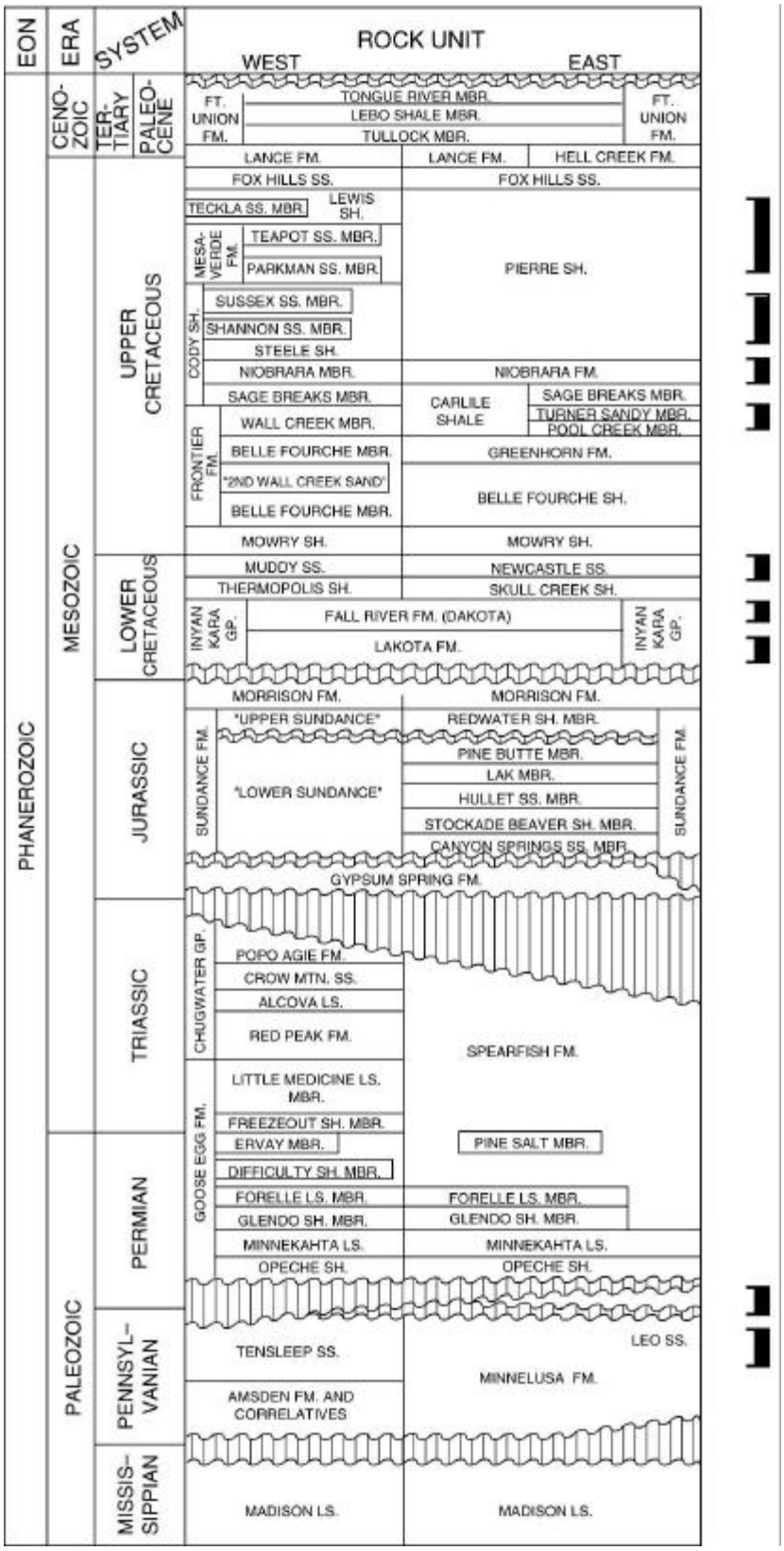

Figure 33: Stratigraphic column for the Powder River Basin. Brackets on the right side mark the productive intervals (Dolton and Fox, 1995).

The Pennsylvanian-Permian Interval

The producing formations of this interval include the Pennsylvanian Minnelusa Sandstone and the Permian Minnekahta Limestone. This play consists of 160 fields that have approximately 500 MMBO (Million Barrels of Oil). The hydrocarbon traps related to this major play are largely the result of paleotopography, reservoir truncation, and sandstone pinchouts at the top of the Minnelusa. The reservoirs themselves are aeolian sand dunes sealed at the top by the impermeable Opeche Shale. Source rocks for the hydrocarbons seem to be the dark marine shales of Desmoinesian age, lying underneath the Minnelusa, or the Phosphoria Formation to the west (Dolton and Fox, 1995).

Within the study area, there are only a few localized oil fields producing from the Minnelusa Sandstone. Several of these localized fields form an arcuate pattern around the magnetic high seen in the northwest portion of the study area (Figure 34).

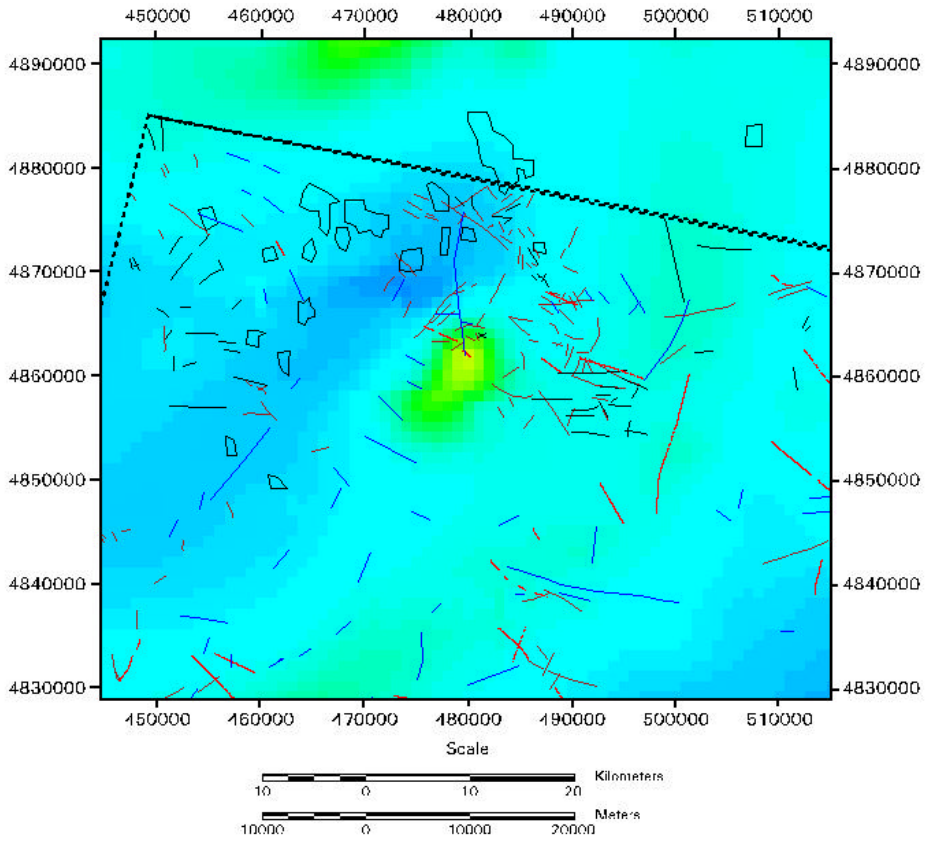

Figure 34: Map showing the Pennsylvanian-Permian oil fields between Raven Creek and Eagle Rock (polygons from northeat to southwest) surrounding a magnetic high. Topographic Lineaments (brown), Tonal Anomalies and Vegetation Lineaments (black), DEM Lineaments (red), and Drainage Anomalies (blue) are also shown. Geophysical legend in Appendix A.

The Landsat and DEM derived topographic lineaments may serve as good surface expressions of this structure and, possibly, suggest a cause for the observed position of the reservoir. This is a good example of how lineaments and magnetic data can be used to analyze reservoir location.

The NEWMAG™ high-resolution residual magnetic data shows two magnetic trends, both trending roughly northeast-southwest, that the three easternmost Minnelusa fields follow (Figure 35). These trends, correspond to the Black Hills monocline, which can be seen in the subsurface structure map of the Dakota Formation (Barlow and Haun, Inc. Geologists, 1987). The three oil fields, formed from oil trapped in anticlines at the Dakota level, overlay this small linear magnetic high. The Red Bird field, shown in Figure 35b, is completely flanked on the east side by intersecting DEM Lineaments marking the structural high on which it sits.

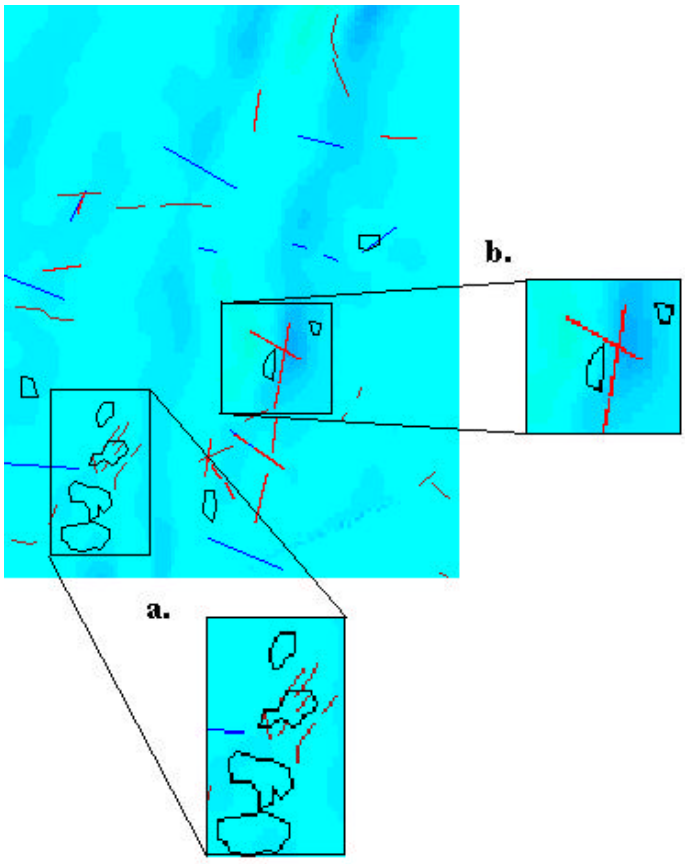

Figure 35: NEWMAG™ data with lineaments and Minnelusa oil field locations. a) Inset showing possible linear control in the Beaverhole field. b) DEM Lineaments related to the subsurface basement high flanking the east side of an oil field. Index figure of NEWMAG™ data and legend in Appendix A.

In summary, the major structural features that affect the Pennsylvanian-Permian hydrocarbon reservoirs in the field area, are possibly represented on the surface as indicated by the presence of topographic lineaments from Landsat and DEM, and drainage anomalies coincident with highs seen in the magnetic data. Examples are the strong high in the northwest portion of the study area and the linear trends related to the Black Hills Monocline and the Hartville Uplift in the southeast portion of the study area. The lineaments that appear to be the most coincident with these structures are the topographic lineaments, the DEM lineaments and the drainage anomalies.

The Lower Cretaceous Interval

The major producing formations in the Powder River Basin that are Lower Cretaceous in age are the Lakota Sandstone, Fall River Sandstone (Dakota), Muddy Sandstone, Skull Creek Shale, and the Mowry Shale. Traps in the Lakota Sandstone are completely stratigraphic as they occur within channel sandstones sealed by fine-grained alluvium. The majority of the traps associated with the Fall River Sandstone are stratigraphic pinchouts with increasing shale content to the west; however, large hydrocarbon reservoirs have been discovered in structural traps formed by plunging anticlinal noses. Many different types of stratigraphic traps characterize reservoirs producing from the Muddy Sandstone. Lastly, the Skull Creek Shale produces from fractures and fracture intersections - a more unconventional play. The source bed for all of these reservoirs is presumed to be the very organic-rich Mowry Shale, which immediately overlies these formations. The fields of the Lower Cretaceous interval account for more than 720 MMBO and 1050 BCFG (Billion Cubic Feet of Gas) in the Powder River Basin. The vast majority of this amount is from the Muddy Sandstone play, while the Lakota Sandstone play is underexplored and does not contribute significantly to these numbers (Dolton and Fox, 1995).

Images created from the integration of total intensity and high-resolution residual magnetic data with the lineaments show many coincidences with reservoir location (Figure 36). An increase in number of all lineaments as well as a dominant northeast orientation in the western portion of the study area indicates the influence of subsurface, possible basement, structure on surface features. In fact, the overlay depicts a northeast-

trending magnetic high corresponding to the zone with an increase in lineament density (Figure 36). Several fields can be seen on this high that possibly owe their existence to the feature. The most notable of these fields, the Big Muddy East field, lies just to the east of this magnetic high in the southwestern portion of the study area. A number of lineaments belonging to the DEM Lineament and Topographic Lineament classes relate to this magnetic gradient and an east-plunging anticline at the Dakota level (Barlow and Haun, Inc. Geologists, 1987). Continuing to the north, the Cole Creek South field also overlays the edge of this magnetic high, to which it may be related. Topographic

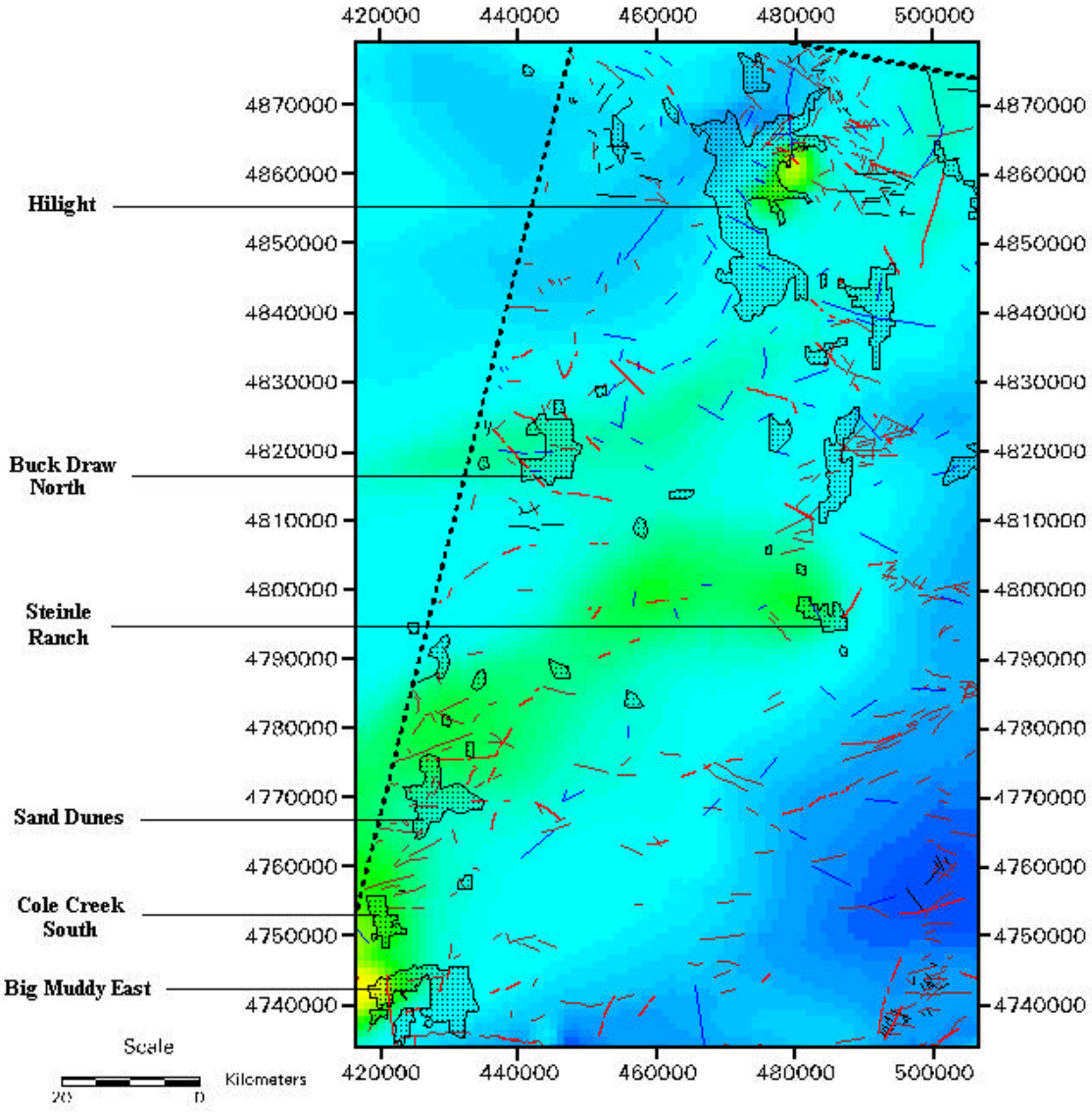

Figure 36: Location of Landsat topographic lineaments (brown), tonal anomalies and linear vegetation lineaments (black), DEM lineaments (red), drainage anomalies (blue), and Lower Cretaceous reservoirs (stippled) overlaid on USGS total intensity magnetic data. Geophysical legend in Appendix A.

lineaments identified from the Landsat image and the DEM, as well as drainage anomalies, appear just to the northeast of this reservoir and therefore may stem from the subsurface structure. The Sand Dunes field, just north of the Cole Creek South field, overlays the arcuate edge of the same magnetic high. The circular-shaped edge is associated with lineaments that trend in many directions, which differs from the overall northeast-trending orientation of the lineaments on this high. Therefore, it appears that this reservoir location is strongly related to the basement structure. However, it is suggested that this high may be a tongue of coarse clastic sedimentary rocks formed from eroded igneous rocks (Robbins, 1993). Nevertheless, the last major reservoir that appears to be related to the same magnetic high is the Steinle Ranch field. This field also overlays the gradient between the magnetic high and low at the very eastern portion of the high. Two of major lineaments tending northeast, and conjugally northwest, mark this gradient and possibly the eastern termination of this magnetic high.

Toward the northwestern portion of the study area, just north of the aforementioned magnetic high, another magnetic high can be seen. This high is much smaller, but still trends in the same general east-northeast direction. In fact, the trend of this high becomes more northeasterly from east to west. Curiously, many of the major lineaments of all classes overlying this magnetic high trend northwest. Perhaps these lineaments represent structures forming conjugally to the lineaments trending northeast along this feature. In support of this statement, those lineaments trending northwest are commonly found to intersect those trending east-northeast. A major Fall River (Dakota) Sandstone reservoir, the Buck Draw North field, overlays this high toward the western portion of the study area. The southern portion of the reservoir changes shape to a more easterly orientation. This abrupt change corresponds to a major drainage anomaly trending in the same direction.

The Hilight field, a major Muddy Sandstone reservoir, lies near a small, but striking, circular magnetic high in the northwest portion of the study area. The concentration of lineaments, dominantly drainage anomalies, in the region immediately northeast of this noteworthy high appear to correspond. The most apparent correspondence of the location of this large field with the magnetic high is the abrupt change in trend direction from northeast to north-northwest of the field. Therefore, this

magnetic high and the linear structures related to it may be the cause of the major abrupt change of the Hilight field.

Many of the major correlations between reservoir location and linear structures supported by magnetic data are seen in the western portion of the study area. However, through the support of high-resolution residual magnetic data (NEWMAG™), another major oil field appears to be affected by lineaments related to basement structure. Toward the southwestern portion of the Fiddler Creek, another Muddy Sandstone field, orientation to the southwest stops bluntly into a northwest-trending segment (Figure 37). A few DEM lineaments and drainage anomalies lie parallel and perpendicular to this southeasterly trend and also surround the small magnetic high at the end of the northeast-trending segment. The NEWMAG™ data, along with southeast lineament orientation, may therefore yield clues to the sudden change in orientation of this field, as it seems to follow the residual magnetic high. The same change in trend is not seen in the Clareton Field just to the southeast.

The major oil fields of the Lower Cretaceous producing interval appear to be strongly affected by magnetic highs seen both in USGS total intensity magnetics and

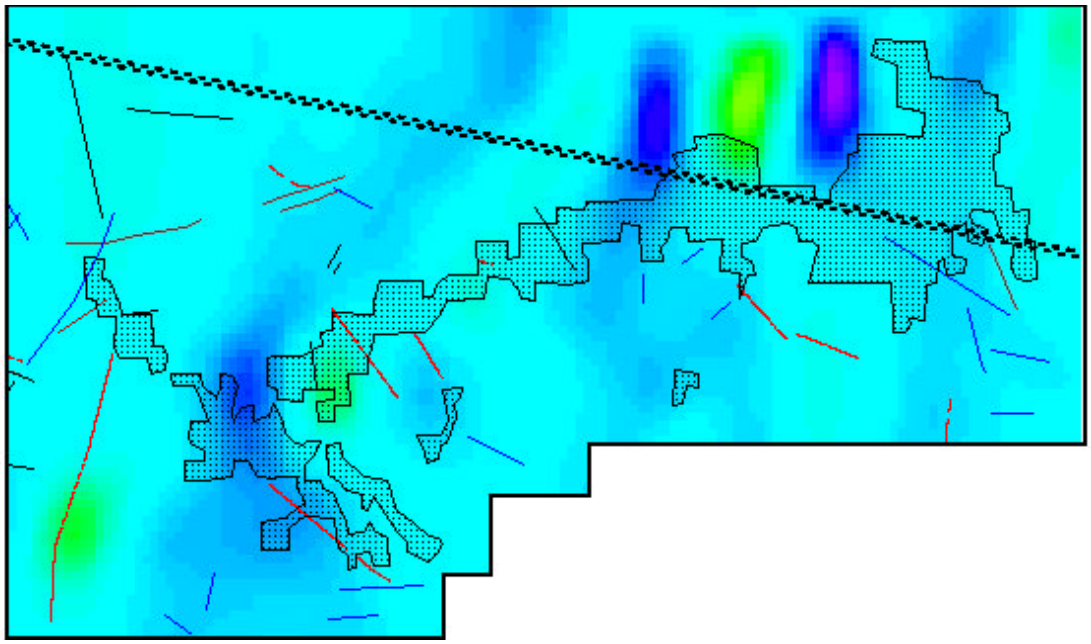

Figure 37: Fiddler Creek oil field location and lineaments of all classes overlayed on NEWMAG™ high-resolution residual magnetic data. Index figure of NEWMAG™ data and legend in Appendix A.

NEWMAG™ high-resolution residual magnetics. Lineaments, mainly belonging to the Landsat and DEM derived topographic lineaments, DEM lineaments and the drainage anomalies, are found parallel and perpendicular to these magnetic highs. Insight has been obtained from analysis of the lineaments relating to magnetic highs. It appears that the drainage anomalies are dominantly perpendicular to the trend of the basement structure. This is evident in both Figures 36 and 37.

The Upper Cretaceous Interval

The major plays that comprise the Upper Cretaceous interval are the Turner Sandstone, Sussex-Shannon Sandstone, and Mesaverde-Lewis (Parkman). There are also unconventional fractured shale plays, including the Niobrara and Mowry Shales. The Turner Sandstone is a low-porosity sandstone that produces from traps associated with generally thin bar complexes of irregular shape. The Sussex-Shannon Sandstone play consists of marine shelf sandstone reservoirs. Traps in this play are typically classic updip pinchouts of porous sandstone that terminate into impermeable shale. Lastly, the Mesaverde-Lewis (Parkman) play involves hydrocarbon traps in marine sandstones. Like the Sussex-Shannon, the traps associated with this play are typically updip stratigraphic pinchouts along sinuous marine bar sands. Total production from the Upper Cretaceous interval exceeds 310 MMBO and 270 BCFG. The fractured shale plays do not contribute significantly to these numbers (Dolton and Fox, 1995).

Many lineaments are associated with the Flat Top field located in the southern portion of the study area (Figure 38). An overlay of the lineaments and the oil field locations with the magnetic data does not indicate evidence of basement structure relating to these lineaments. However, the detailed structure map of the Dakota Formation (Barlow and Haun, Inc. Geologists, 1987) depicts a large and arcuate nonplunging anticline as the primary trapping mechanism for this field. The axis of this anticline is shown in Figure 37. Therefore, lineaments, especially topographic ones, may not always stem from basement structure.

Interesting results were found from the overlay with the lineament and oil field locations with the NEWMAG™ data. Todd field, a small linear east-west-trending field in the northern portion of the study area, directly overlays the apex of a north-south-

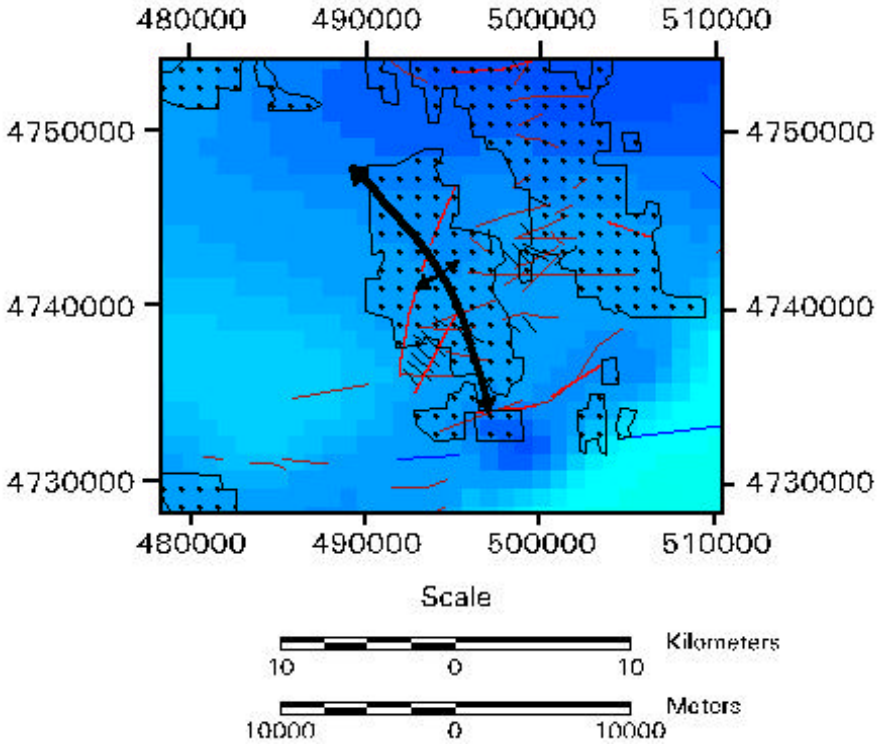

Figure 38: Map showing the Flat Top oil field. The location of lineaments as well as the axis of a large anticline at the Dakota level is also shown. Geophysical legend in Appendix A.

trending magnetic high (Figure 39a). A large DEM lineament directly crosses this magnetic high, perhaps representing the surface expression of this feature. In the southwestern portion of the study area, the Brooks Ranch field lies just to the west of a residual magnetic high (Figure 39b). This is the same residual high that possibly affects the Big Muddy East field of the Lower Cretaceous interval. Lineaments belonging to the Topographic and DEM classes may represent this structure on the surface as seen in Figure 39b. Coincidentally, a structural high is also found to lie above this magnetic anomaly at the Dakota level. In the central part of the study area, another oil field, Poison Draw, can be seen in relation to a residual magnetic high (Figure 39c). This northwest-trending field lies just to the southeast of a subtle magnetic high, also trending northwest. The high concentration of many lineaments of all types, but especially those belonging to the Landsat and DEM derived topographic lineaments class, may owe their origin to this linear high.

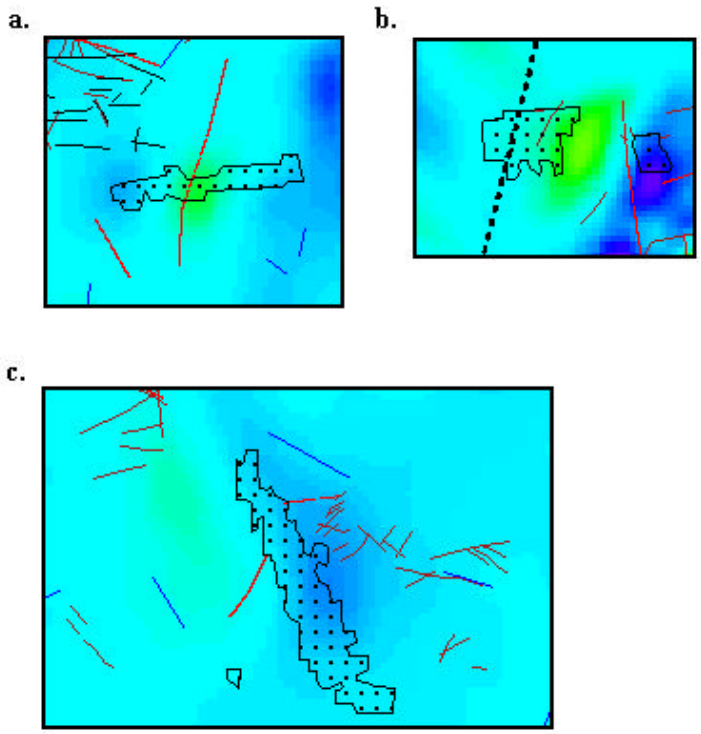

Figure 39: Overlays of lineament and oil field location on NEWMAG™ magnetic data. a) Todd field. b) Brooks Ranch field. c) Poison Draw. Index figure of NEWMAG™ data and legend in Appendix A.

Summary of Lineament Influence on Hydrocarbon Reservoirs

The employment of the GIS functionality of overlay appears to be very useful in understanding the relationships between lineament location and magnetic anomalies. This overlay method allows for analysis of the origin of the lineaments by means of basement structure analysis. This method bridges the thousands of feet between surface features and the structure of the basement. Lineaments may not always represent the surficial expression of structures originating from basement anomalies, but may reflect structure in the underlying sedimentary package. Therefore, it is very useful to have formation structure maps of the overlying strata to provide further information.

The lineaments that seem to be more consistently related to subsurface structure are those belonging to the topographic lineaments, the DEM lineaments and the drainage anomalies classes. The orientations of the lineaments are usually parallel or perpendicular to the structure, as seen in Figures 35b, 36, 37, and 38. This pattern could represent conjugate sets of fractures as may be indicated near the Buck Draw North field

in Figure 36. The drainage anomalies seem to be typically perpendicular to the trend of the coincident structure. Nevertheless, these patterns of lineaments, along with a higher concentration in one area, are strong indicators of subsurface structure. This information is critical in areas such as the Powder River Basin where hydrocarbon reservoirs are prevalent. Overlay methods with magnetic data may not be the most precise method of reservoir location analysis, but could reduce the area of study significantly. This may be a useful and cost effective approach to planning seismic surveys for future exploration.

Chapter 7: Conclusions

Lineament studies are oftentimes viewed as untrustworthy due to the subjectiveness of the lineament identification process. This skeptical view of lineament studies may arise from the assumption that all lineaments have equal value, regardless of their appearance on the data sets employed for identification. Furthermore, the use of subsurface geophysical techniques greatly enhances the value of lineament investigations, because the geophysical data facilitates the interpretation of geological structure. This investigation has shown that the classification of lineaments from a Landsat TM image, DEM, and DLG files, yields a far richer lineament interpretation, as well as providing information about each lineament type.

Rose diagrams generated for each lineament class, combined with work done by Gries (1983), suggests that many of the topographic lineaments derived from Landsat, representing valleys, ridges and escarpments, can be related to structural directions associated with the later portion of the Laramide Orogeny. Furthermore, the topographic lineaments derived from the DEM support this analysis. The drainage anomalies, derived from the DLG data, and the tonal anomalies and linear vegetation patterns, derived from Landsat, appear to reflect structures formed from the Early Laramide Orogeny. This is an important result as the northern portion of the Laramie Range, where most of the tonal anomalies and linear vegetation growth were mapped, is believed to have been strongly deformed during the latter stages of the orogeny (Gries, 1983). Lineament trends also seen in the major uplifts in the study area reflect that the Hartville Uplift primarily during the early stages of the Laramide Orogeny with perhaps futher deformation during the later stages. The Northern Laramie Range lineaments show trend directions consistent with the counterclockwise rotation of compressive stress as detailed by Gries (1983). Lastly, the Black Hills, formed during the early Laramide, perhaps show the effects of Late Laramide deformation. The major northeast and northwest trend directions indicated by all types of lineaments may be very significant, particularly to how the relate to trends identified by Slack (1981) and Marrs and Raines (1984). The northeast trending lineaments appear to correlate to the Fiddler Creek and Clareton trends of Slack (1981) and the Arminto/Upton, Natrona/Ross, Casper/Bill, and Orpha/Redbird of Marrs and

Raines (1984). The lineaments that also show northwesterly trends, the Landsat-derived lineaments and the drainage anomalies, may correlate to the Buffalo/Douglas northwest trend of linear structures identified by Marrs and Raines (1984).

Landsat TM topographic lineaments, consisting of linear ridges and valley, were found to be concentrated in areas where there is either exposed brittle rock or a strong magnetic or gravity high. This can also be said of the topographic lineaments identified from the DEM. The DEM lineaments were in most cases complementary, rather than duplicative of the Landsat-derived topographic lineaments. In many places, patterns of the topographic lineaments indicated the presence of conjugate fracture sets. Therefore, it can be inferred that the topographic lineaments strongly reflect geological structures both surface and subsurface. Drainage anomalies, identified from the DLG files, were also shown to provide valuable information regarding the subsurface structure. Lineaments belonging to this class were often found to lie perpendicular to magnetic trends seen in both USGS total intensity and NEWMAG™ high-resolution residual magnetic data. A circular pattern of drainage anomalies was found to exist in two main regions of the study area. An overlay of these lineaments with both types of magnetic data indicated that these patterns coincide with arcuate gradients between magnetic highs and lows. The lineaments belonging to the tonal anomalies and linear vegetation growth class, derived from the Landsat TM image, were not readily related to subsurface structure. However, these lineaments did occur in greater density in areas of exposed brittle igneous and sedimentary rocks. The vegetation lineaments portray obvious joint and fracture sets in the brittle rocks and could, therefore, be a useful class of lineaments for surficial structure analysis.

GIS functionality is becoming increasingly popular in structural geology analysis. The most common GIS functionality employed in the analysis portion of this study was the use of overlay. However, GIS functionality was also found to be particularly useful in the preprocessing of the data. Specifically, the systematic comparison of all lineaments to with nearby cultural features, and the elimination of those lineaments found to closely transportation routes mapped in the DLG files, was very important in reducing the number of spurious lineaments, and thus increasing the likelihood that the lineaments in the final data set were indeed of geological origin. However, some cultural lineaments

may themselves follow geological “avenues” such as major faults and fractures. Thus a lineament that parallels a cultural feature is not necessarily a spurious lineament. The DEM can be used to resolve the ambiguity, based on the assumption that transportation features rarely modify the landscape significantly at the scale used in this study. The original topographic lineament data, including lineaments derived from the Landsat image and the DEM, were stratified based on different topographic classes. These classes are slope-breaks, ridge-tops, and valleys. Information from the DEM was utilized to identify slope-breaks and ridge tops, whereas the valleys were identified from the DLG hydrological files. It was found that each topographic lineament class was useful, possibly reflecting the range of topography found in this area. Studies covering smaller localities might find that only certain types of lineaments are useful. For example, a geologist mapping structure in broad flat terrain may find that slope-break lineaments are the most valuable. Conversely, a geologist mapping structure in areas of high relief may place more emphasis on valley and ridge-top lineaments.

The Powder River Basin is widely known as one of the nation’s most prolific hydrocarbon producing interior basins. There are three main producing intervals in the Powder River Basin – the Pennsylvanian-Permian, Lower Cretaceous and Upper Cretaceous. Many of the reservoirs belonging to these producing intervals appear to be linearly arranged, most oriented to the northwest, suggesting strong structural control. Overlaying the lineaments and the locations of the reservoirs on the total intensity and high-resolution magnetic yielded interesting results. Subtle and strong magnetic highs seen in the total intensity and high-resolution magnetic data often coincide with a higher concentration of lineaments. These lineaments parallel and cross these highs at the surface, often intersecting. Many major and minor oil fields are located in these areas, possibly owing their existence to basement structural features and related lineaments. Among the most prominent of these fields are Hilight, Buck Draw North, Cole Creek South, Big Muddy East, Sand Dunes, Steinle Ranch, Todd, Poison Draw and Fiddler Creek.

In summary, this study has led to the development of valuable insights regarding the properties of lineaments and their structural significance. Also, the employment of GIS functionality with information contained within the DEM and DLG files has shown

to be very powerful in the classification and categorization of these lineaments. Ultimately, the final analysis of the influence of these lineaments came from the integration of the surface information with the subsurface geophysics. This stage of the investigation allowed for generalizations to be made about which lineaments seem to be surface expressions of subsurface structure interpreted from geophysical data. The lineament data combined with the subsurface magnetic geophysics also provided possible reasons for the locations of some hydrocarbon reservoirs.

Recommendations for Future Investigations

This lineament analysis involved many steps. Perhaps one of the most difficult to implement was the elimination of cultural lineaments from the interpreted lineament files. This step was performed with raster images of the lineaments rather than using the original digitized vector layers. Perhaps an easier way to conduct this operation would be to use vector GIS functionalities of buffer and erase. After the cultural lineaments were removed, lineaments were converted back into vectors for rose diagram generation. A second aspect of this procedure is that for those lineaments with more than two nodes, the azimuth was determined by the straight line from starting to end node. To eliminate this problem, future studies should include only lineaments with two node points. In areas where lineaments are curvilinear, several lineaments of two nodes each should be drawn, rather than one large lineament.

Structural analysis of the lineaments in this study was generalized based on the coincidence of a large concentration of lineaments with interpreted structure in the magnetic and gravity geophysics. This method is useful in evaluating which lineaments are more credible as surface expressions of subsurface structure. However, incorporation of 2-D seismic geophysics that cross certain lineaments could be considered as the next step in the subsurface analysis of these lineaments. Seismic lines could be obtained in areas of high lineament concentration to study their effects at depth.

Lastly, overlays of the location of hydrocarbon reservoirs and the lineaments on to the magnetic data showed significant results. In many cases where there were magnetic highs, or gradients between highs and lows, there was a higher concentration of lineaments that were parallel or perpendicular to these apparent structures. Many oil

fields were found to lie either directly over these highs, or on the fringes near the gradient. To provide evidence that these reservoirs are affected by the structures identified in the magnetic data, one or two additional steps should be carried out. The first step would be to include overlays of lineament and reservoir location with published productive formation structure maps. Also, seismic lines could be acquired across the area of question. These steps would also continue the study of which lineaments appear to show the strongest correlation with subsurface structures.

Appendix A: Legends for Geophysical Maps

mGal Legend for all figures containing USGS gravity data

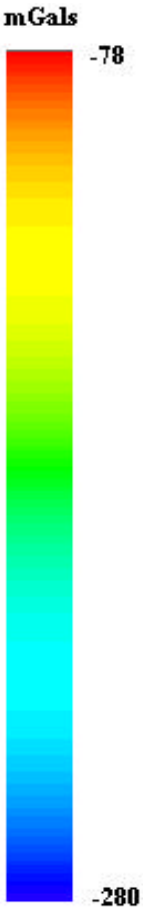

Gamma Legend for all figures containing USGS total intensity magnetic data

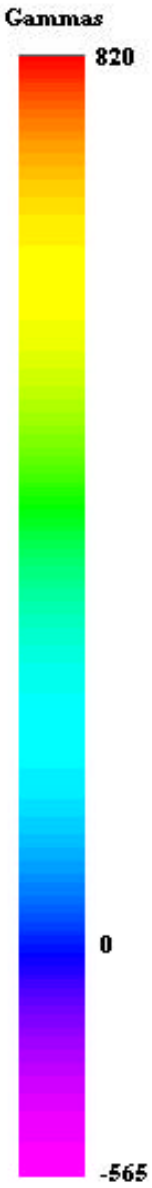

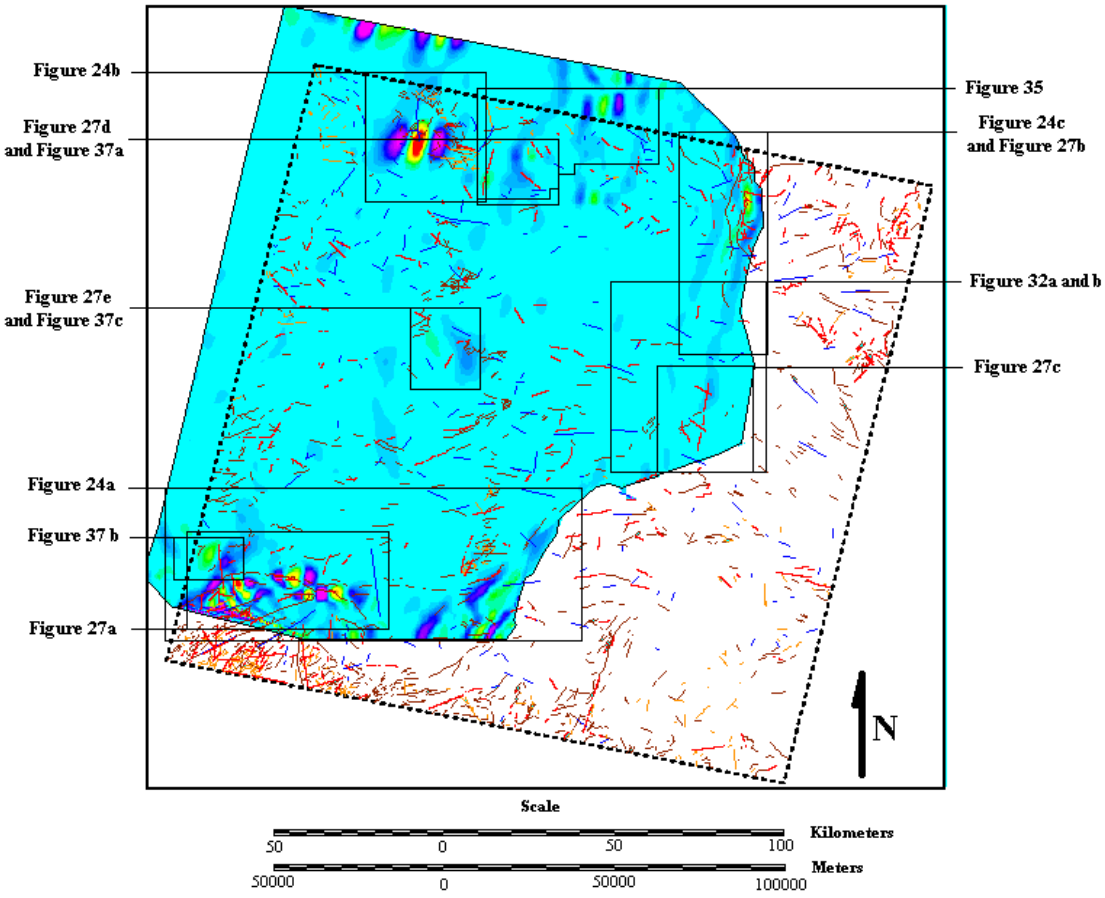

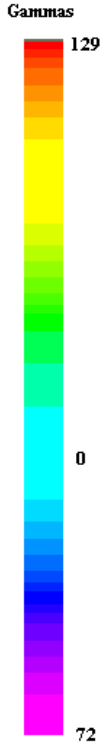

Index Map of Newmag™ Coverage and Figure Locations

Legend

- Landsat Image Outline
- Landsat Topographic Lineament
- Tonal Anonaly or Linear Vegetation Growth
- DEM Topographic Lineament
- Drainage Anomaly

References

Barlow and Haun, Incorporated Geologists, 1987. Structure contour map of the Powder River Basin and Casper Arch: scale 1:190,080, 2 sheets.

Beaver, D. E., Eliason, J. R., and Thiessen, R. L., 1992. Regional digital analysis of major crustal structures in Washington State: *in* Basement Tectonics 7. Proceedings of the International Conference, pp. 329-340.

Berg, R. R., 1968. Point-bar origin of Fall River Sandstone reservoirs, northeastern Wyoming: *AAPG Bulletin*, v. 52, pp. 2116-2122.

Blackstone, D. L., 1949. Structural pattern of the Powder River Basin: *Wyoming Geological Association Guidebook, 4th Annual Field Conference*, pp. 35-36.

Blackstone, D. L., 1990. Precambrian basement map of Wyoming: Outcrop and structural configuration: Wyoming Geological Survey Map Series MS-27, scale 1:1,000,000.

Brown, W. G., 1981. Surface and subsurface examples from the Wyoming foreland as evidences of a regional compressional origin for the Laramide Orogeny, [abs.], Rocky Mountain Foreland Basement Tectonics: University of Wyoming Contributions to Geology, v. 19, pp. 175-177.

Berquist, C. R., 1996. Techniques for conversion of paper maps to digital and the creation of new digital geologic maps in Virginia [abs.], Geological Society of America Abstracts with Programs, v. 28, n. 7, p. 264.

Campagna, D. J., and Levandowski, D. W., 1991. The recognition of strike-slip fault systems using imagery, gravity, and topographic data sets. *Photogrammetric Engineering and Remote Sensing*, v. 57, n. 9, pp. 1195-1201.

Chorowicz, J., Kim, J., Manoussis, S., Rudant, J.-P., Foin, P., and Veillet, I., 1989. A new technique for recognition of geological and geomporphological patterns in Digital Terrain Models: *Remote Sensing of the Environment*: v. 29, pp. 229-239.

Chorowicz, J., Ichoku, C., Raizanoff, S., Youn-Jong, K., Cervelle, B., 1992. A combined algorithm for automated drainage network extractior: *Water Resources Research*, v. 23, n. 5, pp. 1293-1302.

Condie, K. C., 1976. The Wyoming Archean province in the western United States, *in* Windley, B. F., ed., The early history of the Earth: New York, Wiley and Sons, pp. 499-510.

DeBruin, R. H., and Boyd, C. S., 1990. Oil and gas fields map of the Powder River Basin, Wyoming: Geological Survey of Wyoming, MS-31, scale 1:316,800.

Dix, O. R. and Jackson, M. P. A., 1981. *Statistical analysis of lineaments and their relation to fracturing, faulting, and halokinesis in the East Texas Basin*. Bureau of Economic Geology, The University of Texas at Austin, Austin TX, Report 110.

Dolton, G. L., and Fox, J. E., 1996. Powder River Basin Province: *in* Gautier, D. L., Dolton, G. L., Takahashi, K. I., Varnes, K. L., *eds.*, 1995 National Assessment of U. S. Oil and Gas Resources – Results, Methodology, and Supporting Data. U. S. Geological Survey Digital Data Series DDS-30, Release 2.

Douglas, D. H., 1986. Experiments to locate ridges and channels to create a new type of digital elevation model. *Cartographica*, v. 23, n. 4, pp. 29-61.

Duval, J. S., Pitkin, J. A., and Macke, D. L., 1977. Aeromagnetic map of part of the southern Powder River Basin, Wyoming: USGS Open File Report 77-621, 1 sheet, scale 1:125,000.

Erdas, 1997. *Erdas Field Guide*, 4th Edition. Erdas, Atlanta, GA, 656p.

Florinsky, I. V., Quantitative topographic method of fault morphology recognition, *Geomorphology*, v. 16, n. 2, pp. 103-119.

Fishman, J., Bhatt, M., Aiken, C. L. V., Fleischmann, K. H., Balde, M., de la Fuente Mauricio, F., 1996. The integration of remote sensing, GIS converted geology and GPS controlled gravity in an analysis of the structure of Ecuador [abs.], Geological Society of America Abstracts with Programs, v. 28, n. 7, p. 265.

Gay, S. P., 1995. The basement fault block pattern: Its importance in petroleum exploration, and its delineation with residual aeromagnetic techniques: *in* R. W. Ojakangas, *ed.*, Proceedings Volume of the 10th Basement Tectonics Conference. Pp. 1-41.

Gries, R., 1983. North-south compression of Rocky Mountain foreland structures: *in* Lowell, J. D., *ed.*, Rocky Mountain Foreland Basins and Uplifts. Rocky Mountain Association of Geologists, pp. 9-32.

Hardcastle, K. C., 1995. Photolineament factor: A new computer-aided method for remotely sensing the degree to which bedrock is fractured. *Photogrammetric Engineering and Remote Sensing* 61 (6): 739-747.

Hedge, C. E., Houston, R. S., Tweto, O. L., Peterman, Z. E., Harrison, J. E., an Reid, R. R., 1986. The Precambrian of the Rocky Mountain region: U. S. Geological Survey Professional Paper 1241-D, 17 p.Hoppin, R. A., 1974. Lineaments: their role in tectonics of central Rocky Mountains: *AAPG Bulletin*, v. 58, pp. 2260-2273.

Jaworski, C., 1997. Using Gis to produce quaternary geologic maps of Wyoming [abs.], Geological Society of America Abstracts with Programs, v. 29, n. 7, p. 293.

Jenson, S. K., and Domingue, J. O., 1988. Extracting topographic structure from digital elevation data for geographic information system analysis. *Photogrammetric Engineering and Remote Sensing*, v. 54, n. 11, pp. 1593-1600.

Johnson, E. A., 1992. Depositional history of Jurassic rocks in the area of the Powder River Basin, northeastern Wyoming and southeastern Montana: U. S. Geological Survey Bulletin 1917-J, pp. J1-J38.

Johnson, E. A., 1993. Depositional history of Triassic rocks in the area of the Powder River Basin, northeastern Wyoming and southeastern Montana: U. S. Geological Survey Bulletin 1917-P, pp. P1-P30.

Kent, B. H., 1986. *Evolution of thick coal deposits in the Powder River Basin, northeastern Wyoming*. Geological Society of America Special Paper 210, pp. 105-120.

Kleinkopf, M. D., and Redden, J. A., 1975. Bouguer gravity, aeromagnetic, and generalized geologic maps of part of the Black Hills of South Dakota and Wyoming: USGS Geophysical Investigations Map GP-903, 11 p., 1 sheet, scale 1:125,000.

Levandowski, D., Cetin, H., and Reichard, J., 1993. Photogeomorphic and gravity mapping of extensional faulting and associated structures in unconsolidated sediments of Newark and Railroad Valleys, Nevada. *Proceedings of the Ninth Thematic Conference on Geologic Remote Sensing*, v. 1, pp. 169-180.

Linn, J. K., 1996. Computer demonstration utilizing ArcView for display and analysis of geologic and geophysical data [abs.], Geological Society of America Abstracts with Programs, v. 28, n. 7, p. 264.

Love, J. D., and Christiansen, A. C., 1985. Geologic map of Wyoming: Wyoming Geological Survey Map, 2 sheets, scale 1:500,000.

Love, J. D., and Weitz, J. L., 1951. Geologic Map of the Powder River Basin and adjacent areas, Wyoming. U. S. Geological Survey, Oil and Gas Investigations, OM 122, scale 1:316,800.

Mah, A., Taylor, G. R., Lennox, P. and Balia, L., 1995. Lineament analysis of Landsat Thematic Mapper Images, Northern Territory, Australia. *Photogrammetric Engineering and Remote Sensing* 61 (6): 761-773.

Mallory, W. W., ed., 1972. Geologic atlas of the Rocky Mountain region, United States of America: Denver, Rocky Mountain Association of Geologists, 331 p.

Marrs, R. W., and G. L. Raines, 1984. Tectonic framework of Powder River Basin, Wyoming and Montana, interpreted from Landsat imagery: *AAPG Bulletin*, v. 68, pp. 516-529.

Maughan, E. K., 1983. Tectonic setting of the Rocky Mountain region during the Late Paleozoic and Early Mesozoic, *in* Symposium on genesis of Rocky Mountain ore deposits; changes with time and tectonics: Denver Region Exploration Geologists Society Proceedings Volume, pp. 39-50.

McMahon, M. J., and North, C. P., 1993. Three-dimensional integration of remotely sensed geological data: A methodology for petroleum exploration: *in* Exploration, environment and engineering. *Proceedings of the Ninth Thematic Conference on Geologic Remote Sensing*. V. 1, pp. 221-233.

McMillen, K. J., 1989. Cambrian seismic stratigraphy and extensional tectonics of the Powder River Basin, Wyoming [abs.]: GSA 85th Annual Meeting Abstracts with Programs, Cordilleran Section, v. 21, n. 5, p. 116.

Michael, R. C., and I. S. Merin, 1986. Tectonic framework of Powder River Basin, Wyoming and Montana, interpreted from Landsat imagery: Discussion: *AAPG Bulletin*, v. 70, pp. 453-455.

Mitchell, G. C., and Rogers, M. H., 1993. Extensional tectonic influence on Lower and Upper Cretaceous stratigraphy and reservoirs. *The Mountain Geologist*, v. 30, n. 2, pp. 54-68.

Moore, W. R., 1985. Seismic profiles of the Powder River Basin, Wyoming, *in* Gries, R. R., and Dyer, R. C., eds., Seismic exploration of the Rocky Mountains: Denver,

Rocky Mountain Association of Geologists and Denver Geophysical Society, p. 187-199.

Mueller, P. A., Wooden, J. L., and Nutman, A. P., 1992. 3.96 Ga zircons from an Archean quartzite, Beartooth Mountains, Montana: *Geology*, v. 20, n. 4, pp. 327-330.

Neves, D. S., and Thiessen, R. L., 1993. The extraction of 3-D geological structure using geomorphological features in Digital Elevation Models: *in* Exploration, environment and engineering. *Proceedings of the Ninth Thematic Conference on Geologic Remote Sensing*, v. 1, pp. 1029-1040.

Offield, T. W., Abbott, E. A., Gillespie, A. R., and Loguercio, S. O., 1977. Structure mapping on enhanced Landsat images of southern Brazil: Tectonic control of mineralization and speculations on metallogeny. *Geophysics*, v. 42, n. 3, pp. 482-500.

Oldow, J.S., 1996. Digital geological and geophysical database of northern Venezuela [abs.], Geological Society of America Abstracts with Programs, v. 28, n. 7, p. 264.

O'Leary, D. W., Friedman, J. D., and H. A. Pohn, 1976. Lineament, linear, lineation: some proposed new standards for old terms. *Geological Society of America Bulletin* 87 (10): 1463-1469.

O'Leary, D. W., and Simpson, S. L., 1977. Remote sensor applications to tectonism and seismicity in the northern part of the Mississippi Embayment. *Geophysics*, v. 42, n. 3, pp. 542-548.

Parizek, R. R., Lavin, P. M., Greenfield, R. J., Weiss, R. A., Shuman C. A., and Moran, M. L., 1990. *Nature and hydrologic significance of fracture traces, lineaments, and fracture zones related to ground-water monitoring.* U.S. E.P.A., Office of Research and Development, Environmental Monitoring Systems Laboratory, Technical Document CR813660-01-0, 165pp.

Rasmussen, D. L., and D. W. Bean, 1984. Dissolution of Permian salt and Mesozoic syndepositional trends, central Powder River Basin, Wyoming, *in* J. Goolsby and D. Morten, eds., *The Permian and Pennsylvanian geology of Wyoming*: WGA Guidebook, pp. 281-295.

Ray, R. R., and Berg, C. R., 1985. Seismic interpretaion of the Casper Arch thrust, Tepee Flats Field, Wyoming, *in* Gries, R. R., and Dyer, R. C., eds., Seismic exploration

of the Rocky Mountains: Rocky Mountain Association of Geologists and Denver Geophysical Society, p. 51-58.

Robbins, S. L., and Grow, J. A., 1990. Structural and basement lithological implications of gravity and seismic-reflection data across the central Powder River Basin from the Black Hilss to the Bighorn Mountains [abs.]: USGS Circular 1060, p. 71.

Robbins, S. L., 1994. Gravity and aeromagnetic studies of the Powder River Basin and surrounding areas, southeastern Montana, northeastern Wyoming, and western South Dakota. USGS Bulletin 1917-R, 17 p., 4 sheets, scale 1:1,000,000.

Ross, J. A., 1997. Digital geologic map production and publication at the Kansas Geological Survey [abs.], Geological Society of America Abstracts with Programs, v. 29, n. 7, p. 293.

Rowan, L. C. and Bowers, T. L., 1995. Analysis of linear features mapped in Landsat Thematic Mapper and side-looking airborne radar images of the Reno 1° by 2° Quadrangle, Nevada and California: Implications for mineral resource studies. *Photogrammetric Engineering and Remote Sensing* 61 (6): 749-759.

Rowan, L. C. and P. H. Wetlaufer, 1975. *Iron-absorption band analysis for the discrimination of iron-rich zones.* U.S. Geological Survey, Type III Final Report, Contract S-70243-AG.

Salas, G. P., 1975. Relationship of mineral resources to linear features in Mexico as determined from Landsat data. Proceedings of the First Annual William T. Pecora Memorial Symposium, October, 1975, Sioux Falls, South Dakota, 14 p.

Sharp, R. P., 1948. Early Tertiary fanglomerate, Big Horn Mountains, Wyoming: *Journal of Geology*, v. 56, p. 1-15.

Shurr, G. W., 1979. Lineament control of sedimentary facies in the northern Great Plains, United States, *in* M. H. Podwysocki and J. L. Earle, eds., *Proceedings of Second International Conference on Basement Tectonics, Newark, Delaware, 1976*: Basement Tectonics Committee, Denver, Colorado, pp. 413-422.

Slack, P. B., 1981. Paleotectonics and hydrocarbon accumulation, Powder River Basin, Wyoming: *AAPG Bulletin*, v. 65, pp. 730-743.

Snyder, G. L., Hughes, D. J., Hall, R. P., and Ludwig, K. R., 1989. Distribution of Precambrian mafic intrusives penetrating some Archean rocks of western North America: U. S. Geological Survey Open-File Report 89-125, 36 p.

Srinivasan, R. and B. A. Engel, 1991. Effect of slope prediction methods on slope and erosion estimates. *Applied Engineering in Agriculture* **7**, 779-783.

Stewart, J. H., 1976. Late Precambrian evolution of North America; plate tectonics implication: *Geology*, v. 4, n. 1, pp. 11-15.

Winston, D., 1988. Proposed intracratonic setting of western middle Proterozoic basins [abs.]: Geological Society of America 41st Annual Meeting Abstracts with Programs, Rocky Mountain Section, v. 20, n. 6., p. 474.

Warner, T. A., 1998. An evaluation of lineament analysis for hydrocarbon exploration. In review by *Geocarto*.

Warner, T. A., 1997. *Integration of remotely sensed geobotanical and structural methods for hydrocarbon exploration in West-central West Virginia*. Final report for DOE-sponsored Research Contract DE-FG21-95MC32159. Morgantown, WV, 55pp.

Warner, T. A., D. J. Campagna, C. S. Evans, D. W. Levandowski and H. Cetin, 1991. Analyzing remote sensing geobotanical trends in Quentico Provincial Park, Ontario, Canada, using digital elevation data. *Photogrammetric Engineering and Remote Sensing*, v. 57 (9): 1179-1183.

Weimer, R. J., 1980. Recurrent movements on basement faults, a tectonic style for Colorado and adjacent areas: *Rocky Mountain Association of Geologists Symposium*, Denver, Colorado, pp. 23-35.

Yin, Z. Y. and G. A. Brook, 1992. The topographic approach to locating high-yield wells in crystalline rocks: Does it work? *Groundwater* 30: 96-102.